Synovial Fluid Analysis and The Evaluation of Patients With Arthritis

Brian F. Mandell
Editor

Springer

Synovial Fluid Analysis and The Evaluation of Patients With Arthritis

Brian F. Mandell
Editor

Synovial Fluid Analysis and The Evaluation of Patients With Arthritis

Springer

Editor
Brian F. Mandell
Rheumatologic and Immunologic Disease
Cleveland Clinic
Cleveland
OH, USA

ISBN 978-3-030-99611-6 ISBN 978-3-030-99612-3 (eBook)
https://doi.org/10.1007/978-3-030-99612-3

This Springer imprint is published by the registered company Springer Nature Switzerland AG
The registered company address is: Gewerbestrasse 11, 6330 Cham, Switzerland

This book is dedicated to the memory of Drs. Isaias Spilberg and H. Ralph Schumacher. It was "Chic" Spilberg at Washington University in St Louis, Missouri, who 50 years ago welcomed me into the experimental world of crystal-induced inflammation, introducing me to the polarizing microscope (and to South American authors who wrote beautiful fiction).

Decades later, in the rheumatology department at the Hospital of the University of Pennsylvania, I had the opportunity to work as a fellow and then colleague with Ralph Schumacher. Ralph had the most genuine and intense clinical and scientific curiosity of anyone I have ever met. He had a special passion for the microscope (light and electron) and the analysis of synovial fluids throughout his professional career. Any fluid that was left unaspirated in a patient could not be examined, and thus could not be used to generate questions; and if there were no questions generated, there could be no learning. No clinical fluid sample could be

declared free of crystals without a good 10-minute scouring under the polarizing scope.

Ralph (pictured below with his electron microscope) initiated the synovial fluid workshop at the annual scientific meeting of the American College of Rheumatology. He regularly reviewed fluids sent to him from physicians around the world, always on the lookout for the unusual or unrecognized structure. He wrote with his colleague Dr. Antonio Reginato, another iconic figure and wonderful teacher at Penn, a text and atlas of synovial fluid analysis [1] which is unfortunately out of print. I am hoping that our current book can take its place on the shelves of the current generation of rheumatologists.

My sincere thanks to all of the contributors to this book, all experts in the field, who have contributed their energy and expertise to the project. I offer my special acknowledgment to Professor Eliseo Pascual, internationally known for his clinical and teaching contributions in several areas of rheumatology, especially related to crystal identification. His immediate enthusiasm and assistance in tying up some loose ends of this project, I gratefully acknowledge with thanks and enormous respect.

H Ralph Schumacher with his electron microscope at the Philadelphia VA Hospital

1. *Atlas of Synovial Fluid Analysis and Crystal Identification. Schumacher HR and Reginato A. Lea and Febiger. 1991*

Contents

Contributors

Mariano Andrés Rheumatology Unit, Dr. Balmis General University Hospital-Institute of Sanitary and Biomedical Research (ISABIAL), Alicante, Spain

Clinical Medicine Department, Miguel Hernandez University, San Juan de Alicante, Spain

Sharon Cowley Division of Rheumatology, Mater Misericordiae University Hospital, Dublin, Ireland

N. Lawrence Edwards Department of Medicine, University of Florida, Gainesville, FL, USA

John D. FitzGerald Department of Medicine, Division of Rheumatology, University of California, Los Angeles, David Geffen School of Medicine, Los Angeles, CA, USA

Susan M. Harrington Pathology and Laboratory Medicine Institute, Cleveland Clinic, Cleveland, OH, USA

Tim L. Jansen Department of Rheumatology VieCuri MC, Venlo, The Netherlands

Department Med Cell Biophysics (MCB), University of Twente, Enschede, The Netherlands

Robert T. Keenan Arthrosi Therapeutics, San Diego, CA, USA

Joshua A. Lieberman Department of Laboratory Medicine and Pathology, University of Washington, School of Medicine, Seattle, WA, USA

Brian F. Mandell Rheumatologic and Immunologic Disease, Cleveland Clinic, Cleveland, OH, USA

Geraldine McCarthy Division of Rheumatology, Mater Misericordiae University Hospital, Dublin, Ireland

Maria C. Modesto-Caballero Osakidetza, OSI EE-Cruces, Cruces University Hospital, Barakaldo, Spain

Francesca Oliviero Rheumatology Unit, Department of Medicine – DIMED, Biomedical Campus "Pietro D'Abano", University of Padova, Padova, Italy

Kenneth S. O'Rourke Division of Rheumatology, Maine Medical Center, Portland, ME, USA

Eliseo Pascual Rheumatology Unit, Dr. Balmis General University Hospital-Institute of Sanitary and Biomedical Research (ISABIAL), Alicante, Spain

Clinical Medicine Department, Miguel Hernandez University, San Juan de Alicante, Spain

Fernando Perez-Ruiz Osakidetza, OSI EE-Cruces, Cruces University Hospital, Barakaldo, Spain

Biocruces-Bizkaia Health Research Institute, Barakaldo, Spain

Medicine Department of the Medicine and Nursing School, University of the Basque Country, Barakaldo, Spain

Michael H. Pillinger Division of Rheumatology, NYU Grossman School of Medicine/NYU Langone Medical Center, VA New York Harbor Health Care System, New York, NY, USA

Leonardo Punzi Centre for Gout and Metabolic Bone and Joint Diseases, Rheumatology, SS Giovanni and Paolo Hospital, Venice, Italy

Ann K. Rosenthal The Division of Rheumatology, Department of Medicine, Medical College of Wisconsin and The Zablocki VA Medical Center, Milwaukee, WI, USA

Stephen J. Salipante Department of Laboratory Medicine and Pathology, University of Washington, School of Medicine, Seattle, WA, USA

Carla R. Scanzello Division of Rheumatology, University of Pennsylvania Perelman School of Medicine, Philadelphia, PA, USA

Michael J. Crescenz VA Medical Center, Philadelphia, PA, USA

Chapter 1
The Impact of Synovial Fluid Analysis on Clinical Practice – Introduction

Brian F. Mandell

In their 1953 seminal study [1] on 1500 specimens from patients at the Massachusetts General Hospital "*Synovial Fluid Changes in Joint Disease*" (Fig. 1.1), Ropes and Bauer wrote that evaluation of synovial fluid is necessary to learn of the "physiological and metabolic alterations in articular tissues…. and obtain clues as to the pathogenic mechanisms involved". They cited a reference crediting Paracelsus (1493–1541) with the initial recognition of viscous fluid in joint cavities, and in their 150 page text they described features of normal and pathologic synovial fluids (SF). They honed in on the concept of SF as a filtrate from blood, and distinguished two major groups of fluids: traumatic and "infectious inflammatory". They described the relationship between concentrations of small and macro molecules in SF and blood. They described intra-articular pressure, SF pH and how synovial fluid cell counts evolved over time in several patients with rheumatoid arthritis. They noted the inflammatory nature of fluids from patients with clinically diagnosed gout, but did not describe the crystals. This was years before the pathogenic monosodium urate crystals were characterized by polarized microscopy in synovial fluids, but 268 years after the microscopist Antoni van Leeuwenhoek had described the "long, transparent little particles, many pointed at both ends" contained in the "chalk" draining from a hole in a relative's gouty elbow (cited from ref. [2]).

Expanding on the observations of Joseph Hollander at the University of Pennsylvania that crystalline structures could be observed by routine light microscopy in synovial fluids obtained from patients with clinically diagnosed gout, Dan McCarty with Hollander using polarized microscopy described in 1961 the presence of birefringent crystals with negative elongation properties in the fluids of gouty patients [3]. The crystals were dissolved by incubation with uricase, proof of their biochemical composition. Additionally, they noted that polarized microscopy

B. F. Mandell (✉)
Rheumatologic and Immunologic Disease, Cleveland Clinic, Cleveland, OH, USA
e-mail: mandelb@ccf.org

B. F. Mandell (ed.), *Synovial Fluid Analysis and The Evaluation of Patients With Arthritis*, https://doi.org/10.1007/978-3-030-99612-3_1

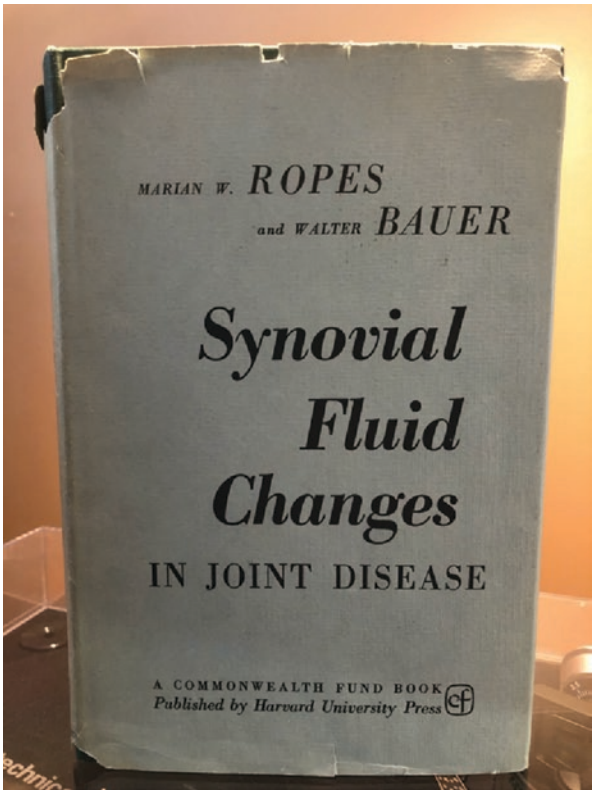

Fig. 1.1 Cover of Ropes and Bauer's 1953 treatise of SF analysis

was a more sensitive diagnostic technique than standard light microscopy for recognizing these crystals. In 1962 Seegmiller, Howell, and Malawista [4] at the NIH and Faires and McCarty [5] independently demonstrated that the intra-articular injection of monosodium urate crystals into human knees was sufficient to induce a very painful acute arthritis which mimicked an acute gout flare. The inflammatory effect of injected urate crystals reportedly had been previously demonstrated by Freudweiler in 1899 [6], in a paper published in German with apparently little academic recognition. McCarty went on to describe the presence and pathogenic role of calcium pyrophosphate crystals in patients with "pseudogout" (calcium pyrophosphate arthritis, CPPA) [7] and the association of calcium phosphate crystals (apatite) with "Milwaukee shoulder and knee syndrome" [8]. H Ralph Schumacher studied synovial histopathology and wrote and lectured on the diagnostic value of synovial fluid analysis using light, polarizing and electron microscopy for decades at the University of Pennsylvania.

Moving forward some 68 years from the publication of Ropes and Bauer's text, national and international societies have recommended synovial fluid analysis including polarized microscopy for the diagnosis of crystal-associated arthritis. Practice guidelines uniformly emphasize the need for synovial fluid aspiration and analysis to diagnose septic arthritis and exclude its mimic crystal-induced arthritis

(with the awareness that the two can be simultaneously present). With the increasing availability of ultrasound imaging in rheumatology and musculoskeletal clinics, arthrocentesis even of small joints with minimal effusions should be a readily available diagnostic procedure. And yet, synovial fluid analysis is still underutilized in the evaluation of patients with undefined arthritis. This prompted a forceful editorial by Leonardo Punzi et al. in 2015 [9] following a call 3 years earlier [10] for greater investment in the teaching of synovial fluid analysis in the United States during rheumatology fellowship and in other musculoskeletal medicine training programs. Great strides have not been made to increase the teaching and utilization of SF analysis since those two commentaries, from two different continents, were written. We are hoping that this book will provide practical practice landmarks as well as serve as a reference source on SF analysis for both tyros and experienced musculoskeletal clinicians.

The evaluation of SF provides insight into the real-time biologic status of the joint being evaluated. While a specific and definitive diagnosis can be established from SF analysis in a small number of disorders (e.g., infection, gout, CPPA), there is additional information provided that may be as useful (or more so) as obtaining a rheumatoid factor or HLA-B27 genetic test which are ordered more frequently and more indiscriminately. Unlike with other body fluids, the fluid pH, levels of glucose or protein/albumin have little diagnostic value. But the cell count with differential has much to offer. The total white cell count provides the initial critical information as to whether the fluid results from an inflammatory or non-inflammatory process. Not every patient with inflammatory arthritis will present with a red/hot and extremely tender joint capsule, especially if receiving high-dose steroids, anti-TNF or anti-IL6 therapy. Conversely, a non-inflammatory effusion associated with an occult intra-articular fracture, osteonecrosis, hypertrophic osteoarthropathy or villonodular synovitis may rapidly accumulate causing marked pain and tenderness suggestive of an inflammatory process. Fluid analysis can rapidly focus the differential diagnosis. Acute and severe ankle arthritis in a patient with sickle cell anemia can be due to AVN, but might also be from synovial infarction (distinguished by its inflammatory SF). Crystal analysis is necessary to recognize those patients with coexistent infection and crystal-associated arthritis, very important to recognize as the septic joint may not respond clinically as expected to appropriate drainage and antibiotic therapy until the crystal-induced inflammation is also addressed. Failure to recognize this scenario can result in the patient receiving additional unnecessary surgical or antibiotic treatments for (incorrectly) presumed resistant infection.

Looking at the differential white cell count in SF can provide soft evidence toward or away from certain forms of oligo- or polyarthritis, i.e., extremely high neutrophil counts are more likely from psoriatic than rheumatoid arthritis. This discussion, initiated by Ropes and Bauer [1], is expanded in Chap. 5 in this text.

As internal medicine residents during training become increasingly facile with the use of point of care ultrasound, they will hopefully as matriculated rheumatology fellows become more uniformly expectant to be trained in the use of musculoskeletal ultrasound for diagnosis of synovitis and for guidance of injection and aspiration. Once the barrier of lack of confidence in performing arthrocentesis

dissolves, there should be more emphasis on learning the nuances of crystal recognition and SF analysis. Within this text are several chapters, written by true experts in synovial fluid analysis and crystal identification, that should help hone the skills of others by providing the authors' insights accumulated over many years of diagnosing and treating patients with crystal-associated arthritis.

Reviewing the many images in this text should be helpful, but there is no substitute for gaining experience with frequent careful scanning of SFs from patients with different diseases affecting their joints. As emphasized in several chapters, analysis for CPP and lipid crystals in particular warrants observation using both standard as well as compensated polarized light – both have value. Experience utilizing the fine focus and condenser adjustments is essential to maximize recognition of artifacts, distinguish between intracellular granules and small crystals, and identify birefringence and the direction of elongation of crystals.

Just as technology has moved forwards in providing us with additional tools for advanced imaging and identification of crystal-associated arthritis, e.g., ultrasound and dual-energy CT, there are ongoing advances in SF analysis. Thus, we have also included in this text a state-of-the-art review of currently available molecular diagnostic testing for infection, as well as a forward-looking discussion of evolving non-traditional techniques that may be used to diagnose the presence of specific crystals in synovial fluids.

References

1. Ropes MW, Bauer W. Synovial fluid changes in joint disease. Cambridge, Mass: Harvard University Press; 1953.
2. Porter R, Rousseau GS. Gout. The Patrician Malady. P34. New Haven and London: Yale University Press; 1998.
3. McCarty DJ, Hollander JL. Identification of urate crystals in gouty synovial fluid. Ann Int Med. 1961;54:452–60.
4. Seegmiller JE, Howell RR, Malawista SE. The inflammatory reaction to sodium urate: its possible relationship to the genesis of acute gouty arthritis. JAMA. 1962;180:469.
5. Faires JS, McCarty DJ. Acute arthritis in man and dog after intrasynovial injection of sodium urate crystals. Lancet. 1962;280:682–5.
6. Nuki G, Simkin PA. A concise history of gout and hyperuricemia and their treatment. Arth Res Therapy. 2006;8:S1. https://doi.org/10.1186/ar1906.
7. McCarty DJ, Kohn NN, Faires JS. The significance of calcium phosphate crystals in the synovial fluid of arthritic patients: the "pseudogout" syndrome. Ann Int Med. 1962;56:711–37.
8. Halverson PB, Cheung HS, McCarty DJ, et al. "Milwaukee shoulder"--association of microspheroids containing hydroxyapatite crystals, active collagenase, and neutral protease with rotator cuff defects. II Synovial fluid studies Arthritis Rheum. 1981;24:474–83.
9. Punzi L, Ramonda R, Oliviero F. Why are rheumatologists still reluctant to perform joint-fluid analysis? Joint Bone Spine. 2015;82:139–40.
10. Schumacher HR, Chen LX, Mandell BF. The time has come to incorporate more teaching and formalized assessment of skills in synovial fluid analysis into rheumatology training programs. Arth Care Res. 2012;9:1271–3.

Chapter 2
Synovial Structure and Physiology in Health and Disease

Carla R. Scanzello

Introduction

The synovium is a connective tissue that lines the cavity of articular joints. It lies just beneath the fibrous joint capsule, and extends to the bone-cartilage interface without encroaching on articular cartilage (Fig. 2.1a)**.** The tissue of the synovium is generally separated into two regions: a superficial lining layer (intima) which is one to three cell layers thick and faces the joint space, and a sublining layer (subintima) which contains blood vessels, lymphatics, and nerves (Fig. 2.1b)**,** and a variable amount of adipose tissue [3]. The subintima eventually transitions to the denser, more fibrous joint capsule. The appearance of the subintimal layer can vary even within the same joint; three basic patterns have been identified: areolar, fibrous, and fatty [4]. Areolar synovium is characterized by loose subintimal connective tissue and is highly vascular; fibrous synovium is denser and poorly vascularized, and fatty synovium has a higher proportion of adipocytes in the sublining.

One of the unique features of the synovium is that the lining and sublining layers are not separated by an organized basement membrane as in other barrier tissues throughout the body (i.e., epithelial linings such as pleura). Although many of the molecular components of basement membranes are still found in the synovial extracellular matrix (including perlecan, fibronectin, and laminin) [5], it is more loosely organized. This lack of a structured, basement membrane makes the lining semipermeable to many molecular species, allowing for filtration of plasma components which comprise a portion of the synovial fluid that bathes the joint space. Still, the

C. R. Scanzello (✉)
Division of Rheumatology, University of Pennsylvania Perelman School of Medicine, Philadelphia, PA, USA

Michael J. Crescenz VA Medical Center, Philadelphia, PA, USA
e-mail: cscanz@pennmedicine.upenn.edu; carla.scanzello@va.gov

B. F. Mandell (ed.), *Synovial Fluid Analysis and The Evaluation of Patients With Arthritis*, https://doi.org/10.1007/978-3-030-99612-3_2

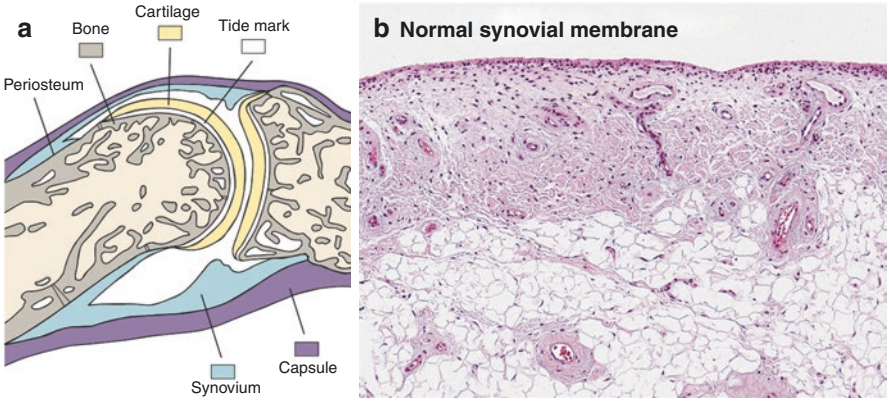

Fig. 2.1 (**a**) A normal human interphalangeal joint, in sagittal section, as an example of a synovial joint. The location of the synovium, facing the joint space and attaching to the inner surface of the joint capsule and the outer surface of the bone up to the bone/cartilage junction, is shown. (Reused with permission from Sokoloff and Bland [1]. Copyright 1975 the Williams & Wilkins Co, Baltimore.) (**b**) Photomicrograph of a thin section of normal human synovial tissue (H&E, 10X). The thin (1–2 cell layer) synovial lining layer is at the top of the section, which lines the loose connective tissue of the sublining layer below it. Varying degrees of adipose (present in the lower part of the frame) can be seen within the sublining layer. (Reused with permission from Gravallese, et al. [2]. Copyright 2021 Elsevier, Philadelphia)

lining and sublining layers have distinct functions [4]. Cells of the intima (synoviocytes) are responsible for production of synovial fluid that provides nutrition for the articular cartilage and lubricates the articular surfaces. In addition, intimal cells protect the joint from inflammatory damage by providing a barrier that prevents cellular extravasation, and by clearing debris. The vasculature and lymphatics of the subintima allow trafficking of substances into and out of the joint space [3]. These functions are critical for the maintenance of joint health throughout our lifespan. This chapter will provide an overview of the structure and function of synovial membrane and its cellular components, and review pathologic changes to the synovium seen in common rheumatologic diseases that compromise its normal function.

Synovial Intima

Synoviocytes that comprise the intimal layer are of two main types: type A synoviocytes which are macrophages of hematopoietic origin, and type B synoviocytes which are fibroblasts of mesenchymal origin (Fig. 2.2a). Early electron microscopy studies of the synovium [8] led to the identification of these cell types and demonstrated that type A synoviocytes contain vacuoles, a prominent Golgi apparatus, and filopodia, but they have little rough endoplasmic reticulum. In contrast, type B

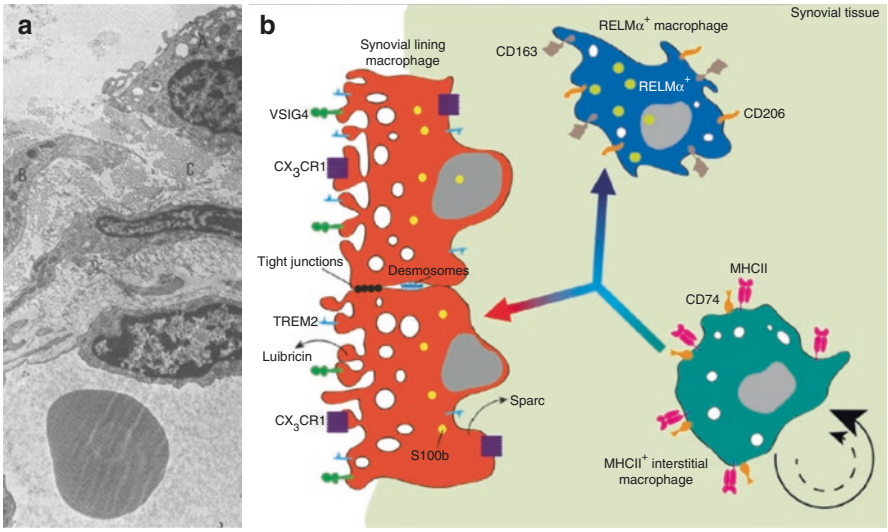

Fig. 2.2 (**a**) Transmission electron microscopy of monkey synovial lining cells. **"**A" indicates a Type A synoviocyte (macrophage) on the lining surface with many processes, vacuoles, and dense bodies. **"**B" indicates a deeper type B synoviocyte (fibroblast) which has more rough endoplasmic reticulum. "C" indicates collagen bundles in the matrix. A small superficial vessel occupies the bottom of the Fig. 9000X. (Reused with permission from Schumacher [6]. Copyright 1975 Association for Clinical Scientists.) (**b**) Origin and phenotypic characteristics of synovial lining macrophages. Resident CX_3CR1^+ lining macrophages and RELMα+ sublining macrophages are replenished throughout adulthood by a resident interstitial macrophage that resides in the sublining. (Reused with permission from Culemann, et al. [7]. Copyright 2019 Elsevier, Philadelphia)

synoviocytes contain fewer vacuoles and abundant rough endoplasmic reticulum, suggesting an important function in protein synthesis. Type A cells express typical macrophage markers, including nonspecific esterase and CD68, while type B cells express high levels of uridine diphosphoglucose dehydrogenase (UDPGD, an enzyme involved in hyaluronic acid synthesis) and CD55. In the normal, healthy state, type B (fibroblast-like) cells predominate while type A cells make up about 10–20% of the lining cells.

Type B Synoviocytes

The developmental origin of the synovium, and specifically fibroblast-like synoviocytes, remained a mystery until recently, when several groups demonstrated that synovial tissue develops early during embryogenesis from the same mesenchymal precursor cells that give rise to other joint tissues including cartilage, bone, meniscus, and ligaments [9–11]. These cells, identified by expression of growth differentiation factor-5 (GDF-5) condense to form a lining layer. This is facilitated by

expression of cadherin-11, a key adhesion molecule that mediates adherens junction formation and regulates the formation of the synovial lining during development [12, 13]. As mentioned above, these cells are rich in endoplasmic reticulum suggesting a synthetic function, and they produce synovial extracellular matrix components including collagen type 1, fibronectin, and proteoglycans. In addition, type B lining cells express UDPGD, hyaluronate synthetase 1 (HAS1), and proteoglycan 4 (PRG4) which encodes lubricin. They are the main producers of synovial fluid lubricin and hyaluronic acid which together provide boundary lubrication of cartilage [14] and shock absorption [15], allowing friction-free and pain-free motion of the joint during activity. Lubricin also prevents pathologic deposition of protein onto the surface of articular cartilage.

In addition to these important synthetic functions, type B synoviocytes have phagocytic capacity and the ability to present antigens, and thus may act as "immune sentinels" poised to activate immune responses when needed. They express decay-accelerating factor (CD55) [16] which inactivates intermediates of the complement cascade, suggesting an immunoregulatory function. However, under inflammatory conditions, these cells can produce large amounts of metalloproteinases, inflammatory cytokines, and molecules involved in activation of osteoclasts (i.e., RANKL), contributing to pathology throughout the joint. Heterogeneity in synovial fibroblast cadherin-11 expression can contribute to the invasiveness of the synovium at the pannus-cartilage interface in rheumatoid arthritis [12, 17]. Croft et al. [18] showed that $CD90^{-}$ synovial lining fibroblasts expressed FAPα (fibroblast activation protein-α), and through adoptive transfer demonstrated that these cells mediated bone and cartilage destruction in a murine model of inflammatory arthritis. Epigenetic changes to synovial fibroblasts have been implicated in modulating a change from an immunoregulatory role in health, to an active pathogenic role in chronic arthritis.

Type A Synoviocytes

Synovial intimal macrophages express high levels of the fractalkine receptor CX_3CR1 [19], and scavenger receptors such as CD163 and MERTK [20] which contribute to phagocytic capacity. This feature allows them to participate in clearing debris and dying cells from the joint space. Although the synovial lining is not a true epithelial barrier, synovial lining macrophages have unique features which allow them to maintain a barrier between the joint space and the sublining capillaries. Specifically, they attach to neighboring cells through desmosomes and tight junctions [19], allowing the lining to maintain the joint space as an immune-privileged site in the healthy state by limiting cellular movement into the joint. In joint disease, this barrier function can become compromised, allowing an influx of inflammatory leukocytes into the joint space and synovial fluid that compromises the integrity of other joint tissues.

Synovial Subintima

Lining vs. Sublining Macrophages

Both the lining and sublining regions contain resident populations of macrophages that are critical to maintaining joint health. The op/op osteopetrotic mouse, which is deficient in macrophages because of an absence of macrophage colony-stimulating factor, also lacks synovial lining macrophages [21], suggesting that type A cells share a common lineage with other tissue macrophages. For many years it was assumed that both lining and sublining macrophages were derived from monocyte precursors from the bone marrow and were replenished from the circulation throughout adulthood. But several new findings have advanced our understanding of synovial macrophage origins and function. In 2019, two reports demonstrated that CX_3CR1^+ embryonic macrophages (ESMs) begin to populate the developing synovium in the mouse early, between day E12.5 and E15 [19, 22]. In contrast, bone-marrow-derived synovial macrophages (BMSMs), characterized by expression of CD11b and Ly6c, are not observed until later, after day 19. Most synovial resident macrophages in the adult mouse appear to be of embryonic origin and express the cytokines IL-4 and IL-10 consistent with an immune regulatory role, while BMSMs preferentially express M1 pro-inflammatory type cytokines such as IL-1β and TNFα [22]. Resident macrophages of the lining (type A synoviocytes) are continuously replenished throughout adulthood from a pool of proliferating $MHCII^+$ sublining resident macrophages, and not from circulating bone-marrow-derived monocytes. The same $MHCII^+$ sublining precursors that give rise to the lining macrophages (type A synoviocytes) also give rise to a population of CX_3CR1^- resident sublining macrophages (Fig. 2.2b). These resident macrophages express resistin-like molecule-α (RELMα) and CD163, associated with alternatively activated (M2) macrophages, and they may be important in limiting pathologic synovial inflammation. The function of synovial macrophages is influenced both by their origin (embryonic vs. bone-marrow/circulation) and their spatial location within the synovium (lining vs. sublining). The specific mechanisms that regulate the differentiation and function of macrophage populations in human disease need further investigation, to determine if specific subgroups can be targeted for therapy.

Subintimal Stromal Cells

The sublining stroma is a highly variable loose connective tissue characterized by a loose collagenous matrix, and populated by fibroblasts which produce the matrix. Mizoguchi et al. [17] identified three distinct populations of human synovial fibroblasts, using cell-surface markers and transcriptomics. In addition to the $CD90^-CD34^-$ lining fibroblasts previously described, they found a population of

sublining $CD90^+CD34^-$ cells that surround blood vessels and capillaries. This population highly expressed RANKL, and promoted osteoclastogenesis in vitro suggesting a role in synovial bone erosion. A third $CD34^+$ fibroblast subset was found to be distributed in the lining and sublining, and in contrast to $CD34^-$ cells, secreted IL-6, CXCL12, and CCL2 in response to TNFα. Thus, this population may promote cellular recruitment driving synovitis. These distinct populations have relevance to OA as well as inflammatory arthritis, as OA lining fibroblasts ($CD90^-CD34^-$) correlated with synovial macrophage content, and sublining ($CD90^+CD34^+$) fibroblasts correlated with synovial T-cell content [23]. Clearly, there is phenotypic heterogeneity of synovial fibroblasts, and single-cell sequencing showed that there was a continuum of fibroblast phenotypes between the synovial sublining and lining [24] suggesting a plasticity in phenotype that needs further elucidation.

Consistent with the common origin of synovium and other joint tissues [9, 11], the synovial stroma is a rich source of mesenchymal stem cells (MSCs) which can give rise to different cell lineages, including chondrocytes, osteoblasts, and adipocytes. Synovial-derived MSCs have a high chondrogenic potential compared to other tissue sources of MSCs [10], consistent with older reports of the importance of synovium in cartilage repair [25]. Bone-marrow (BM) and adipose-derived MSCs have been shown to have potent immunosuppressive effects in vitro on T-lymphocyte responses, and augment T regulatory cell development [26]. The effects on T cells may be due to both cytokine production [27] and mechanisms requiring cell-contact [28], but more work is needed evaluating mechanisms specifically in synovial-derived MSCs. MSCs in synovium increase in arthritis [29, 30], and animal models of joint tissue injury, due to both infiltration from BM sources and local proliferation of resident populations [31]. $CD271^+$ MSCs expanded in arthritis may become pathogenic and lose their immunosuppressive functions [29, 32]. Whether the immunomodulatory function of synovial MSCs can be harnessed for cell-based arthritis therapeutics is under investigation by several groups (reviewed in [33]).

Subintimal Vasculature

The synovial subintimal contains a rich network of vessels and lymphatics which allows for movement of molecules, nutrients, and metabolites into and out of the joint to maintain the health of the avascular articular cartilage. The vasculature of the synovial sublining is most dense closest to the lining layer, and contains highly fenestrated capillaries and venules [8, 34]. In healthy joints, low molecular weight substances diffuse across their concentration gradients. Plasma components and nutrients diffuse through fenestrated capillaries and into the synovial fluid, while low-molecular-weight metabolites produced within the joint are taken up by sublining venules and cleared. Larger molecular weight substances (such as Hyaluronic acid, a key component of synovial fluid) are generally retained in the joint space or cleared much more slowly by the synovial lymphatics [35]. In addition, synovial lymphatics are an important conduit to clear cells from the synovial tissue and fluid that accumulate during chronic inflammation.

Synovial Inflammation in Disease

Synovial Tissue Pathology

As discussed above, tissue macrophages are the most numerous resident leukocytes of the synovium. A small population of resident mast cells are also present in the normal synovium [36] as well as scattered perivascular T lymphocytes [3], but B lymphocytes are rare to nonexistent [37]. The pattern of inflammatory cell content in the sublining region can change drastically in rheumatic diseases, with infiltration by both myeloid and lymphoid cells. Moreover, synovial lining hyperplasia occurs, with increased cell layers, formation of synovial villi, and deposition of fibrin on the lining surface [38]. The sublining vascular density can be either increased or decreased, and the subintima can become fibrotic, particularly in chronic synovitis. Although there is significant overlap in the features of synovial membrane pathology between common rheumatic diseases [39], there are also some features more typical of certain diseases; these are summarized in Table 2.1.

Table 2.1 Features of synovial pathology in different forms of arthritis

Disease	Leukocyte infiltrate	Intimal hyperplasia	Subintimal vascularity	Other typical features
Rheumatoid Arthritis [39–41]	Predominantly lymphocytes (30–50%, T > B cells), macrophages (20–40%); neutrophils <5%	↑↑↑ (≥5 cells thick, but often with 6–8)	↑↑	Large lymphocytic aggregates (w/ germinal centers) in up to 30–50% of patients; synovial pannus that erodes bone
Osteoarthritis [40, 42]	Predominantly macrophages (40–80%); T-lymphocytes (10–30%); B-lymphocytes/plasma cells <10%	↑ (≤4 cells)	↑	Large lymphocytic aggregates are seen but rare
Gout [39, 43, 44]	Slightly higher proportions of neutrophils compared with RA	↑↑ (≥5 cells)		MSU crystals can be seen in synovial tophi and on surface
Spondyloarthritis [41, 45, 46]	Similar to RA, with Greater proportions of neutrophils and mast cells	↑↑ (≥5 cells)	↑↑↑	Large lymphocytic aggregates can be seen occasionally
Septic Arthritis (acute bacterial) [39, 40]	More neutrophils than other diseases (10–20%); macrophages (30–40%); lymphocytes (20–40%, T > B)	↑↑ (≥5 cells)		

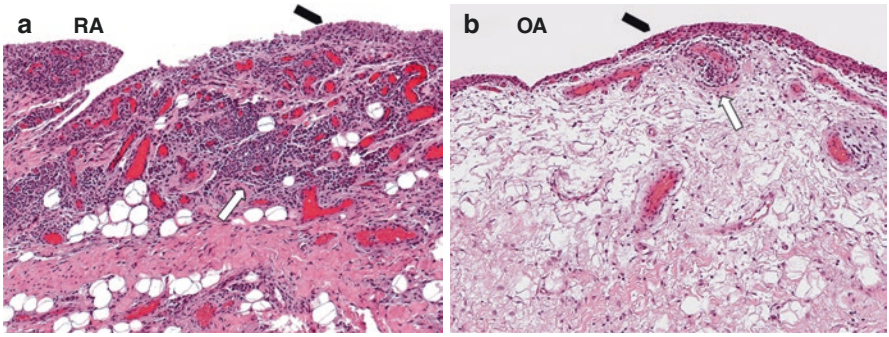

Fig. 2.3 Synovial pathology in (**a**) rheumatoid arthritis and (**b**) osteoarthritis. Varying degrees of synovial lining hyperplasia (black pointers), perivascular lymphocytic infiltrates (white arrows) are shown in both tissues, with increased vascularity exhibited in (**a**). Hematoxylin and eosin stain, 10X. (Images courtesy of E. DiCarlo, MD, Professor of Clinical Pathology, Weill Cornell Medical College and Attending Pathologist, Hospital for Special Surgery)

A number of histopathologic grading systems have been developed to characterize pathologic features of the synovium observed in rheumatic diseases. The most commonly applied histopathology score is that developed by Krenn and colleagues [38, 47], which can discriminate highly inflammatory (i.e., rheumatoid arthritis, Fig. 2.3a) synovium from less inflammatory (i.e. osteoarthritis, Fig. 2.3b) synovial pathology. However, there is considerable overlap, and even low-grade synovitis in OA has clinical relevance as it is associated with severity of symptoms and progression of disease (reviewed in [48]). Routine histopathology has been used to describe distinct "pathotypes" of rheumatoid arthritis synovitis (lympho-myeloid, diffuse myeloid, and pauci-immune), and this classification has shown some promise for predicting responses to available treatments [49]. However, as discussed in the preceding sections, advanced techniques such as single-cell sequencing are revealing distinct patterns of synovial cellular infiltration and activation that may have important implications for prognosis, and predicting responses to therapy. These studies will likely impact clinical trial design for RA treatments in the near future [50], but currently synovial biopsy and pathologic evaluation has limited utility in the clinical setting.

Mechanisms of Cell Homing in Synovitis

The factors that instigate synovitis vary in different rheumatic diseases (i.e., crystals in gouty arthritis, tissue injury in osteoarthritis), and are still not entirely clear in all contexts. What is becoming clear is that the recruitment and retention of inflammatory cells into the synovium is driven by chemokines and adhesion molecules, many of which are produced by activated synovial macrophages, fibroblasts, and endothelial cells (Fig. 2.4). This has been best studied in rheumatoid arthritis. CCL2 (also

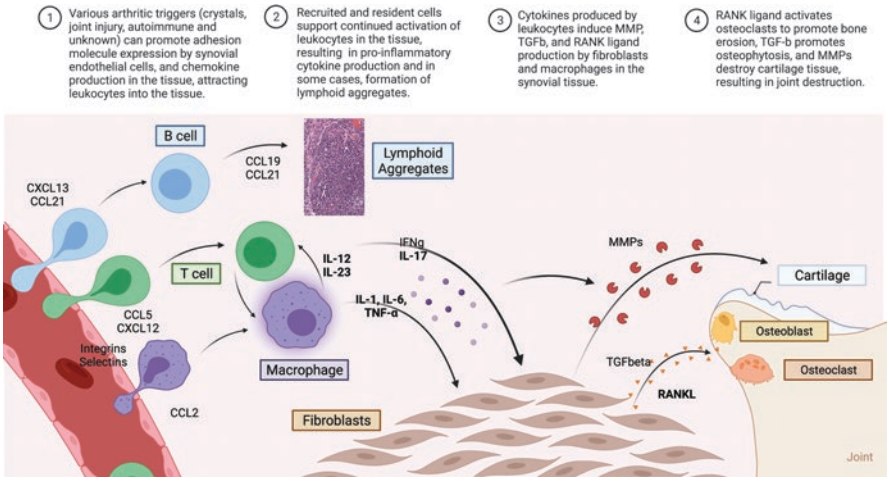

Fig. 2.4 Schematic of the development of synovial inflammation, and its impact on other joint tissues in rheumatic diseases. Molecular mediators in bold type are targets of common biologic therapies used to treat different types of arthritis. (Figure created with BioRender.com. Image of lymphocytic aggregate courtesy of E. DiCarlo, MD, Professor of Clinical Pathology, Weill Cornell Medical College and Attending Pathologist, Hospital for Special Surgery)

known as Monocyte Chemotactic Protein-1, or MCP-1) is an important chemokine that attracts peripheral blood monocytes into the synovium, as well as CD4+ T lymphocytes [51, 52]. CCL5 (Regulated upon Activation, Normal T Cell Expressed and Secreted, or RANTES), and CXCL12 (Stromal Cell Derived Factor-1, or SDF-1) may also drive T-cell recruitment [53–55], and may promote angiogenesis and bone destruction [56]. CCL3 and CCL4 recruit and retain the Th1 T-lymphocyte subset, while CCL20 may support recruitment of Th17 cells. The chemokines CXCL13 and CCL21 drive recruitment and retention of B-lymphocytes and plasma cells, and play an important role in the formation of lymphoid aggregate structures that are observed in up to 20% of patients with RA [57]. Endothelial cells and stromal cells within inflamed synovium express adhesion molecules, including integrins and selectins, which help recruit and retain leukocytes in the tissue [58–60]. Neutrophils make up a large proportion of cells in RA synovial fluid but are not necessarily retained in the tissue. Macrophages and fibroblasts produce neutrophil chemotactic factors such as IL-8 and ENA-78, which are found in high quantities in RA SF [52].

Once chronic synovitis is established, the resident and infiltrating cells produce a wide variety of cytokines, growth factors, and enzymes that contribute to joint damage. Many of these have become well-known targets of arthritis therapy (Fig. 2.4). Infiltrating synovial monocytes and macrophages produce cytokines such as IL-1β, TNFα, and IL-6, which activate synovial fibroblasts, endothelial cells, and lymphocytes to perpetuate synovitis. Successful treatments targeting these "monokines" (cytokines produced primarily by monocytes and macrophages) are in common use for rheumatoid arthritis, spondyloarthritis and gout [61–63]. Synovial

myeloid cells produce IL-12 and 23, which support the differentiation and survival of Th1 and Th17 cell types, respectively. Blockade of IL-12/23 [64], as well as IL-17 [65], has proven successful in treating psoriatic arthritis and spondyloarthritis. In addition, targeting both T lymphocytes (via CTLA4-Ig) and B lymphocytes (via anti-CD20) directly has proven useful in the treatment of inflammatory arthritis. TGF-β, a growth factor produced by synovial macrophages, is linked to osteoblast activation and osteophyte formation in models of osteoarthritis [66]. It is not yet clear whether pharmacologic targeting of this molecule for therapy will be possible. However, inflammatory matrix metalloproteinases produced by synovial macrophages and fibroblasts, including ADAMTS-5, MMP13, and Cathepsin K, are responsible for cartilage matrix damage in OA. Agents selectively targeting ADAMTS5 [67] and Cathepsin K [68] are under development for treatment of OA.

Pathologic Changes to Synovial Vasculature and Lymphatics

Both vascularization of the subintima, as well as clearance of substances from the joint space, can be altered in arthritic diseases. Synovial vascularization can be increased in synovium from patients with OA, but is more marked in RA [34]. Increased synovial doppler signal by ultrasound, a surrogate marker of increased blood flow, is more common in active RA where it is a predictor of disease activity [69]. In RA synovium though, new capillary growth does not meet the needs of the increasing mass of inflamed synovium, contributing to tissue hypoxia and acidification [52]. Despite increased synovial lymphatic vessels [70], lymphatic clearance was shown to be decreased in both OA and RA [71]. An interesting recent report showed that synovial lymphatic function decreases during development of OA in a post-traumatic mouse model, and may be a target for treatment [72]. Whether interventions designed to modulate synovial vascularity or lymphatic function will translate to effective treatments for human disease characterized by synovial inflammation, remains to be seen. But research efforts to understand how to target synovial vasculature for drug delivery to treat synovitis and its consequences are being explored [73].

Summary and Conclusions

The synovial membrane plays several critical roles in the maintenance of joint homeostasis. It provides a permeable barrier between the vasculature and the joint space to allow nutrient and metabolite trafficking, which is central to maintaining the health of the avascular cartilage. Synovial intimal fibroblasts produce key molecular substances (lubricin and hyaluronic acid, among others) that contribute to the functional properties of synovial fluid. These substances maintain adequate shock absorption and lubrication of the joint required for smooth, friction-free articulation during movement. Synovial lining macrophages have the unique ability to

form a barrier between the sublining vasculature and the joint space that prevents cellular egress into the joint space. Available evidence suggests that both lining and sublining resident macrophages in health are skewed toward phenotypes that might serve to limit pathologic inflammation in the synovial tissue. The sublining also contains fibroblasts and mesenchymal stem cells that may contribute to maintaining a non-inflammatory environment. However, in many rheumatic diseases, other leukocytes are recruited to the synovium under the influence of various chemotactic factors, which creates pathologic synovitis that can compromise the function of the synovium. The inflammatory mediators produced by infiltrating cells can influence the function of resident cells, and promote arthritic joint damage. There is a lot of overlap in histopathologic features of synovitis across the spectrum of arthritides. Still there are some features that are more common in certain types of arthritis (Table 2.1). In some diseases synovitis may be a primary cause of joint damage, while in others it may be a consequence of joint damage. Regardless, many of the cellular and molecular products of synovial inflammation have become targets for therapy in various arthritic conditions, while others are under investigation. Modern techniques such as single-cell RNA sequencing are revealing the complexity of cell phenotypes that contribute to the function of the synovium in health and disease, and are providing better insights into the clinical heterogeneity of patients with arthritis and response to arthritis therapies.

References

1. Sokoloff L, Bland JH. The musculoskeletal system. Baltimore: Williams & Wilkins; 1975.
2. Gravallese EM, Smolen JS, van der Heijde D, Weinblatt ME, Weisman MH, Hochberg MC. Rheumatology. 8th ed. Philadelphia: Elsevier; 2021. In press
3. Smith MD. The normal synovium. Open Rheumatol J. 2011;5:100–6.
4. Veale DJ, Firestein GS. Chapter 2: synovium. In: Firestein GS, Budd RC, Gabriel SE, Korestsky GA, McInnes IB, O'Dell JR, editors. Firestein and Kelley's textbook of rheumatology. 11th ed. Philadelphia, PA: Elsevier; 2021. p. 20–33.
5. Dodge GR, Boesler EW, Jimenez SA. Expression of the basement membrane heparan sulfate proteoglycan (perlecan) in human synovium and in cultured human synovial cells. Lab Investig. 1995;73(5):649–57.
6. Schumacher HR. Ultrastructure of the Synovial Membrane. Annals Clin & Lab Sci. 1975;5:489–99.
7. Culemann S, Gruneboom A, Kronke G. Origin and function of synovial macrophage subsets during inflammatory joint disease. Adv Immunol. 2019;143:75–98.
8. Schumacher HR Jr. Ultrastructure of the synovial membrane. Ann Clin Lab Sci. 1975;5(6):489–98.
9. Roelofs AJ, Zupan J, Riemen AHK, Kania K, Ansboro S, White N, et al. Joint morphogenetic cells in the adult mammalian synovium. Nat Commun. 2017;8:15040.
10. Decker RS, Um HB, Dyment NA, Cottingham N, Usami Y, Enomoto-Iwamoto M, et al. Cell origin, volume and arrangement are drivers of articular cartilage formation, morphogenesis and response to injury in mouse limbs. Dev Biol. 2017;426(1):56–68.
11. Shwartz Y, Viukov S, Krief S, Zelzer E. Joint development involves a continuous influx of Gdf5-positive cells. Cell Rep. 2016;15(12):2577–87.

12. Lee DM, Kiener HP, Agarwal SK, Noss EH, Watts GF, Chisaka O, et al. Cadherin-11 in synovial lining formation and pathology in arthritis. Science. 2007;315(5814):1006–10.
13. Valencia X, Higgins JM, Kiener HP, Lee DM, Podrebarac TA, Dascher CC, et al. Cadherin-11 provides specific cellular adhesion between fibroblast-like synoviocytes. J Exp Med. 2004;200(12):1673–9.
14. Abubacker S, Dorosz SG, Ponjevic D, Jay GD, Matyas JR, Schmidt TA. Full-length recombinant human proteoglycan 4 interacts with Hyaluronan to provide cartilage boundary lubrication. Ann Biomed Eng. 2016;44(4):1128–37.
15. Jay GD, Lane BP, Sokoloff L. Characterization of a bovine synovial fluid lubricating factor. III. The interaction with hyaluronic acid. Connect Tissue Res. 1992;28(4):245–55.
16. Stephenson W, Donlin LT, Butler A, Rozo C, Bracken B, Rashidfarrokhi A, et al. Single-cell RNA-seq of rheumatoid arthritis synovial tissue using low-cost microfluidic instrumentation. Nat Commun. 2018;9(1):791.
17. Mizoguchi F, Slowikowski K, Wei K, Marshall JL, Rao DA, Chang SK, et al. Functionally distinct disease-associated fibroblast subsets in rheumatoid arthritis. Nat Commun. 2018;9(1):789.
18. Croft AP, Campos J, Jansen K, Turner JD, Marshall J, Attar M, et al. Distinct fibroblast subsets drive inflammation and damage in arthritis. Nature. 2019;570(7760):246–51.
19. Culemann S, Gruneboom A, Nicolas-Avila JA, Weidner D, Lammle KF, Rothe T, et al. Locally renewing resident synovial macrophages provide a protective barrier for the joint. Nature. 2019;572(7771):670–5.
20. Kurowska-Stolarska M, Alivernini S. Synovial tissue macrophages: friend or foe? RMD Open. 2017;3(2):e000527.
21. Brown NJ, Hutcheson J, Bickel E, Scatizzi JC, Albee LD, Haines GK 3rd, et al. Fas death receptor signaling represses monocyte numbers and macrophage activation in vivo. J Immunol. 2004;173(12):7584–93.
22. Tu J, Hong W, Guo Y, Zhang P, Fang Y, Wang X, et al. Ontogeny of synovial macrophages and the roles of synovial macrophages from different origins in arthritis. Front Immunol. 2019;10:1146.
23. Labinsky H, Panipinto PM, Ly KA, Khuat DK, Madarampalli B, Mahajan V, et al. Multiparameter analysis identifies heterogeneity in knee osteoarthritis synovial responses. Arthritis Rheumatol. 2020;72(4):598–608.
24. Wei K, Korsunsky I, Marshall JL, Gao A, Watts GFM, Major T, et al. Notch signalling drives synovial fibroblast identity and arthritis pathology. Nature. 2020;582(7811):259–64.
25. Hunziker EB, Rosenberg LC. Repair of partial-thickness defects in articular cartilage: cell recruitment from the synovial membrane. J Bone Joint Surg Am. 1996;78(5):721–33.
26. De Bari C. Are mesenchymal stem cells in rheumatoid arthritis the good or bad guys? Arthritis Res Ther. 2015;17:113.
27. Krampera M, Cosmi L, Angeli R, Pasini A, Liotta F, Andreini A, et al. Role for interferon-gamma in the immunomodulatory activity of human bone marrow mesenchymal stem cells. Stem Cells. 2006;24(2):386–98.
28. Luz-Crawford P, Hernandez J, Djouad F, Luque-Campos N, Caicedo A, Carrere-Kremer S, et al. Mesenchymal stem cell repression of Th17 cells is triggered by mitochondrial transfer. Stem Cell Res Ther. 2019;10(1):232.
29. Del Rey MJ, Fare R, Usategui A, Canete JD, Bravo B, Galindo M, et al. CD271(+) stromal cells expand in arthritic synovium and exhibit a proinflammatory phenotype. Arthritis Res Ther. 2016;18:66.
30. Sekiya I, Ojima M, Suzuki S, Yamaga M, Horie M, Koga H, et al. Human mesenchymal stem cells in synovial fluid increase in the knee with degenerated cartilage and osteoarthritis. J Orthop Res. 2012;30(6):943–9.
31. Sergijenko A, Roelofs AJ, Riemen AH, De Bari C. Bone marrow contribution to synovial hyperplasia following joint surface injury. Arthritis Res Ther. 2016;18:166.

32. Lee HJ, Lee WJ, Hwang SC, Choe Y, Kim S, Bok E, et al. Chronic inflammation-induced senescence impairs immunomodulatory properties of synovial fluid mesenchymal stem cells in rheumatoid arthritis. Stem Cell Res Ther. 2021;12(1):502.
33. Lopez-Santalla M, Bueren JA, Garin MI. Mesenchymal stem/stromal cell-based therapy for the treatment of rheumatoid arthritis: an update on preclinical studies. EBioMedicine. 2021;69:103427.
34. Haywood L, Walsh DA. Vasculature of the normal and arthritic synovial joint. Histol Histopathol. 2001;16(1):277–84.
35. Doan TN, Bernard FC, McKinney JM, Dixon JB, Willett NJ. Endothelin-1 inhibits size dependent lymphatic clearance of PEG-based conjugates after intra-articular injection into the rat knee. Acta Biomater. 2019;93:270–81.
36. Dean G, Hoyland JA, Denton J, Donn RP, Freemont AJ. Mast cells in the synovium and synovial fluid in osteoarthritis. Br J Rheumatol. 1993;32(8):671–5.
37. Singh JA, Arayssi T, Duray P, Schumacher HR. Immunohistochemistry of normal human knee synovium: a quantitative study. Ann Rheum Dis. 2004;63(7):785–90.
38. Krenn V, Morawietz L, Haupl T, Neidel J, Petersen I, Konig A. Grading of chronic synovitis--a histopathological grading system for molecular and diagnostic pathology. Pathol Res Pract. 2002;198(5):317–25.
39. Goldenberg DL, Cohen AS. Synovial membrane histopathology in the differential diagnosis of rheumatoid arthritis, gout, pseudogout, systemic lupus erythematosus, infectious arthritis and degenerative joint disease. Medicine (Baltimore). 1978;57(3):239–52.
40. Della Beffa C, Slansky E, Pommerenke C, Klawonn F, Li J, Dai L, et al. The relative composition of the inflammatory infiltrate as an additional tool for synovial tissue classification. PLoS One. 2013;8(8):e72494.
41. Baeten D, Demetter P, Cuvelier C, Van Den Bosch F, Kruithof E, Van Damme N, et al. Comparative study of the synovial histology in rheumatoid arthritis, spondyloarthropathy, and osteoarthritis: influence of disease duration and activity. Ann Rheum Dis. 2000;59(12):945–53.
42. Krenn V, Perino G, Ruther W, Krenn VT, Huber M, Hugle T, et al. 15 years of the histopathological synovitis score, further development and review: a diagnostic score for rheumatology and orthopaedics. Pathol Res Pract. 2017;213(8):874–81.
43. Schumacher HR. Pathology of the synovial membrane in gout. Light and electron microscopic studies. Interpretation of crystals in electron micrographs. Arthritis Rheum. 1975;18(6 Suppl):771–82.
44. Towiwat P, Chhana A, Dalbeth N. The anatomical pathology of gout: a systematic literature review. BMC Musculoskelet Disord. 2019;20(1):140.
45. Canete JD, Celis R, Noordenbos T, Moll C, Gomez-Puerta JA, Pizcueta P, et al. Distinct synovial immunopathology in Behcet disease and psoriatic arthritis. Arthritis Res Ther. 2009;11(1):R17.
46. van de Sande MG, Baeten DL. Immunopathology of synovitis: from histology to molecular pathways. Rheumatology (Oxford). 2016;55(4):599–606.
47. Krenn V, Morawietz L, Burmester GR, Kinne RW, Mueller-Ladner U, Muller B, et al. Synovitis score: discrimination between chronic low-grade and high-grade synovitis. Histopathology. 2006;49(4):358–64.
48. Scanzello CR. Role of low-grade inflammation in osteoarthritis. Curr Opin Rheumatol. 2017;29(1):79–85.
49. Nerviani A, Di Cicco M, Mahto A, Lliso-Ribera G, Rivellese F, Thorborn G, et al. A Pauci-immune synovial Pathotype predicts inadequate response to TNFalpha-blockade in rheumatoid arthritis patients. Front Immunol. 2020;11:845.
50. Lakhanpal A, Smith MH, Donlin LT. Rheumatology in the era of precision medicine: synovial tissue molecular patterns and treatment response in rheumatoid arthritis. Curr Opin Rheumatol. 2021;33(1):58–63.

51. Moadab F, Khorramdelazad H, Abbasifard M. Role of CCL2/CCR2 axis in the immunopathogenesis of rheumatoid arthritis: latest evidence and therapeutic approaches. Life Sci. 2021;269:119034.
52. Firestein GS. Chapter 75: Pathogenesis of rheumatoid arthritis. In: Firestein GS, Budd RC, Gabriel SE, Korestsky GA, IB MI, O'Dell JR, editors. Firestein and kelley's textbook of rheumatology. 11th ed. Philadelphia, PA: Elsevier; 2021. p. 1200–35.
53. Stanczyk J, Kowalski ML, Grzegorczyk J, Szkudlinska B, Jarzebska M, Marciniak M, et al. RANTES and chemotactic activity in synovial fluids from patients with rheumatoid arthritis and osteoarthritis. Mediat Inflamm. 2005;2005(6):343–8.
54. Kanbe K, Chiba J, Inoue Y, Taguchi M, Yabuki A. SDF-1 and CXCR4 in synovium are associated with disease activity and bone and joint destruction in patients with rheumatoid arthritis treated with golimumab. Mod Rheumatol. 2016;26(1):46–50.
55. Nagafuchi Y, Shoda H, Sumitomo S, Nakachi S, Kato R, Tsuchida Y, et al. Immunophenotyping of rheumatoid arthritis reveals a linkage between HLA-DRB1 genotype, CXCR4 expression on memory CD4(+) T cells, and disease activity. Sci Rep. 2016;6:29338.
56. Pablos JL, Santiago B, Galindo M, Torres C, Brehmer MT, Blanco FJ, et al. Synoviocyte-derived CXCL12 is displayed on endothelium and induces angiogenesis in rheumatoid arthritis. J Immunol. 2003;170(4):2147–52.
57. Manzo A, Paoletti S, Carulli M, Blades MC, Barone F, Yanni G, et al. Systematic microanatomical analysis of CXCL13 and CCL21 in situ production and progressive lymphoid organization in rheumatoid synovitis. Eur J Immunol. 2005;35(5):1347–59.
58. Klimiuk PA, Sierakowski S, Latosiewicz R, Cylwik JP, Cylwik B, Skowronski J, et al. Soluble adhesion molecules (ICAM-1, VCAM-1, and E-selectin) and vascular endothelial growth factor (VEGF) in patients with distinct variants of rheumatoid synovitis. Ann Rheum Dis. 2002;61(9):804–9.
59. Salmi M, Rajala P, Jalkanen S. Homing of mucosal leukocytes to joints. Distinct endothelial ligands in synovium mediate leukocyte-subtype specific adhesion. J Clin Invest. 1997;99(9):2165–72.
60. Kriegsmann J, Keyszer GM, Geiler T, Lagoo AS, Lagoo-Deenadayalan S, Gay RE, et al. Expression of E-selectin messenger RNA and protein in rheumatoid arthritis. Arthritis Rheum. 1995;38(6):750–4.
61. Mysler E, Caubet M, Lizarraga A. Current and emerging DMARDs for the treatment of rheumatoid arthritis. Open Access Rheumatol. 2021;13:139–52.
62. Sepriano A, Ramiro S, van der Heijde D, Landewe R. Biological DMARDs and disease modification in axial spondyloarthritis: a review through the lens of causal inference. RMD Open. 2021;7(2).
63. Schlesinger N. Canakinumab in gout. Expert Opin Biol Ther. 2012;12(9):1265–75.
64. Ritchlin C, Rahman P, Kavanaugh A, McInnes IB, Puig L, Li S, et al. Efficacy and safety of the anti-IL-12/23 p40 monoclonal antibody, ustekinumab, in patients with active psoriatic arthritis despite conventional non-biological and biological anti-tumour necrosis factor therapy: 6-month and 1-year results of the phase 3, multicentre, double-blind, placebo-controlled, randomised PSUMMIT 2 trial. Ann Rheum Dis. 2014;73(6):990–9.
65. Boutet MA, Nerviani A, Gallo Afflitto G, Pitzalis C. Role of the IL-23/IL-17 axis in psoriasis and psoriatic arthritis: the clinical importance of its divergence in skin and joints. Int J Mol Sci. 2018;19(2).
66. Scharstuhl A, Glansbeek HL, van Beuningen HM, Vitters EL, van der Kraan PM, van den Berg WB. Inhibition of endogenous TGF-beta during experimental osteoarthritis prevents osteophyte formation and impairs cartilage repair. J Immunol. 2002;169(1):507–14.
67. Brebion F, Gosmini R, Deprez P, Varin M, Peixoto C, Alvey L, et al. Discovery of GLPG1972/S201086, a potent, selective, and orally bioavailable ADAMTS-5 inhibitor for the treatment of osteoarthritis. J Med Chem. 2021;64(6):2937–52.

68. Conaghan PG, Bowes MA, Kingsbury SR, Brett A, Guillard G, Rizoska B, et al. Disease-modifying effects of a novel Cathepsin K inhibitor in osteoarthritis: a randomized controlled trial. Ann Intern Med. 2020;172(2):86–95.
69. Naredo E, Collado P, Cruz A, Palop MJ, Cabero F, Richi P, et al. Longitudinal power Doppler ultrasonographic assessment of joint inflammatory activity in early rheumatoid arthritis: predictive value in disease activity and radiologic progression. Arthritis Rheum. 2007;57(1):116–24.
70. Xu H, Edwards J, Banerji S, Prevo R, Jackson DG, Athanasou NA. Distribution of lymphatic vessels in normal and arthritic human synovial tissues. Ann Rheum Dis. 2003;62(12):1227–9.
71. Bell RD, Rahimi H, Kenney HM, Lieberman AA, Wood RW, Schwarz EM, et al. Altered lymphatic vessel anatomy and markedly diminished lymph clearance in affected hands of patients with active rheumatoid arthritis. Arthritis Rheumatol. 2020;72(9):1447–55.
72. Wang W, Lin X, Xu H, Sun W, Bouta EM, Zuscik MJ, et al. Attenuated joint tissue damage associated with improved synovial lymphatic function following treatment with Bortezomib in a mouse model of experimental posttraumatic osteoarthritis. Arthritis Rheumatol. 2019;71(2):244–57.
73. Yang YH, Rajaiah R, Ruoslahti E, Moudgil KD. Peptides targeting inflamed synovial vasculature attenuate autoimmune arthritis. Proc Natl Acad Sci U S A. 2011;108(31):12857–62.

Chapter 3
Arthrocentesis

Kenneth S. O'Rourke

Arthrocentesis and soft tissue aspiration and injection are critically important skills in the bedside evaluation and management of patients with rheumatic disease. This chapter will focus primarily on the common technical aspects, as procedural competence applicable to all these skills is grounded in an understanding of basic principles. *Content will be presented in an order analogous to the typical, sequential palpation-guided procedural steps*.

A description of the procedural details specific for individual joints and soft tissues is beyond the scope of this chapter; the reader is directed to a visual review [1]. Outside of the mandatory requirement for the use of sterile equipment, a skin antiseptic, and aseptic practice, there are options in equipment choice, medications, and technique that lead to innumerable practice variations. As has been simply stated, "the number of rheumatologists doing procedures equals the number of different ways of performing them." [2].

Indications and Contraindications

The indications for *aspiration* of a joint or soft tissue site include to exclude infection, resolve diagnostic uncertainty (e.g., search for crystals, separate inflammatory from noninflammatory etiologies, evaluate adjoining sites for communication), and to provide for therapeutic decompression. Indications for *injection* include to similarly resolve diagnostic uncertainty (e.g., injection of anesthetic), deliver a therapeutic substance, or to irrigate (e.g., tidal joint irrigation).

Other than needle passage through an overlying purulent ulcer/cellulitis or disrupted skin that may harbor bacteria (e.g., psoriatic plaque), there is no absolute

K. S. O'Rourke (✉)
Division of Rheumatology, Maine Medical Center, Portland, ME, USA

B. F. Mandell (ed.), *Synovial Fluid Analysis and The Evaluation of Patients With Arthritis*, https://doi.org/10.1007/978-3-030-99612-3_3

Table 3.1 Contraindications to joint aspiration or injection

Absolute contraindications for joint aspiration or injection:
Needle passage through an overlying purulent ulcer/cellulitis or disrupted skin that may harbor bacteria (e.g., psoriatic plaque)
Relative contraindications to intra-articular corticosteroid injections:
Unstable joint
Intra-articular fracture
Avascular necrosis
Known drug hypersensitivity
Poor response to previous injections (injections required more frequently than every 3 months)
Poorly controlled diabetes
Significant coagulopathy

contraindication for joint aspiration or injection. However, unavoidable needle tracking through an area of periarticular erythema should not prevent arthrocentesis in the setting of probable septic arthritis, because the risk of introducing an infection into the joint is far less than the potential harm of undiagnosed joint infection [3]. Due to the possibility of an unsuspected septic arthritis, any joint considered for corticosteroid injection should have synovial fluid—if aspirated—sent for culture. Contraindications for joint aspiration or injection and relative contraindications for intra-articular corticosteroid injection are outlined in Table 3.1.

Prosthetic Joint A prosthetic joint should be aspirated when there is a concern for infection. Proposed threshold levels of synovial fluid total white blood cell count that support a high likelihood of a septic artificial joint (e.g., 1700 cells/mm^3 for the knee [4], 4200 cells/mm^3 for the hip [5]) are based on prospective studies, considerably lower than analogous threshold white blood cell levels in synovial fluid from a native joint.

Pregnancy Pregnancy is *not* a contraindication to corticosteroid injection. Fluorinated steroids can cross the placenta, but prednisolone is inactivated by placental type 2 11-beta-hydroxysteroid dehydrogenase [6]. Corticosteroid injection in a pregnant patient is therefore best performed using a nonfluorinated steroid (e.g., methylprednisolone) to minimize fetal exposure.

Concurrent Anticoagulation Concurrent treatment with an anticoagulant is also not a contraindication to arthrocentesis. Two small prospective studies suggest that joint or soft tissue injection and aspirations are of low risk in patients receiving warfarin with international normalization ratio (INR) <3.7 and not receiving a nonsteroidal anti-inflammatory drug [7, 8]. This was further supported by a large, retrospective review [9] of 640 arthrocentesis (knees, shoulders, hips) in 514 consecutive patients, all receiving long-term warfarin noting no differences observed in clinically significant bleeding (early or late), late joint infection, or joint pain that caused

a subsequent physician visit, between those whose INR was ≥2 during the entire periprocedural period and those for whom warfarin was held for 3–5 days and the INR was <2. The safety of arthrocentesis in patients on direct oral anticoagulants was also confirmed in a single-site, retrospective study of 1050 consecutive arthrocentesis/joint injection procedures (483 unique patients) revealing no bleeding complications [10]. In general, prudence dictates that arthrocentesis in an anticoagulated patient be performed using the smallest gauge needle adequate to perform the task with careful attention to proper needle position to minimize tissue trauma. Post-procedure pressure over the needle puncture site, compression bandage, and/or ice may be required to reduce the risk of excessive bleeding.

Informed Consent

The informed consent process is mandatory, and should include a discussion of the indication(s), sequential steps, potential benefits, and risks. Local policies vary as to the required type of documentation of this discussion.

Arthrocentesis and soft tissue injections are typically safe when performed with the appropriate tools and techniques. The risk of inducing a septic arthritis with arthrocentesis is rare when using aseptic practice. The most common procedural risk of arthrocentesis is associated with intra-articular steroid injection, specifically a post-injection flare thought to be due to a steroid crystalline synovitis. Symptoms in this setting occur within a few hours and may last as long as 48–72 hours after the injection. Table 3.2 summarizes the risks associated with arthrocentesis including those associated with corticosteroid injection.

Table 3.2 Risks of arthrocentesis

Risk	Estimated rate, %	Comments
Post-injection flare	2–15%	Due to steroid crystalline synovitis Symptoms start within hours, may last 48–72 hours
Steroid arthropathy	<1%	Instability of weight-bearing joints following excessive injections, secondary to avascular necrosis Based on subprimate animal studies and anecdotal case reports Primate models show no deleterious effects
Septic arthritis	~0.002%	Onset usually delayed 3–4 days after injection Estimated rate based primarily on retrospective reviews
Hypothalamic-pituitary axis suppression	Variable	Usually with large corticosteroid total mg injected, or multijoint injections Evidenced by improvement of noninjected joints, transient eosinophilia, increased plasma 17-hydroxycorticosteroids, decreased plasma cortisol, transient worsening of serum glucose control

(continued)

Table 3.2 (continued)

Risk	Estimated rate, %	Comments
Tendon rupture	<1% (hands/wrists) Up to 10% (Achilles, plantar fascia)	Case reports Avoided by: Using small-gauge needles that disallow plunger depression when needle tip is intra-tendinous Gently filling tendon sheaths
Cutaneous atrophy	<1–8%	Onset 1–4 months after corticosteroid injection; may improve over a few months or persist
Depigmentation	<1–5%	Onset 1–2 months after corticosteroid injection; may improve over months/year or persist Higher risk of depigmentation with fluorinated (poorly soluble) steroids
Flushing	1–15%	Face, neck, trunk Onset 2–36 hours after corticosteroid injection; may last minutes to days Higher risk with triamcinolone products
Capsular calcification	Unknown/rare	Mainly corticosteroid interphalangeal joint injections May be delayed (1–2 years) Asymptomatic
Bleeding	Unknown/rare	In patients at risk, minimized by proper needle position to minimize tissue trauma, and post-procedure pressure over the needle puncture site, compression bandage, and/or ice
Hypersensitivity reactions	Rare	Case report [11]
Vasovagal syncope	Unknown	Minimized with supine positioning
Cartilage/nerve damage	Unknown	With inappropriately long needles and/or rapid needle insertion
Livedoid dermatitis	Rare	Case report [12]

Mandatory Requirements: Skin Antiseptic, Sterile Equipment, Aseptic Practice

There are only three mandatory performance requirements for safe procedural practice: use of a skin antiseptic, sterile equipment, and aseptic practice. Even within these three steps there is room for considerable variation in individual practice.

Skin Antiseptic The traditional choices for skin antisepsis are topical alcohol, iodine, and chlorhexidine. Table 3.3 summarizes their advantages and disadvantages.

Sterile Equipment A selection of variously sized sterile, disposable syringes and needles should be immediately available. The syringe size choice is based on the size of the effusion to aspirate, the amount of injectate to instill, and/or the size of the potential target site, be it intra-articular or extra-articular (e.g., tendon sheath,

Table 3.3 Skin antiseptics [13–15]

Antiseptic	Advantage	Disadvantage
Alcohol (isopropyl pad "swipe")	Inexpensive Results in rapid, large decrease in skin flora	No detergent action, thus less effective on "dirty" skin Dries clear, reducing visual recognition of application extent
Iodine (e.g., povidone iodine topical)	Broad antibacterial spectrum Color on skin demarcates cleansed area	Must dry on skin for 1–2 minutes to obtain full advantage of the sustained iodine release (iodophors: water-soluble complexes of iodine bound to a carrier)
Chlorhexidine topical (e.g., chlorhexidine gluconate)	Binds to skin and provides a residual activity Broad antibacterial spectrum	Higher cost Dries clear, reducing visual recognition of application extent
Hexachlorophene topical	Effective against gram-positive bacteria	Does not kill gram-negative bacteria nor fungi Can be absorbed Can be toxic

peri-neural). Always "break" the seal on a syringe before use by pulling back on the plunger fully, then pushing it down fully. Needle length and gauge should reflect the size and depth of the intended target and whether the procedural intent is for injection only or aspiration and injection (Table 3.4). Smaller-gauge needles (25-gauge and smaller), when inadvertently placed in a tendon or ligament will not allow for depression of the syringe's plunger, providing a negative feedback mechanism and reducing the likelihood of intra-tendinous injection.

Additional equipment to have available would include a (1) tube for synovial fluid cell count (liquid anticoagulant, as undissolved powder may interfere with crystal evaluation; ethylenediaminetetraacetic acid [EDTA] as an anticoagulant is preferred over lithium heparin, as the latter may form crystals), (2) sterile container for synovial fluid culture, (3) sterile hemostat (when clamped to an inserted needle, will facilitate loosening tightly applied syringes off the needle should the procedure require interchanging syringes), (4) sterile gauze and adhesive bandages, (5) slides, cover slips, and nail polish (to seal edges of cover slip, to prevent drying for viewing of synovial fluid later). An optional 3-way stopcock may be considered for single-needle-insertion aspiration then injection without breaking needle-syringe continuity (re-sterility, and to avoid fluid running out the end of needle hub between syringe exchanges) [16].

Aseptic Practice Gloves are necessary under the practice of universal precautions, and in the United States are mandated by the Occupational Safety and Health Administration (OSHA; standard number 1910.1030). Gloves do not have to be sterile if a "no-touch" procedure is used following skin antisepsis, and come in latex-free style for patients with latex hypersensitivity. The use of masks, eye protection, and drapes are not necessary unless there is a risk of splash.

Table 3.4 Needle size and suggested use

Gauge	Diameter size, mm	Generally available lengths, inches	Suggested for local anesthesia, tendon sheath or peri-neural injection, or joint injection *without* aspiration	Suggested for joint aspiration
18	1.2	1, 1.5		+
20	0.90	1, 1.5		+
21	0.80	1, 1.5, 2		+
22	0.70	1, 1.5, 3.5[a]		Possibly too small to ensure successful aspiration
23	0.60	3/4, 1, 1.25	Possibly too large for patient comfort and/or safety	Consider only in small joints[b]
25[c]	0.50	5/8, 7/8, 1, 1.5	+	Consider only in small joints[b]
26[c]	0.45	3/8, 1/2	+	
27[c]	0.40	1/2, 1.25, 1.5	+	
30[c]	0.30	1/2, 1	+	

[a] Spinal needle, useful primarily for deep injections (e.g., hip joint, trochanteric bursa)
[b] Diagnostic aspirate may be limited to amount in the needle hub
[c] The tip of a 25-gauge or smaller diameter needle, when inadvertently placed in a tendon or ligament, will not allow for depression of the syringe's plunger, providing a negative feedback mechanism

Everything Else Is Optional: Anesthesia, Injectate, Technique

Local Anesthesia There is considerable variation among practitioners in the use of local anesthetics in adult patients, both prior to planned injection, as well as for their potential use when mixed with a corticosteroid as part of the joint or soft tissue injectate. Local anesthesia (Table 3.5) in adults may allow for improved needle localization with better patient tolerance when the target is a deformed joint or soft tissue area wherein the need for redirecting the initial needle track approach may be more likely. Local anesthesia may also provide 1–2 hours of post-procedure pain relief and may reduce the overall pain of the entire procedure [17]. Justifications for eschewing the regular use of pre-procedural local anesthesia in adults, irrespective of anesthetic delivery method (e.g., refrigerant spray, topical anesthetic cream, or injectable solution), include: minor patient discomfort associated with the procedure in well-trained hands, the added pain that may be associated with an injectable anesthetic, the risk that a bactericidal anesthetic (e.g., lidocaine) inadvertently introduced into synovial fluid may contaminate subsequent synovial fluid culture, and the time delay associated with pre-procedure anesthesia.

Locally injectable anesthetics may themselves elicit pain during instillation. Pain from an injected anesthetic may be due to tissue expansion (rapid high-volume expansion is more painful), the structure of the anesthetic (the ester procaine is less

Table 3.5 Commonly used local anesthetics

Compound (concentrations)	Pharmacology	Comments
Ethyl chloride topical (100%) fine spray	Anesthesia from rapid cooling (5-second spray can reduce skin temperature to 5 °C–10 °C)	May have an antimicrobial effect [21] although not seen with jet spray [22] Endpoint for application is skin frosting (generally ≤10 seconds) Insufficient analgesic effect in deep tissues
Procaine solution (1%, 2%)	An ester Lasts 2–3 hours	Less painful than lidocaine Out of favor due to frequent hypersensitivity reactions to ester compounds (most commonly from PABA, an ester metabolite)
Lidocaine solution (0.5%, 1%, 2%)	An amide Lasts 1–2 hours No cross-reactivity to ester class anesthetics Bactericidal	*To buffer doses of 1% to 2% lidocaine*: 1 mL of 8.4% sodium bicarbonate to 9 mL lidocaine 5 mL of 4.3% sodium bicarbonate to 30 mL lidocaine
Bupivacaine solution (0.25%, 0.5%)	An amide Lasts 2–5 hours 4 times as potent as lidocaine	*To buffer doses of 0.25% bupivacaine*: 1 mL of 8.4% sodium bicarbonate to 90 mL bupivacaine
Diphenhydramine solution (1%)	Shorter acting than lidocaine	More painful than lidocaine May cause a local skin reaction May be sedating *For 1% solution*: 50 mg of parenteral diphenhydramine (1 mL of standard 5% parenteral solution) with 4 mL sterile normal saline
Lidocaine-prilocaine topical cream (2.5%/2.5%)	Topical cream or disc	Must apply to skin puncture site 30–60 minutes prior

PABA para-aminobenzoic acid

painful than amide lidocaine), its temperature (warming a refrigerated solution will reduce pain with injection), and/or its acidity [18, 19]. Anesthetics are commonly pH ~ 5–7, made acidic to extend shelf life and promote solubility (lidocaine premixed with epinephrine has a pH ~ 3.3–5.5 in order to maintain epinephrine stability in solution). Buffering an anesthetic solution, particularly amides (lidocaine or bupivacaine) with sodium bicarbonate (Table 3.6) can reduce pain with instillation [20]. Buffering does not affect the efficacy of epinephrine in a premixed solution, does not precipitate the anesthetic, and does not reduce the anesthetic effect for up to 1 week at room temperature and 2 weeks in refrigerated storage [20].

Mixing an anesthetic with a corticosteroid for joint or soft tissue injection is optional. Such a mixture can dilute the corticosteroid concentration to minimize local adverse effects during extra-articular injections, deliver the corticosteroid over a larger area, break up adhesions due to larger-volume injectate during intra-articular

Table 3.6 Possible sequences of joint or soft tissue injection

1. Double needle serial insertion: Injection of a local anesthetic is followed by instillation of the injectate (e.g., corticosteroid alone or mixed with anesthetic) at the target using a separate needle and syringe
2. Single needle insertion: Injectate (e.g., corticosteroid alone or mixed with anesthetic) is directly injected at the target without prior injectable local anesthesia)
3. Single needle insertion beginning with the injection of an anesthetic solution, followed by stabilization of the needle (using sterile glove or hemostat), removal of the syringe, and replacement with a syringe prefilled with injectate for instillation
4. Single needle insertion using the following additional hardware: 2 syringes connected by a 3-way stopcock [16] 2 syringes connected by a reciprocating syringe mechanism for single-handed operation [24]

use, and may reduce the pain from corticosteroid-induced synovitis. However, large-volume anesthetic instillation increases the risk of muscle weakness during soft tissue injections adjacent to motor nerves. Flocculation in the syringe may occur with mixing, the result of precipitating the corticosteroid with the preservative (commonly methylparaben) in the anesthetic, and is more commonly observed with methylprednisolone than with other steroids. Although the clinical outcome of this interaction is not proven to interfere with potential efficacy of the corticosteroid, flocculation can be avoided by using a preservative-free anesthetic.

For those with latex allergy, remove the rubber stopper on a lidocaine bottle before removing liquid.

Injection Technique There are a variety of possible sequences of joint or soft tissue injection following skin cleansing (Table 3.6). These involve double needle insertions and single needle insertions. One technique involves the use of a reciprocating syringe, which allows the index and middle fingers to stay in position while the thumb moves to the alternative plunger to change between aspiration and injection [23]. The reciprocating syringe may reduce procedural-related pain, shorten the procedure time, and improve physician satisfaction/performance of arthrocentesis [23, 24].

Joint aspiration should be performed prior to instillation of corticosteroids. Aspiration of a large effusion may itself be pain relieving, and in the knee may alone improve muscle activation [25, 26]. Two studies note improved clinical response with draining of effusion prior to steroid injection [27, 28].

Injectate

There are a wide variety of reported agents used for intra-articular and soft tissue injection.

Corticosteroids Corticosteroids are the most commonly used medications for joint and soft tissue injection (Table 3.7). Steroids used for injection are less soluble than

Table 3.7 Commonly used corticosteroids for joint and soft tissue injection [30, 31]

Corticosteroid	Solubility, % weight/volume	Available concentrations, mg/mL	Relative anti-inflammatory potency	Equivalent dose, mg
Nonfluorinated				
Hydrocortisone acetate	0.002	25, 50	1	20
Methylprednisolone acetate	0.001	20, 40, 80	5	4
Prednisolone tebutate	0.001	20	4	5
Fluorinated				
Betamethasone sodium phosphate/acetate	NA	3	25	0.75
Dexamethasone sodium phosphate	0.01	4, 10	25	0.75
Triamcinolone acetonide	0.004	10, 40	5	4
Triamcinolone diacetate	(data unavailable)	40	5	4
Triamcinolone hexacetonide	0.0002	5, 20	5	4

NA not applicable

hydrocortisone and thus provide a relative depot source for prolonged anti-inflammatory action. However, with reduced solubility comes a higher risk for local adverse effects, particularly with injections into nonencapsulated (soft tissue) sites and/or superficial areas, including skin depigmentation and subcutaneous fat atrophy [29].

Nonfluorinated corticosteroids are more soluble than fluorinated products (Table 3.7) and thus are preferred, in general, for soft tissue injections to minimize local toxicity. Fluorinated corticosteroids (e.g., triamcinolone products) are the least soluble injectable corticosteroids and are preferred for intra-articular injections, as the joint capsule will help to reduce the spread of the medication into periarticular tissues, reducing the risk of local adverse effects, and their lower solubility prolongs the anti-inflammatory effect [30]. The suggested corticosteroid injectate volume varies based on the injection site and the product used (Table 3.8).

Viscosupplements Viscosupplementation refers to the intra-articular injection of hyaluronic acid derivatives (Table 3.9). Products vary according to molecular weight and suggested frequency of injections. Injections should be performed with a needle gauge sufficiently large (e.g., 21-gauge) to avoid damaging the product during instillation and should not be mixed in the same syringe with an anesthetic. Depending on the specific product used, viscosupplementation has been associated with post-injection joint pain in up to 25% of patients. Uncommon post-injection acute painful effusions (synovial white blood cell counts up to 100,000 cells/mm^3) have been reported [32]. Acute effusions typically start within hours of the injection and generally last several hours. There are isolated reports of acute gout and pseudogout after hyaluronic acid injections.

Table 3.8 Suggested corticosteroid injectate volumes for selected joint and soft tissue injections

Adult joint	**Triamcinolone product, mg**	**Total volumes, mL (steroid + anesthetic)**
Knee	40–80	Up to 10
Ankle	20–40	1–5
Shoulder	20–40	Up to 10
Elbow	20–40	1–5
Wrist	20	1–3
Subtalar	20–30	1–5
CMC/IP/MCP/MTP	5–10	0.25–2
Adult bursa	**Methylprednisolone acetate[a], mg**	**Total volumes, mL (steroid + anesthetic)**
Subacromial	20–40	Up to 10
Greater trochanter	20–40	Up to 10
Pes anserine	10–20	1–5 mL

CMC carpometacarpal, *IP* interphalangeal, *MCP* metacarpophalangeal, *MTP* metatarsophalangeal
[a] Representative of a nonfluorinated corticosteroid for extra-articular/soft tissue injections

Table 3.9 Viscosupplements used in the treatment of knee osteoarthritis [33–36]

Viscosupplement (proprietary name)	Supplied	Dose (following joint aspiration)
Hexadecylamide hyaluronan (Hymovis)	24 mg/3 ml	24 mg weekly ×2
High-MW hyaluronan (Orthovisc)	30 mg/2 ml syringe	30 mg weekly ×3–4
Hylan gel-fluid 20 (Synvisc; Synvisc-one)	16 mg/2 ml; 48 mg/6 ml	16 mg weekly ×3; 48 mg ×1
Hyaluronan hydrogel (gel-one)	30 mg/3 ml	30 mg ×1
Sodium hyaluronate (Euflexa)	20 mg/2 ml	20 mg weekly ×3
Sodium hyaluronate (Hyalgan)	20 mg/2 ml	20 mg weekly ×5
Sodium hyaluronate (Supartz)	25 mg/2.5 ml	25 mg weekly ×5
Sodium hyaluronate (Monovisc)	88 mg/4 ml	88 mg ×1
Sodium hyaluronate (GelSyn-3)	16.8 mg/2 ml	16.8 mg weekly ×3
Sodium hyaluronate (Genvisc 850)	25 mg/2.5 ml	25 mg weekly ×5
Sodium hyaluronate (TriVisc)	25 mg/3 ml	25 mg weekly ×3
Sodium hyaluronate (Visco-3)	25 mg/2.5 ml	25 mg weekly ×3
Stabilized hyaluronic acid (Durolane)	60 mg/3 ml	60 mg ×1

MW molecular weight

Anesthetics and Analgesics Apart from their use prior to the injection of other medications or as part of a mixture with a corticosteroid, short-acting anesthetics (e.g., Table 3.4) may be injected alone into joints and or soft tissue locations as a diagnostic tool to differentiate between local and referred pain in situations where the clinical exam is uncertain. Other analgesics instilled intra-articularly are gener-

Table 3.10 Synoviorthesis applications and other reported injectates: selected examples [40–43]

Radionucleotides	Other chemicals	Biologics
Dysprosium-165	Osmic acid	Orgotein (superoxide dismutase)
Erbium-169	Nitrogen	Botulinum toxin
Gold-198	mustard	Trans-capsaicin
Rhenium-186	Thiotepa	Cell therapies
Yttrium-90	Methotrexate	Gene therapy
Lutetium-177	Sodium	Growth factors (e.g., rhFGF18)
Phosphate-32	morrhuate	TNF and IL-1 inhibitors
	Rifamycin SV	Albumin
	Aspirin	Platelet-rich plasma and other blood-derived cell concentrates
	Dextrose solution	

ally reported in the context of orthopedic procedures (total joint arthroplasty or arthroscopy). These agents include opioids, such as fentanyl and tramadol [37] and onabotulinumtoxinA [38], but not morphine as it causes local histamine release and may cause hyperalgesia.

Other Injectate Products A number of other agents have been used for intra-articular injection. Simple saline has been used for intra-articular tidal irrigation or lavage [39]. For use in percutaneous knee lavage, saline is best delivered through a large-bore (e.g., 14- or 16-gauge) needle or similar sized blunt trocar with side ports.

Synoviorthesis, or a medical synovectomy, may be achieved thru the injection of various substances including radionucleotides, chemical agents, and more recently biologic agents (Table 3.10). Synoviorthesis is typically indicated for a patient with resistant monoarthritis, either inflammatory (e.g., rheumatoid arthritis) or recurrent post-hemorrhagic (e.g., hemophilic arthropathy [40]), synovitis, unresponsive to conservative care (including intra-articular injection with standard agents) and/or in a patient not deemed a surgical candidate.

Post-procedure Recommendations

Most practitioners advocate some limited period of rest or reduced activity following joint or soft tissue injection. Postprocedural rest may prolong the benefit from a corticosteroid injection by reducing steroid diffusion from the joint and minimizing leakage of the steroid out of the needle track, both of which may maximize the intra-articular duration of action. Rest may also prevent damage from overuse in those obtaining immediate pain relief [44]. Optimal regimens endorsing the means of rest (e.g., bed rest, rigid, or flexible fixation) and rest duration unique to each specific joint or soft tissue injection are not well defined, and prospective, randomized studies are few.

Failed Arthrocentesis and the Use of Image-Guided Procedures

Accuracy Despite a clinician's thorough knowledge of anatomy, meticulous attention to technique, and operator experience, radiologic studies of joint and soft tissue injections have demonstrated the frequency of inaccuracy of needle localization, or the inability to aspirate a clinically detectable effusion, when based solely on palpation of body surface landmarks (Table 3.11). Reasons for inaccuracy include the unintended localization of the needle tip in an intra-articular fat pad in certain joints; joint position during aspiration; choice of specific intra-articular portal when more than 1 option is described; highly viscous synovial fluid being too difficult to aspirate; a needle lumen obstructed by fat, debris, or skin plug; and mistaken exam findings [45].

For the knee, in particular, the large, triangular medial fat pad may obstruct joint aspiration. The supine knee-extended position is more likely to yield fluid on aspiration than a flexed-knee (e.g., sitting) position [49]. The lateral midpatellar location has shown greater success than either anteromedial or anterolateral sites for injecting viscosupplement when no effusion is present, as determined by contrast injection [50]. An anterolateral knee portal has been described as being as effective as the lateral midpatellar portal [51].

Ultrasound Image guidance can improve the accuracy and, potentially, the outcome of joint and soft tissue injections. The competent performance of musculoskeletal ultrasound requires monetary (equipment) and time (training) investment. Ultrasound needle guidance is associated with increased accuracy and higher success rate for synovial fluid aspiration [52–58]. When contrasted against palpation-guided procedures, studies assessing the degree of additional improvement in

Table 3.11 Accuracy of needle placement guided by body surface landmarks

Site	Imaging used to assess accuracy	Skin portal for needle entry	Accuracy of needle placement by surface anatomy, n (%)
Subacromial space [46]	Radiographs with radio-opaque contrast in injectate	Anterolateral	15/20 (75)
		Posterior	15/20 (75)
		Lateral	12/20 (60)
Subacromial space [47]	MR with gadolinium in injectate	Posterior	13/17 (76)
		Anteromedial	10/16 (62.5)
Glenohumeral joint [48]	MR with gadolinium in injectate	Anterior	11/41 (26.8)
Knee joint [49]	Fluoroscopy with radio-opaque contrast in injectate	Anterolateral	57/80 (71)
		Anteromedial	60/80 (75)
		Lateral midpatellar	74/80 (93)

MR magnetic resonance

clinical outcome from the use of ultrasound guidance have yielded mixed results (improvements [52, 55], or none-to-small short-term clinical improvements of ultrasound-guided when compared with palpation-guided technique [54, 59–62]). Despite demonstrated accuracy over palpation-guided technique, it is not clear that the varied incremental clinical efficacy described in studies of procedures guided by ultrasound is sufficient to justify its routine use, and its associated patient costs, for all procedures. Ultrasound-guided procedures should be considered for difficult to palpate/reach joints, complicated joint effusions (loculations/adhesions), in patients with poor anatomic landmarks, or for small targets (e.g., tendon sheaths, neurovascular tunnels). The reader is directed to a recent set of relevant reviews of joint-specific ultrasound-guided techniques [63].

References

1. Torralba KD: Approach to joint injections and aspirations. 2021 Virtual Rheumatology Practicum – Adult (Lecture 3). https://wwwyoutubecom/watch?v=l41Z0Vt3T1I. Accessed 22 Aug 2021.
2. Gardner GC. Teaching arthrocentesis and injection techniques: what is the best way to get our point across? J Rheumatol. 2007 Jul;34(7):1448–50.
3. Charalambous CP, Tryfonidis M, Sadiq S, Hirst P, Paul A. Septic arthritis following intra-articular steroid injection of the knee–a survey of current practice regarding antiseptic technique used during intra-articular steroid injection of the knee. Clin Rheumatol. 2003;22:386–90.
4. Trampuz A, Hanssen AD, Osmon DR, Mandrekar J, Steckelberg JM, Patel R. Synovial fluid leukocyte count and differential for the diagnosis of prosthetic knee infection. Am J Med. 2004;117:556–62.
5. Schinsky MF, Della Valle CJ, Sporer SM, Paprosky WG. Perioperative testing for joint infection in patients undergoing revision total hip arthroplasty. J Bone Joint Surg Am. 2008;90:1869–75.
6. Murphy VE, Fittock RJ, Zarzycki PK, Delahunty MM, Smith R, Clifton VL. Metabolism of synthetic steroids by the human placenta. Placenta. 2007;28:39–46.
7. Thumboo J, O'Duffy JD. A prospective study of the safety of joint and soft tissue aspirations and injections in patients taking warfarin sodium. Arthritis Rheum. 1998;41:736–9.
8. Salvati G, Punzi L, Pianon M, et al. Frequency of the bleeding risk in patients receiving warfarin submitted to arthrocentesis of the knee [article in Italian]. Reumatismo. 2003;55:159–63.
9. Ahmed I, Gertner E. Safety of arthrocentesis and joint injection in patients receiving anticoagulation at therapeutic levels. Am J Med. 2012;125:265–9.
10. Yui JC, Preskill C, Greenlund LS. Arthrocentesis and joint injection in patients receiving direct oral anticoagulants. Mayo Clin Proc. 2017;92:1223–6.
11. Karsh J, Yang W. An anaphylactic reaction to intra-articular triamcinolone: a case report and review of the literature. Ann Allergy Asthma Immunol. 2003;90:254–8.
12. McKinney C, Sharma N, Jerath R. Livedoid dermatitis (Nicolau syndrome) following intra-articular glucocorticoid injection. J Clin Rheumatol. 2014;20:339–40.
13. Laufman H. Current use of skin and wound cleansers and antiseptics. Am J Surg. 1989;157:359–65.
14. Leclair J. A review of antiseptics. Cleansing agents. Todays OR Nurse. 1990;12:25–8.
15. Sebben JE. Sterile technique and the prevention of wound infection in office surgery–Part II. J Dermatol Surg Oncol. 1989;15:38–48.
16. Simkin PA, Gardner GC. The 3-way stopcock: a useful adjunct in the practice of arthrocentesis. Arthritis Rheum. 2005;53:627–8.

17. Park KS, Peisajovich A, Michael AA, Sibbitt WL Jr, Bankhurst AD. Should local anesthesia be used for arthrocentesis and joint injections? Rheumatol Int. 2009;29:721–3.
18. Hogan ME, vanderVaart S, Perampaladas K, Machado M, Einarson TR, Taddio A. Systematic review and meta-analysis of the effect of warming local anesthetics on injection pain. Ann Emerg Med. 2011;58:86–98.
19. Alonso PE, Perula LA, Rioja LF. Pain-temperature relation in the application of local anaesthesia. Br J Plast Surg. 1993;46:76–8.
20. Quaba O, Huntley JS, Bahia H, McKeown DW. A users guide for reducing the pain of local anaesthetic administration. Emerg Med J. 2005;22:188–9.
21. Burney K, Bowker K, Reynolds R, Bradley M. Topical ethyl chloride fine spray: does it have any antimicrobial activity? Clin Radiol. 2006;61:1055–7.
22. James WS 3rd, Drez D Jr. Ethyl chloride: an ineffective bacteriostatic or cidal agent for arthrocentesis. Am J Sports Med. 1988;16:539–40.
23. Draeger HT, Twining JM, Johnson CR, Kettwich SC, Kettwich LG, Bankhurst AD. A randomised controlled trial of the reciprocating syringe in arthrocentesis. Ann Rheum Dis. 2006;65:1084–7.
24. Sibbitt W Jr, Sibbitt RR, Michael AA, et al. Physician control of needle and syringe during aspiration-injection procedures with the new reciprocating syringe. J Rheumatol. 2006;33:771–8.
25. Rutherford DJ, Hubley-Kozey CL, Stanish WD. Knee effusion affects knee mechanics and muscle activity during gait in individuals with knee osteoarthritis. Osteoarthr Cart. 2012;20:974–81.
26. Pietrosimone B, Lepley AS, Murray AM, Thomas AC, Bahhur NO, Schwartz TA. Changes in voluntary quadriceps activation predict changes in muscle strength and gait biomechanics following knee joint effusion. Clin Biomech. 2014;29:923–9.
27. Gaffney K, Ledingham J, Perry JD. Intra-articular triamcinolone hexacetonide in knee osteoarthritis: factors influencing the clinical response. Ann Rheum Dis. 1995;54:379–38127.
28. Weitoft T, Rönnblom L. Randomised controlled study of postinjection immobilisation after intra-articular glucocorticoid treatment for wrist synovitis. Ann Rheum Dis. 2003;62:1013–5.
29. Cole BJ, Schumacher HR Jr. Injectable corticosteroids in modern practice. J Am Acad Orthop Surg. 2005;13:37–46.
30. Wittich CM, Ficalora FD, Mason TG, Beckman TJ. Musculoskeletal injection. Mayo Clin Proc. 2009;84:831–7.
31. Speed CA. Injection therapies for soft-tissue lesions. Best Pract Res Clin Rheumatol. 2007;21:333–47.
32. Rutjes AW, Jüni P, da Costa BR, Trelle S, Nüesch E, Reichenbach S. Viscosupplementation for osteoarthritis of the knee: a systematic review and meta-analysis. Ann Intern Med. 2012;157:180–91.
33. Balazs EA, Denlinger JL. Viscosupplementation: a new concept in the treatment of osteoarthritis. J Rheumatol. 1993;39:3–9.
34. Bellamy N, Campbell J, Robinson V, Gee T, Bourne R, Wells G. Viscosupplementation for the treatment of osteoarthritis of the knee. Cochrane Database Syst Rev. 2006;2:CD005321.
35. Arrich J, Piribauer F, Mad P, Schmid D, Klaushofer K, Müllner M. Intra-articular hyaluronic acid for the treatment of osteoarthritis of the knee: systematic review and meta-analysis. CMAJ. 2005;172:1039–43.
36. Two new intra-articular injections for knee osteoarthritis. Med Lett Drugs Ther. 2018;60(1554):142–5.
37. Mitra S, Kaushal H, Gupta RK. Evaluation of analgesic efficacy of intra-articular bupivacaine, bupivacaine plus fentanyl, and bupivacaine plus tramadol after arthroscopic knee surgery. Arthroscopy. 2011;27:1637–43.
38. Singh JA, Mahowald ML, Noorbaloochi S. Intraarticular botulinum toxin a for refractory painful total knee arthroplasty: a randomized controlled trial. J Rheumatol. 2010;37:2377–86.

39. Ike RW. Tidal irrigation versus conservative medical management in patients with osteoarthritis of the knee: a prospective randomized study. Tidal Irrigation Cooperating Group. J Rheumatol. 1992;19:772–9.
40. Rodriguez-Merchan EC, Goddard NJ. The technique of synoviorthesis. Haemophilia. 2001;7(suppl 2):11–5.
41. Caviglia HA, Fernandez-Palazzi F, Galatro G, Perez-Bianco R. Chemical synoviorthesis with rifampicin in haemophilia. Haemophilia. 2001;7(suppl 2):26–30.
42. Cruz-Esteban C, Wilke WS. Innovative treatment approaches for rheumatoid arthritis. Non-surgical synovectomy Baillieres. Clin Rheumatol. 1995;9:787–801.
43. van der Zant FM, Boer RO, Moolenburgh JD, Jahangier ZN, Bijlsma JW, Jacobs JW. Radiation synovectomy with (90)yttrium, (186)rhenium and (169)erbium: a systematic literature review with meta-analyses. Clin Exp Rheumatol. 2009;27:130–9.
44. Wallen MM, Gillies D. Intra-articular steroids and splints/rest for children with juvenile idiopathic arthritis and adults with rheumatoid arthritis. Cochrane Database Syst Rev. 2006;25:CD002824.
45. Roberts WN. Primer: pitfalls of aspiration and injection. Nat Clin Pract Rheumatol. 2007;3:464–72.
46. Kang MN, Rizio L, Prybicien M, Middlemas DA, Blacksin MF. The accuracy of subacromial corticosteroid injections: a comparison of multiple methods. J Shoulder Elb Surg. 2008;17(1 suppl):61S–6S.
47. Henkus HE, Cobben LP, Coerkamp EG, Nelissen RG, van Arkel ER. The accuracy of subacromial injections: a prospective randomized magnetic resonance imaging study. Arthroscopy. 2006;22:277–82.
48. Sethi PM, Kingston S, Elattrache N. Accuracy of anterior intra-articular injection of the glenohumeral joint. Arthroscopy. 2005;21:77–80.
49. Zhang Q, Zhang T, Lv H, et al. Comparisons of two positions of knee arthrocentesis: how to obtain complete drainage. Am J Phys Med Rehabil. 2012;91:611–5.
50. Jackson DW, Evans NA, Thomas BM. Accuracy of needle placement into the intra-articular space of the knee. J Bone Joint Surg Am. 2002;84-A:1522–7.
51. Chavez-Chiang CE, Sibbitt WL Jr, Band PA, Chavez-Chiang NR, Delea SL, Bankhurst AD. The highly accurate anteriolateral portal for injecting the knee. Sports Med Arthrosc Rehabil Ther Technol. 2011;3:6.
52. Berkoff DJ, Miller LE, Block JE. Clinical utility of ultrasound guidance for intra-articular knee injections: a review. Clin Interv Aging. 2012;7:89–95.
53. Schirmer M, Duftner C, Schmidt WA, Dejaco C. Ultrasonography in inflammatory rheumatic disease: an overview. Nat Rev Rheumatol. 2011;7:479–88.
54. Cunnington J, Marshall N, Hide G, et al. A randomized, double-blind, controlled study of ultrasound-guided corticosteroid injection into the joint of patients with inflammatory arthritis. Arthritis Rheum. 2010;62:1862–9.
55. Sibbitt WL Jr, Kettwich LG, Band PA, et al. Does ultrasound guidance improve the outcomes of arthrocentesis and corticosteroid injection of the knee? Scand J Rheumatol. 2012;41:66–72.
56. Bruyn GA, Schmidt WA. How to perform ultrasound-guided injections. Best Pract Res Clin Rheumatol. 2009;23:269–79.
57. Wu T, Dong Y, Song HX, Fu Y, Hua J. Ultrasound-guided versus landmark in knee arthrocentesis: a systematic review. Semin Arthritis Rheum. 2016;45:627–32.
58. Aly AR, Rajasekaran S, Ashworth N. Ultrasound-guided shoulder girdle injections are more accurate and more effective than landmark-guided injections: a systematic review and meta-analysis. Br J Sports Med. 2015;49:1042–9.
59. Gilliland CA, Salazar LD, Borchers JR. Ultrasound versus anatomic guidance for intra-articular and periarticular injection: a systematic review. Phys Sportsmed. 2011;39(3):121–31.
60. Sage W, Pickup L, Smith TO, Denton ER, Toms AP. The clinical and functional outcomes of ultrasound-guided vs landmark-guided injections for adults with shoulder pathology–a systematic review and meta-analysis. Rheumatology (Oxford). 2013;52:743–51.

61. Bloom JE, Rischin A, Johnston RV, Buchbinder R. Image-guided versus blind glucocorticoid injection for shoulder pain. Cochrane Database Syst Rev. 2012;8:CD009147.
62. Hirsch G, O'Neill TW, Kitas G, Sinha A, Klocke R. Accuracy of injection and short-term pain relief following intra-articular corticosteroid injection in knee osteoarthritis - an observational study. BMC Musculoskelet Disord. 2017;18(1):44.
63. Peck E. Outpatient ultrasound-guided musculoskeletal techniques. Phys Med Rehabil Clin N Am. 2016;27(3):xv–xvi.(this volume has multiple articles on US-guided injection: shoulder, elbow, wrist, hand, hip, knee, ankle, foot, tendinopathy, nerve).

Chapter 4
Biochemical Composition of Synovial Fluid in Health and Disease

Robert T. Keenan

Lubricant Molecules

A primary function of SF is to lubricate the joint reducing friction and mechanical stress on the articular cartilage. Large molecules of SF such as hyaluronan (HA), products of the proteoglycan 4 (PRG4) gene including lubricin and superficial zone protein work synergistically to decrease friction and mechanical damage [1]. Hyaluronan is a non-sulfated glycosaminoglycan composed of repeating disaccharide units of D-glucuronic acid and D-N-acetylglucosamine. It was discovered in 1934 by Myer and Palmer, deriving its name from the Greek-derived *haylos* combined with uronic acid [2]. Produced by fibroblast-derived type B synovial cells, HA has the viscosity of an egg white, and is the most abundant large molecule of SF with concentrations ranging from 1–4 mg/ml [3]. It is a biopolymer molecule several million daltons in size. HA can take the form of hyaluronic acid, or at physiological pH can take the form of a sodium salt [2].

Hyaluronan is a rheological marvel that is extremely lubricious and hydrophilic. In solution, the hyaluronan polymer chain takes on the form of an expanded coil allowing it to hold 1000 times its weight in water [2]. The chains entangle with each other at very low concentrations, and at higher concentrations have an extremely high shear-dependent viscosity separating tissue surfaces that slide along each other. These characteristics give SF the empirical "string sign" that can be demonstrated by letting the thick normal fluid drip out of a syringe one drop at time or by pinching a drop between the thumb and forefinger [4]. A fluid "string sign" of 3 cm or more before breaking is considered normal, while <2.5 cm (more similar to water) is considered abnormal and indicative of inflammatory fluid with degraded HA.

R. T. Keenan (✉)
Arthrosi Therapeutics, San Diego, CA, USA
e-mail: rkeenan@arthrosi.com

B. F. Mandell (ed.), *Synovial Fluid Analysis and The Evaluation of Patients With Arthritis*, https://doi.org/10.1007/978-3-030-99612-3_4

Hyaluronan has other important biological functions. The constant secretion, then degradation has led to the suggestion that it acts as a scavenger for cellular debris [5]. Since the 1940s it has been known that HA is degraded by oxidizing systems via chain cleavage induced by hydroxy radicals, and through this reaction molecular "debris" can be caught in the network of HA and removed at the same rate as the polysaccharide [6, 7]. HA also has a concentration and molecular weight-dependent effect on angiogenesis [2, 8]. High molecular weight and concentrations of HA inhibit capillary formation which may contribute to the avascularity of the joint capsule and cartilage. Interestingly, under certain conditions HA binds to cell surface proteins. Synovial cells can change their expression of HA-binding receptors in disease states, thus HA can influence immunological reactions and inflammatory cell traffic in and out of the synovial fluid [9]. Finally, HA may interact directly or indirectly with pain receptors within the joint, perhaps explaining transient analgesic benefit experienced by some patients following intra-articular HA injections [2, 10].

In states of inflammation and oxidative stress there is accelerated (beyond physiologic) degradation of HA resulting in impairment and loss of viscosity. Degraded HA of low-molecular-weight has different biological activities compared to the high-molecular-weight HA in the healthy joint [2]. Smaller HA chains can serve as endogenous immunostimulating danger signals contributing to inflammation and angiogenesis [2, 11, 12].

There are many commercially available products for HA "viscosupplementation" in OA which may decrease pain and improve function in some patients with mild to moderate disease [13]. An intent with intra-articular injection of exogenous HA is to temporarily improve intra-articular viscosity, stimulate endogenous HA production, stimulate chondrocytes and synthesis of cartilage matrix components, and inhibit enzymatic degradation of chondrocytes and inflammatory processes [14].

Lubricin is a surface-active mucin-like glycoprotein, encoded by the PRG4 gene, which is produced by synovial fibroblasts and chondrocytes along the surface of articular cartilage [15]. The role of lubricin is to retain a protective layer of water molecules, lubricate the joint, and prevent cell and protein adhesion. Along with hyaluronan, it provides protection of the joint by reducing friction. Patients with inflammatory arthritis, joint trauma, or genetic lubricin deficiencies have insufficient amounts to protect the cartilage. There are recombinant forms of lubricin in clinical development for the treatment of OA, autoimmune arthritis, as well as dry eyes and other applications [16].

Proteins

There are similarities between blood plasma and SF protein composition, with the synovial membrane selectively blocking very large plasma proteins from entering into the joint space under normal physiological conditions [17]. The average joint SF contains approximately one-third of the protein concentration found in plasma, or 19–28 mg/ml [17, 18]. The major protein found in SF is albumin (approximately

12 mg/ml or 37% of the plasma concentration); transferrin and globulins make up most of the rest. In contrast, large molecular weight plasma proteins such as fibrinogen are at very low concentrations.

In joint inflammation the concentration and quantity of proteins increase. Patients with synovial inflammation including osteoarthritis (OA), rheumatoid arthritis (RA), gout, systemic lupus erythematosus (SLE), and traumatic arthritis have increased protein concentrations [17]. The inflammation of the synovium compromises the ability of the synovium to selectively filter and retain proteins [2, 17]. For example, active RA patients will have high levels of large plasma proteins such as fibrinogen, β2 macroglobulin, β1 lipoprotein, α2 glycoprotein, and α2 macroglobulin [17]. Small proteins such as C-reactive protein, calprotectin, and defensins also more readily influx into SF during joint inflammation, and may have clinical significance and some diagnostic value. But measurement of the SF protein level, unlike the situation with other body fluids, is not diagnostically useful.

Fibrinogen levels are relatively low in the healthy joint SF, but during inflammatory states such as RA and gout, levels can increase 3–5-fold [19]. Studies have shown influx of fibrinogen and other coagulation proteins into synovial fluid that is not paralleled by increased fibrinolytic activity. While normal joint fluid does not clot, the increased fibrinogen in inflamed synovial fluid can cause clotting when transported in a test tube without EDTA or sodium heparin [20, 21]. In the RA patient, forms of citrullinated fibrinogen may bind to anti-citrullinated protein antibodies (anti-CCP ab) within the synovial fluid and joint [22].

Similar to serum CRP, synovial CRP increases in states of inflammation, particularly infection. Serum CRP is commonly used as a screening test for acute infection, but synovial fluid has been found to have a sensitivity and specificity of 92% and 90%, respectively, in periprosthetic joint infection (PJI). High concentrations of CRP are also found in the synovial fluid of inflammatory arthropathies such as RA [23]. Although thought to be exclusively produced in the liver, there is evidence that fibroblast-like synoviocytes may produce CRP, releasing it into the SF [24] and perhaps into the blood.

There are several small proteins and antimicrobial peptides (AMPs) released by neutrophils and macrophages as part of the innate immune response that can be found in SF during states of infection or sterile inflammation. Cathelicidin LL-37, α-defensin, and calprotectin in SF have potential clinical utility when used with other markers such as CRP, white blood count (WBC) with differential and cultures when a septic joint is suspected. Commercial point-of-care testing is available to detect calprotectin and α-defensin in SF [25, 26], but their clinical utility to differentiate between septic and aseptic inflammatory arthropathies is not fully understood.

Cathelicidin LL-37 is a 37 amino acid peptide produced by neutrophils that has been implicated in the pathogenesis of several inflammatory diseases including SLE, RA, psoriasis, and atherosclerosis [27]. It has been found in SF of RA patients and found to associate with inflammation and to increase apoptosis of osteoblasts [27]. Defensins are small (29–35 amino acids) proteins produced by circulating white blood cells and tissue cells [26]. Defensins are classified into alpha and beta families with α-defensin found in and released by neutrophils, macrophages, and

Paneth cells of the intestine. In the presence of pathogens in SF, neutrophils release α-defensin inducing the depolarization of the bacterial cell membrane promoting lysis and death [26]. In addition to direct antimicrobial activity, α-defensin also contributes to chemotaxis, cytokine induction, and phagocytosis [28]. Consistently high levels of α-defensin observed in the SF of infected joints have led to it being established as a biomarker and part of the diagnostic criteria for PJI [26, 29]. Interestingly, α-defensin is not influenced by prior antibiotic administration, comorbid conditions of the patient (with the possible exception of an autoimmune disease), or type of infectious organism [30]. Elevated levels can be found in inflammatory arthropathies including crystalline (gout and calcium pyrophosphate deposition disease (CPPD)), psoriatic arthritis, and rheumatoid arthritis [29, 31]. Similar to α-defensin levels, increased numbers of neutrophils within the SF contribute to the levels of lactate dehydrogenase (LD), while the serum LD levels remain normal [4].

Calprotectin is another AMP secreted by neutrophils and monocytes that has chemotactic properties. It has been shown to be more sensitive and specific for the diagnosis of PJI than erythrocyte sedimentation rate, CRP, and SF WBC [32, 33]. Unlike cathelicidin LL-37 and α-defensin, calprotectin has been shown to have potential clinical utility as a biomarker to differentiate septic arthritis from other inflammatory arthropathies including CPPD and RA [34].

Small Molecules

Small molecules in SF include glucose, urate, and lactate. Unlike other body fluids where active transport dictates the movement of many molecules, in SF smaller molecule concentrations typically parallel serum levels under normal conditions. For example, glucose levels in SF are typically ~10 mg/dL less than serum levels. In inflammatory states there are often significantly larger decreases in SF glucose levels in a septic joint compared to serum glucose levels [4], but there is too much overlap with other inflammatory joint conditions for this to be a reliable diagnostic test for infection.

Uric acid in the plasma and SF circulates as urate, the mono-deprotonated ionic form of uric acid under normal physiologic conditions [35]. Elevated serum urate levels will elevate SF levels with subsequent monosodium urate monohydrate (MSU) deposition (MSU being the most common crystallized urate) which may ultimately result in gouty arthritis (see Chap. 10). The various factors that cause crystallization of uric acid have not been fully illuminated, and data on how HA and its degradation products influence urate solubility have been conflicting [35].

Measurement of SF protein, glucose, and even the presence of crystals will not aid in differentiating between septic and aseptic arthritis. While WBC with differential, gram stain and culture remain the most important tests to obtain, lactate may have diagnostic potential to distinguish septic arthritis from other inflammatory states including gout [36–38]. SF lactate levels above 10 mmol/L suggest septic arthritis, and levels lower than 4.3 mmol/L are more likely to be aseptic [36].

Another potential biomarker to distinguish septic arthritis from crystalline and aseptic inflammatory arthropathies is the SF lactate/glucose ratio [39]. A large European study evaluating 233 SF specimens found elevated lactate/glucose ratio had a greater area under curve, sensitivity, specificity, and likelihood ratio in septic arthritis, outperforming individual SF lactate and glucose levels.

References

1. Jahn S, Seror J, Klein J. Lubrication of articular cartilage. Annu Rev Biomed Eng. 2016;18:235–58.
2. Tamer TM. Hyaluronan and synovial joint: function, distribution and healing. Interdiscip Toxicol. 2013;6(3):111–25.
3. Mazzucco D, Scott R, Spector M. Composition of joint fluid in patients undergoing total knee replacement and revision arthroplasty: correlation with flow properties. Biomaterials. 2004;25(18):4433–45.
4. Mundt LA, Shanahan K. Graff's textbook of urinalysis and body fluids. 3rd ed. Burlington: Jones & Bartlett; 2016.
5. Laurent TC, Laurent UB, Fraser JR. Functions of hyaluronan. Ann Rheum Dis. 1995;54(5):429–32.
6. Myint P, et al. The reactivity of various free radicals with hyaluronic acid: steady-state and pulse radiolysis studies. Biochim Biophys Acta. 1987;925(2):194–202.
7. Rapta P, et al. High-molar-mass hyaluronan behavior during testing its radical scavenging capacity in organic and aqueous media: effects of the presence of manganese(II) ions. Chem Biodivers. 2009;6(2):162–9.
8. Sattar A, Kumar S, West DC. Does hyaluronan have a role in endothelial cell proliferation of the synovium? Semin Arthritis Rheum. 1992;22(1):37–43.
9. Edwards J. Second international meeting on synovium. Cell biology, physiology and pathology. 21-23 September, Canterbury, United Kingdom. Ann Rheum Dis. 1995;54(5):389–91.
10. Adams ME. An analysis of clinical studies of the use of crosslinked hyaluronan, hylan, in the treatment of osteoarthritis. J Rheumatol Suppl. 1993;39:16–8.
11. Kotla NG, et al. Recent advances and prospects of hyaluronan as a multifunctional therapeutic system. J Control Release. 2021;336:598–620.
12. Tavianatou AG, et al. Molecular size-dependent specificity of hyaluronan on functional properties, morphology and matrix composition of mammary cancer cells. Matrix Biol Plus. 2019;3:100008.
13. Conrozier T, et al. Viscosupplementation for the treatment of osteoarthritis. The contribution of EUROVISCO group. Ther Adv Musculoskelet Dis. 2021;13:1759720X211018605.
14. Strand V, et al. Safety and efficacy of US-approved viscosupplements for knee osteoarthritis: a systematic review and meta-analysis of randomized, saline-controlled trials. J Pain Res. 2015;8:217–28.
15. Szychlinska MA, et al. Altered joint tribology in osteoarthritis: reduced lubricin synthesis due to the inflammatory process. New horizons for therapeutic approaches. Ann Phys Rehabil Med. 2016;59(3):149–56.
16. Jay GD, Waller KA. The biology of lubricin: near frictionless joint motion. Matrix Biol. 2014;39:17–24.
17. Hui AY, et al. A systems biology approach to synovial joint lubrication in health, injury, and disease. Wiley Interdiscip Rev Syst Biol Med. 2012;4(1):15–37.
18. Levick JR. Permeability of rheumatoid and normal human synovium to specific plasma proteins. Arthritis Rheum. 1981;24(12):1550–60.
19. Barnhart MI, et al. Fibrin promotion and lysis in arthritic joints. Ann Rheum Dis. 1967;26(3):206–18.

20. Carmassi F, et al. Fibrin degradation in the synovial fluid of rheumatoid arthritis patients: a model for extravascular fibrinolysis. Semin Thromb Hemost. 1996;22(6):489–96.
21. Faryna A, Goldenberg K. In: Walker HK, Hall WD, editors. Joint fluid, in clinical methods: the history, physical, and laboratory examinations. Boston: Butterworths; 1990.
22. Raijmakers R, et al. Elevated levels of fibrinogen-derived endogenous citrullinated peptides in synovial fluid of rheumatoid arthritis patients. Arthritis Res Ther. 2012;14(3):R114.
23. Sukenik S, et al. Serum and synovial fluid levels of serum amyloid A protein and C-reactive protein in inflammatory and noninflammatory arthritis. J Rheumatol. 1988;15(6):942–5.
24. Fang Z, et al. C-reactive protein promotes the activation of fibroblast-like Synoviocytes from patients with rheumatoid arthritis. Front Immunol. 2020;11:958.
25. Warren J, et al. Diagnostic utility of a novel point-of-care test of calprotectin for Periprosthetic joint infection after Total knee arthroplasty: a prospective cohort study. J Bone Joint Surg Am. 2021;103(11):1009–15.
26. Zeng YQ, et al. Diagnostic accuracy of the synovial fluid alpha-Defensin lateral flow test in Periprosthetic joint infection: a meta-analysis. Orthop Surg. 2021;13(3):708–18.
27. Kahlenberg JM, Kaplan MJ. Little peptide, big effects: the role of LL-37 in inflammation and autoimmune disease. J Immunol. 2013;191(10):4895–901.
28. Fruitwala S, El-Naccache DW, Chang TL. Multifaceted immune functions of human defensins and underlying mechanisms. Semin Cell Dev Biol. 2019;88:163–72.
29. Phillips DS, Workman KK, Kelly M. Nonoperative treatment of a Periprosthetic gout flare in the setting of a positive alpha-Defensin result. Arthroplast Today. 2021;9:65–7.
30. Deirmengian C, et al. Validation of the alpha Defensin lateral flow test for Periprosthetic joint infection. J Bone Joint Surg Am. 2021;103(2):115–22.
31. Plate A, et al. Inflammatory disorders mimicking periprosthetic joint infections may result in false-positive alpha-defensin. Clin Microbiol Infect. 2018;24(11):1212 e1–6.
32. Zhang Z, et al. The value of calprotectin in synovial fluid for the diagnosis of chronic prosthetic joint infection. Bone Joint Res. 2020;9(8):450–7.
33. Salari P, et al. Synovial fluid calprotectin for the preoperative diagnosis of chronic Periprosthetic joint infection. J Arthroplast. 2020;35(2):534–7.
34. Baillet A, et al. Calprotectin discriminates septic arthritis from pseudogout and rheumatoid arthritis. Rheumatology (Oxford). 2019;58(9):1644–8.
35. Martillo MA, Nazzal L, Crittenden DB. The crystallization of monosodium urate. Curr Rheumatol Rep. 2014;16(2):400.
36. Lenski M, Scherer MA. Analysis of synovial inflammatory markers to differ infectious from gouty arthritis. Clin Biochem. 2014;47(1–2):49–55.
37. Long B, Koyfman A, Gottlieb M. Evaluation and management of septic arthritis and its Mimics in the Emergency Department. West J Emerg Med. 2019;20(2):331–41.
38. Carpenter CR, et al. Diagnostic accuracy of synovial lactate, polymerase chain reaction, or clinical examination for suspected adult septic arthritis. J Emerg Med. 2020;59(3):339–47.
39. Berthoud O, et al. Performance of a new rapid diagnostic test the lactate/glucose ratio of synovial fluid for the diagnosis of septic arthritis. Joint Bone Spine. 2020;87(4):343–50.

Chapter 5
Cellular Components of Synovial Fluid in Health and Disease

N. Lawrence Edwards

Origin and Nature of Normal Synovial Fluid

Synovial fluid is an ultrafiltrate of plasma that originates from a highly fenestrated capillary network overlying the synovial membrane. This vascular membrane structure allows for the rapid exchange of water and solutes in and out of the articular space. Within the synovial space, the ultrafiltrate is enriched with hyaluronans and other glycoproteins secreted by synovial lining cells [1]. The synovial fluid functions to supply nutrition to and remove metabolic waste from the avascular articular cartilage as it compresses and expands with weight bearing. Synovial fluid also assists in lubricating articular surfaces and defending against infection. The volume of synovial fluid in a normal joint is quite small and depends on the size of the joint. One study of synovial fluid obtained immediately after death from patients who had no history of joint disease reported an average volume of 2.1 ml (range 0.13 to 3.5 ml) in examined knees [2]. These small volumes are beyond detection by usual physical examination.

As a plasma ultrafiltrate, synovial fluid should be devoid of nucleated cells from circulating blood. However, even in "normal" synovial fluid small numbers of immune cells can be detected. Ropes et al. reported average nucleated cell count of 63 cells/cu.mm which is comparable to similar studies on normal synovial fluid which ranged from 10 to 180 cells [3, 4]. In normal synovial fluid, mononuclear cells dominate with 58% monocyte/macrophages and 25% lymphocytes. Polymorphonuclear cells represent <10% of normal synovial fluid immune cells [2].

The synovial fluid we obtain by arthrocentesis is virtually never "normal". We aspirate diarthrodial joints because of swelling, pain and to aid in the diagnosis of

N. L. Edwards (✉)
Department of Medicine, University of Florida, Gainesville, FL, USA
e-mail: edwarnl@medicine.ufl.edu

B. F. Mandell (ed.), *Synovial Fluid Analysis and The Evaluation of Patients With Arthritis*, https://doi.org/10.1007/978-3-030-99612-3_5

an inflammatory or non-inflammatory arthritis. The distinction between "normal" and "abnormal" synovial fluid can be made on the basis of volume (> or <1.0 ml) and cellularity (> or <100 cells/mm^3). By common convention the total nucleated cell count of normal synovial fluid is <100 cells/mm^3; <1000 cells/mm^3 for non-inflammatory fluid; and >1500–2000 cells/mm^3 for inflammatory fluids [5]. In instances of low cell counts (between 1000 and 2000 cells/mm^3) the differential cell count can aid in the classification with mononuclear cell predominance usually indicating non-inflammatory conditions and polymorphonuclear cell predominance suggesting inflammatory disease [5].

Synovial Fluid Cell Types

Arthrocentesis with white blood cell count has long been a useful procedure to aid in the diagnosis of joint disease. Differential synovial fluid cell count has widespread acceptance for its ability to classify inflammatory from non-inflammatory arthropathies and, most consequentially, to help identify the cause of an acute monoarthritis as likely either crystalline or septic arthritis.

The principal cells that migrate into the synovial fluid from the peripheral circulation are lymphocytes, monocytes, and polymorphonuclear (PMNs) cells. Occasionally other cell types appear in cytocentrifuged synovial fluid specimens such as eosinophils, mast cells, plasma cells, types A and B synovial lining cells, and malignant cells [5]. For the purpose of this review chapter, we will focus on lymphocytes, monocytes/macrophages, PMNs, and eosinophils as they are the most commonly encountered and most useful in generating the differential diagnosis of joint pathology.

Mechanisms of Synovial Cell Counting

Conventional manual counting in a hemocytometric chamber remains the gold standard for enumerating and differentiating immune cells in synovial fluid. Over the past 10–15 years most laboratories have adopted automated cell counters to improve the turn-around time and decrease the inter-reader variability associated with manual techniques. There are, however, limits to the precision and accuracy of the automated approach. Results from automated analyzers are most accurate when the total synovial fluid white cell count is >10,000 cells/mm^3 and the percent PMNs is >60%. Many laboratories will automatically perform a manual analysis when cell counts and cell types lay outside these parameters [6].

Another factor that can greatly affect the interpretation of synovial fluid white cell counting is the time elapsed between performing the arthrocentesis and when

the laboratory analysis actually takes place. Kerolus et al. showed a progressive decline in synovial fluid leukocyte count over a 6-hour period at room temperature. In freshly obtained synovial fluids with WBC counts <10,000 mm^3, the number of leukocytes declined by 16% in the first hour and by 64% at 6 hours. For synovial fluids with higher baseline leukocyte count, the decline was more gradual with 8% loss at 1 hour and 40% loss at 6 hours [7]. Polymorphonuclear cells are considerably more fragile than mononuclear cells and deteriorate at a more rapid pace. The decline in white cell count over time can alter classification of an inflammatory synovial fluid to a non-inflammatory fluid if laboratory testing is not performed in a timely manner. Similarly, a PMN predominant fluid could erroneously appear more like a lymphocytic or monocytic synovial fluid over time [8].

Performing cell staining to help distinguish PMNs, lymphocytes, monocytes, and eosinophils in synovial fluid is more difficult than staining in blood or other body fluids. This is because of the hyaluronan content of synovial fluid that interferes with Wright-Giemsa stain and can lead to erroneous interpretations. Many laboratories will only report the percentages of PMNs and not attempt to distinguish the various mononuclear cells present in synovial fluid.

Other variables that can affect the laboratory's reporting of cell number and cell type in synovial fluid, besides the time to processing and the relative instability of different immune cell classes, are the type of diluent used (isotonic versus hypertonic saline) and the presence or absence of hyaluronidase in the preparation.

Synovial Fluid Lymphocytes and Arthritis

Peripheral lymphocytes are attracted to the joint space by a number of chemoattractants depending on the disease process. A preponderance of this cell type can be observed in inflammatory rheumatic diseases where there is little proliferative synovitis and few osseocartilaginous erosions such as systemic lupus erythematosus, Sjögren Disease, Behcet's syndrome, sarcoidosis, and Mediterranean Fever. A lymphocytic synovial fluid can also be observed early in the course of rheumatoid arthritis and if this characteristic persists, it portends a better overall prognosis [5]. Lymphocytes can also make up the highest percentage of synovial fluid white cells in osteoarthritis although the total number of white cells is generally lower than that of RA by a factor of 10. In osteoarthritic joints, the most consistent sources of chemoattraction are IL-15 and TNFα [9]. The chemoattractant profile for rheumatoid arthritis synovium also includes IL-15 with equal importance given to IL-8, monocyte chemotactic protein-1 (MCP-1), and macrophage inflammatory protein-1α (MIP-1 α) [10].

While synovial polymorphonuclear leukocytes predominate in the acute phases of both gout and CPPD deposition disease, the quiescent phases of both crystalline arthropathies may have more of a lymphocytic profile.

Synovial Fluid Monocytes/Macrophages and Arthritis

Monocytes and macrophages are normal components of the synovium. The monocytes that appear in synovial fluid of both normal and pathologic conditions, however, are recruited from the circulating monocyte pool [11]. Using CD14 and CD16 as specific monocyte or macrophage subset markers, the $CD14^{+}$ $CD16^{neg}$ (classical) subset represents approximately 85% of circulating monocytes, the $CD14^{low}$ $CD16^{+}$ (intermediate) subset approximately 10%, and the $CD14^{+}$ $CD16^{+}$ (double-positive) subset approximately 5%. Double-positive $CD14^{+}$ $CD16^{+}$ monocyte or macrophages are considered pro-inflammatory and are enriched in the synovial fluid monocyte/macrophage population in most conditions that result in a joint effusion. This is especially true in systemic inflammatory diseases and inflammatory arthritis, like rheumatoid arthritis. It is also true with osteoarthritis of the knee – although to a lesser extent. Gómez-Aristizábal and associates demonstrated that in patients with knee osteoarthritis, patient-reported outcome measures for stiffness and quality of life were directly affected by the percent of double-positive monocyte/macrophages in the synovial fluid [11].

Monocyte predominant synovial effusions are rare, but can be seen in various viral infections (Rubella, Parvovirus, Viral Hepatitis, as well as Reactive Arthritis [12]). Monocytic joint effusions have also been reported with systemic lupus erythematosus and transient arthritis associated with urticaria/angioedema [13] as well as amyloidosis [14].

Synovial Fluid Polymorphonuclear Leukocytes and Arthritis

Polymorphonuclear leukocytes or neutrophils are the third largest population of immune cells in normal synovial fluid. They can, however, become the dominant cell type in almost any form of arthritis. During flares of rheumatoid arthritis, the influx of neutrophils has been shown to promote inflammation and boney destruction by factors associated with osteoclast activity [15]. In osteoarthritis, the percentage and number of neutrophils in highly variable but increased synovial fluid neutrophils is associated with higher synovial fluid concentration of $CD4^{+}$ and Treg cells and may be an indicator for a more aggressive subtype of osteoarthritis [15]. Other inflammatory arthritities can present with mildly inflammatory effusions (5–30,000 cells/mm^3) with high neutrophil percentage (50–80%). These include rheumatoid arthritis [16], psoriatic arthritis [17], and Behçet's disease [17].

An almost "pure" neutrophilic synovial fluid with a high synovial cell count is the hallmark of both acute crystalline and septic synovitis and both are triggered by activation of the innate immune system. The expectation that all synovial fluid analysis for these two conditions will render WBC counts of >50,000 cells/mm^3 needs to be tempered by the recognition that the synovial fluid cell concentration will be at an initial low level prior to the crystal triggering or bacterial invasion. How high the synovial fluid WBC count is at the time of joint aspiration depends on how long

the immune activation has been going on. A synovial fluid WBC count of 20,000–30,000 cells/mm^3 early on in the inflammatory process should not dissuade the clinician from looking for crystals or bacteria. In fact, a synovial fluid cell count of >50,000 cells/mm^3 only has a sensitivity of 61% for septic arthritis [18] and a synovial fluid WBC count of >100,000 cells/mm^3 only has a specificity of 77% [19].

It is appropriate and important for clinicians to first consider infectious and crystalline causes of a purulent joint effusion in the setting of fever and acute monoarthritis. However, there are a number of other potential causes of neutrophilic effusions with >50,000 cells/mm^3. These cases of "pseudoseptic arthritis" can be seen with many underlying rheumatologic and inflammatory conditions including rheumatoid arthritis [20], psoriatic arthritis [21], relapsing polychondritis [22], and post joint injection of hyaluronic acid [23]. We should also remember that although tuberculous arthritis most often presents as a chronic mono- or oligoarthritis it does present as an acute monoarthritis about 25% of the time. Acute tuberculous, and non-tuberculous mycobacterial arthritis often presents with a neutrophil dominant effusion [24].

Synovial Fluid Eosinophils and Arthritis

Eosinophils represent <3% of peripheral blood leukocytes in normal subjects and are a rare finding in synovial fluid analysis. The clinical significance of eosinophils appearing in synovial fluid is not well understood and the presence of synovial fluid eosinophils is usually not a reflection of peripheral blood eosinophilia. Even conditions with intense peripheral eosinophilia such as hypereosinophilic syndrome (HES), drug reaction with eosinophilia and systemic symptoms (DRESS) and eosinophilic granulomatosis with polyangiitis (EGPA) do not usually have eosinophils in synovial fluid [25]. The actual frequency of synovial fluid eosinophilia may be underestimated because of incomplete staining during normal preparation or simply overlooked because of the low percentage of the total synovial fluid leukocyte count they may represent.

Minor synovial fluid eosinophilia (less than 10% of total synovial fluid leukocytes) has been reported in both surgical and non-surgical trauma to joints that result in a hemarthrosis. The timing of eosinophil appearance in synovial fluid and the occurrence of bleeding into the synovial space has not been well characterized and has no known clinical implications. Other conditions associated with minor synovial fluid eosinophilia include CPPD arthropathy, complex regional pain syndrome-1 (CRPS-1), psoriatic arthritis, and filariasis [26].

Clinical conditions that have been occasionally associated with major synovial fluid eosinophils (greater than 10% of total leukocytes and sometimes as high as 85–90%) include Lyme disease, CPPD-arthropathy, psoriatic arthritis, following arthrography, septic arthritis and other helminthic infections such as Ascaris lumbricoides, Strongyloides stercoralis, Tricuris trichiura, and Giardia lamblia [27]. There is also an idiopathic form of major synovial fluid eosinophilia [28]. This transient monoarthritis is not associated with peripheral eosinophilia and has little clinical

Table 5.1 Cellular components of SF in health and disease

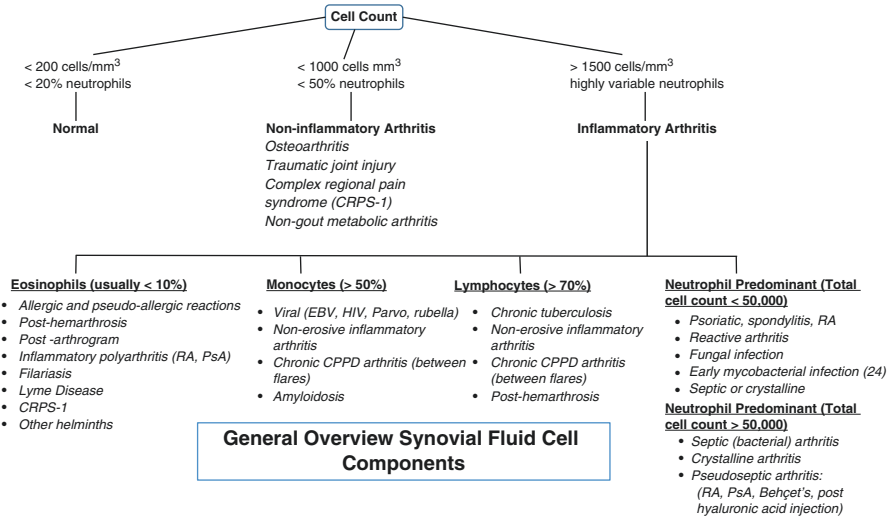

Adapted from Maxime Dougados [5]

evidence of inflammation other than joint effusion containing 2000–10,000 cells/mm^3. The knee is the most common joint involved and resolves rapidly with the use of NSAIDs with no sequelae [25] (Table 5.1).

Summary

Synovial fluid analysis remains an important laboratory tool for distinguishing the more than 100 different types of inflammatory and non-inflammatory arthropathies from each other. As clinicians, we should rely most heavily on our history taking and physical examination to diagnose various musculoskeletal complaints. The enumeration of the various types of immune cells in the synovial fluid can certainly add credence to the suspected diagnosis or insert concern that we have not yet arrived at the proper conclusion. It is important to remember that the cellular content of synovial fluid is highly dynamic and assigning a particular cell concentration or cell type to any inflammatory or non-inflammatory arthritis is an imperfect approach.

References

1. Pascual E, Jovaní V. Synovial fluid analysis. Best Pract Res Clin Rheumatol. 2005;19(3):371–86.
2. Ropes MW, Rossmeisl EC, Bauer W. The origin and nature of normal human synovial fluid. J Clin Invest. 1940;19(6):795–9.

3. McEwen C. Cytologic studies on rheumatic fever. II cells of rheumatic exudates. J Clin Invest. 1935;14(2):190–201.
4. Kling DH. Synovial cells in joint effusion. J Bone and Joint Surg. 1930;12:867–70.
5. Dougados M. Synovial fluid cell analysis. Baillieres Clin Rheumatol. 1996;10(3):519–34.
6. Saadalla A, Aguirre JJ, Wockenfus AM, et al. Evaluation of automated synovial fluid total cell count and percent polymorphonuclear leukocytes on a Sysmex XN-1000 analyzer for identifying patients at risk of septic arthritis. Clin Chim Acta. 2020;510:416–20.
7. Kerolus G, Clayburne G, Schumacher HR Jr. Is it mandatory to examine synovial fluids promptly after arthrocentesis? Arthritis Rheum. 1989;32(3):271–8.
8. Schumacher HR Jr, Sieck MS, Rothfuss S, et al. Reproducibility of synovial fluid analysis. A study among four laboratories. Arthritis Rheum. 1986;29(6):770–4.
9. Scanzello CR, Umoh E, Pressler F, et al. Local cytokine profiles in knee osteoarthritis: elevated synovial fluid interlukin-15 differentiates early from end-stage osteoarthritis. Osteoarth Cartilage. 2009;17(8):1040–8.
10. Al-Mughales J, Blyth TH, Hunter JA, et al. The chemoattractant activity of rheumatoid synovial fluid for human lymphocytes is due to multiple cytokines. Clin Exp Immunol. 1996;106(2):230–6.
11. Gómez-Aristizábal A, Gandi R, Mahomed NN, et al. Synovial fluid monocyte/macrophage subsets and their correlation to patient-reported outcomes in osteoarthritis patients: a cohort study. Arthritis Res Therap. 2019;21(1):26–36.
12. Dougados M, Nguyen M, Menkès CJ, et al. Monocytic arthritis: study of their clinical significance apropos 43 cases. Rev of Rhum Mal Osteoaartic. 1987;54(7–9):545–8.
13. Crawford AM, NcNeil DL, Fritzler MJ, Kinsella TD. The A.H.A. syndrome. Arthritis, hives and acquired anigoederma. Arthritis Rheum. 1984;27:Abstract D62.
14. Gordan DA, Pruzanski W, Ogryzlo MA. Synovial fluid examination for the diagnosis of amyloidosis. Ann Rheum Dis. 1973;32:428–30.
15. Wright HL, Moots RJ, Bucknall RC, Edwards SW. Neutrophil function in inflammation and inflammatory diseases. Rheumatology. 2010;49(9):1618–31.
16. Watson F, Robinson JJ, Phelan M, et al. Receptor expression in synovial fluid neutrophils from patients eith rheumatoid arthritis. Ann Rheum Dis. 1993;52:354–9.
17. Cañete JD, Celis R, Noordenbos T, et al. Distinct synovial immunopathology in Beçhet disease and psoriatic arthritis. Arthritis Res Ther. 2009;11:R17.
18. McGillicuddy DC, Shah KH, Friedberg RP, et al. How sensitive is the synovial fluid white blood cell count in diagnosing septic arthritis? Amer J Emerg Med. 2007;25(7):749–52.
19. Coutlakis PJ, Roberts WN, Wise CM. Another look at synovial fluid leukocytes and infection. J Clin Rheumatol. 2002;8:67–71.
20. Call RS, Ward JR, Samurlson CO. 'Pseudoseptic'artthritis in patients with rheumatoid arthritis. West J Med. 1985;143:471–3.
21. Paul P, Paul M, Dey D, et al. Pseudoseptic arthritis: an initial presentation underlying psoriatic arthritis. Cureus. 2021;13:e14660. https://doi.org/10.7759/cureus.14660.
22. Oppermann BP, Cote JK, Morris SJ, et al. Pseudoseptic arthritis: a case series and review of the literature. Case Rep Inf Dis. 2011; https://doi.org/10.1155/2011/942023.
23. Sedrak P, Hacche P, Horner NS, et al. Differenial characteristics and management of pseudoseptic arthritis following hyaluronic acid injection is a rare complication: a systematic review. J ISAKOS: Disord Orthoped Sports Med. 2021;6:94–101.
24. Foocharen C, Nanagara R, Foocharoen T, et al. Clinical features of tuberculous septic arthritis in Khon Kaen, Thailand: a 10-year retrospective study. Southeast Asian J Trop Med Public Health. 2010;41:1438–46.
25. Vázquez-Triñanes C, Sopheña B, González-González L, et al. Synovial fluid eosinophilia: a case series with a long follow-up and literature review. Rheumatology. 2013;52(2):346–51.
26. Amor B, Benhamou CL, Dougados M, et al. Eosinophilic arthritis and general review of the significance of articular eosinophilia. Rev Rhum Mal Osteoartic. 1983;50(10):659–64.

27. Kay J, Eichenfield AH, Athreya BU, et al. Synovial fluid eosinophilia in Lyme disease. Arthritis Rheum. 1988;31:1384–9.
28. Brown JP, Rola-Plezzcyznski M, Menard HA. Eosinophilic synovitis: clinical observations on a new recognized subset of patients with dermatographism. Arthritis Rheum. 1986;29(9):1147–51.

Chapter 6
Microbiology and Culture Identification of Infections

Susan M. Harrington

Establishing a diagnosis of joint infection and accurately identifying the etiologic agent help to inform therapeutic choices and influence patient management options. Advances in the use of biomarkers and molecular methods have improved diagnosis, but culture of synovial fluid is still the best means for determining the infecting microbe and providing in vitro antimicrobial susceptibility test results. Culture of synovial fluid for diagnosis of joint infection can be challenging depending on clinical presentation, previous therapy, and the particular etiologic agent. Indeed, the sensitivity of culture reported in the literature is highly variable [1, 2]. However, culture techniques have improved with consequent increases in organism recovery. Attention to variables such as collection technique, specimen volume, culture media, and incubation time is essential to maximize successful recovery of pathogens and minimize false positive or negative results. Molecular methods have also brought advances in diagnosis and are addressed in another chapter.

The Pathogens

The etiologic agents of native joint infection vary depending on patient age and risk factors. Gram-positive species are the most common pathogens with *Staphylococcus aureus* being the leading pathogen in almost all risk groups. Other more common pathogens include the pyogenic streptococci, especially *S. agalactiae, S. pneumoniae*, *P. aeruginosa*, enteric gram-negative rods, and *N. gonorrhoeae*. *Kingella kingae* is a pathogen recognized in joint infection of young children. *Brucella*

S. M. Harrington (✉)
Pathology and Laboratory Medicine Institute, Cleveland Clinic, Cleveland, OH, USA
e-mail: Harrins2@ccf.org

B. F. Mandell (ed.), *Synovial Fluid Analysis and The Evaluation of Patients With Arthritis*, https://doi.org/10.1007/978-3-030-99612-3_6

species may be encountered in patients from countries in which livestock are not vaccinated and dairy products are unpasteurized. Polymicrobial infection, including anaerobic bacteria, makes up a few percentage of cases. Mycobacteria, anaerobes, and other species are less common pathogens, but are nevertheless important agents to consider, depending on clinical presentation, risk factors, and underlying illness [3, 4]. The need for special culture or molecular methods should be kept in mind if culture for the most common species does not identify a pathogen.

Prosthetic joint infection (PJI) that occurs within weeks to 3 months of a surgical procedure (early infection) is usually caused by virulent species such as *S. aureus* and gram-negative rods. When prosthetic joints fail a few months to about 2 years after a procedure (delayed infection), these indolent infections are generally caused by less virulent species often found on the skin such as *Cutibacterium* (formerly *Propionibacterium*) *acnes*, coagulase-negative *Staphylococcus* spp., and *Corynebacterium* spp. Late infections that occur 2 or more years after surgery are generally caused by hematogenous seeding from various sources of infection [1].

Specimen Collection

To improve recovery of microbes it is recommended that antibiotics be withheld for 14 days prior to specimen collection [5]. If antibiotics have been administered, collection into blood culture bottles containing resins that chelate antibiotics may help improve yield. Asceptic technique is critical during joint fluid aspiration. The skin should be thoroughly cleansed using chlorhexidine gluconate, tincture of iodine, or other antiseptic agents. The site must be allowed to dry (at least 30 sec) in accordance with directions for the antiseptic. Otherwise, adequate antisepsis may not be achieved. The specimen is aspirated with a needle and syringe for transfer into a sterile specimen transport container(s) for transport to the laboratory.

Microbiologic assessment of synovial fluid should include Gram stain, culture on solid media, and culture in aerobic and anaerobic blood culture bottles (BCB). About 1 ml of fluid should be placed into a sterile transport tube for Gram stain and culture on solid media. Use of tubes with EDTA or heparin for culture should be discouraged as they may inhibit growth of bacteria [6]. Ideally, 1–10 ml of aspirated fluid should be transferred at bedside with equal volumes placed into aerobic and anaerobic BCB. Preference is usually given to the aerobic bottle if limited fluid is available. Of note, if blood culture bottles or other specimen transport containers with a rubber septum are used, the surface of the septum under the protective plastic cap must also be disinfected, according to the manufacturer's directions. When anaerobes are suspected, a small volume of fluid (0.5–1 ml) should be placed into anaerobic transport media. Otherwise, the specimen should be delivered immediately to the laboratory for culture to preserve bacteria with a strictly anaerobic metabolism as these species will not survive significant exposure to air. In general, anaerobes are more likely to survive in larger volume specimens [6].

One of the most challenging aspects of synovial fluid culture is the small volume that may be available and this often influences the choice of media used for culture. If 0.5 ml or less are aspirated, the fluid should not be gathered on a swab for culture. Swab cultures result in poor yields and may lend to specimen contamination [6, 7]. One option is to send the material to the laboratory immediately in the syringe without transfer to a sterile tube. Removal of the needle and capping the syringe prior to transport is required to prevent personal injury. Bedside inoculation of a few drops of fluid to chocolate agar, which supports the growth of nearly all bacteria and yeast, is another approach if only a few drops of fluid are aspirated. However, some laboratories prefer not to provide culture media to clinical areas because it is challenging to ensure proper storage and stability.

Albeit controversial, a technique in which 10 ml sterile saline is instilled into the joint and fluid is re-aspirated has been advocated to overcome the "dry tap" situation. This saline lavage method raises concern over the opportunity for specimen contamination and whether the recovered fluid represents the fluid in the joint. In a large series of hip and knee PJI infections, sensitivity of synovial fluid culture results where adequate fluid volume was obtained was similar to sensitivity of culture using the saline lavage method when compared to results of tissue culture from the same patients. Specificity was slightly less with the dry tap method [2]. If the saline lavage method is used, it is important that as much fluid as possible is placed into aerobic and anaerobic BCB to enhance recovery of small numbers of pathogens.

Specimen Handling and Transport

Specimens should always be transported to the laboratory as soon as possible to prevent loss of viable organisms. Refrigeration is discouraged as it may reduce recovery of some of the more fastidious pathogens such as *Streptococcus pneumoniae* and *Neisseria gonorrhoeae* [6]. Inoculation of BCB at bedside reduces concern over loss during transport of fastidious species or organisms in low numbers because any pathogens present are placed directly into an optimal growth medium. In this case the BCB medium serves as both a transport and a culture medium. However, when rapid transport to the microbiology laboratory is available some centers prefer to receive fluid in the microbiology laboratory in a sterile tube or capped syringe to ensure specimen is available for Gram stain, to prevent aerosolization of infectious agents at bedside, and to minimize contamination that may occur with manipulation outside of the laboratory biosafety cabinet.

In large health care systems where microbiology services have been consolidated to a central laboratory, timely transport of irretrievable specimens such as joint fluid can be challenging. Specimens may be collected at sites without a laboratory or with minimal laboratory testing services. Laboratories at smaller sites may receive the specimen and subsequently transport to a central microbiology laboratory. If biosafety cabinets and trained personnel are available, some systems elect to make

(and read) Gram stains, and inoculate culture plates and BCB at the smaller laboratory site, prior to transport. Although it may seem counter-intuitive, BCB designed for automated blood culture detection systems should not be incubated at the smaller laboratory, if the dedicated blood culture instrument is at the centralized microbiology laboratory. Pre-incubation of BCB can cause subsequent detection on the automated blood culture instrument to be delayed because the instruments detect the change in growth during bacterial log phase. Often, however, smaller laboratories are not equipped to provide any microbiology specimen processing or culture services. Frequent couriers to move specimens to the central microbiology laboratory are essential in these circumstances. The approach to specimen handling and transport practices may vary depending on the health care system and should be optimized through communication between laboratory services personnel and clinicians.

Stains

The Gram stain is a valuable test because it provides early information on the presence of microbes, and can thereby influence therapeutic choices. The presence of inflammatory cells or observation of intracellular organisms on primary stain can be helpful diagnostic aids. Sometimes significant organisms may be present on Gram stain that do not grow in culture and this information may direct further studies or suggest the presence of non-viable, antibiotic-treated microbes. Although Gram stains have high specificity, sensitivity is generally low and stains are less sensitive than culture. Thus, negative stain results should never be used to rule-out infection [1, 5]. Like Gram stain and culture, fungal fluorescent and acid fast stains should be performed if fungal or mycobacterial cultures are ordered.

Culture Media and Incubation

Most bacterial culture media sets will contain at least chocolate agar and Trypticase soy 5% sheep blood agar plates as almost all bacteria and yeasts will grow on these media. Synovial fluid cultures are generally not mixed or heavily contaminated with skin flora and the use of media to select for gram-negative pathogens, e.g., MacConkey agar or gram-positive pathogens is generally not required, but can be helpful. Selective media should be added if multiple bacterial morphologies are observed on Gram stain. For anaerobic culture media such as Brucella blood agar or CDC anaerobic sheep blood agar are added. Synovial fluid culture plates are incubated for at least 5 days (aerobic culture) at 35 °C in a 5% CO_2 atmosphere. Cultures of specimens incubated under anaerobic conditions should be incubated 7 days with extended (14 days) incubation of specimens aspirated from prosthetic joints (see

special considerations for PJI). Somewhat controversial because of the likelihood of contamination, addition of thioglycolate or other broth that supports anaerobes may be incorporated to improve sensitivity, especially if PJI is suspected or BCB have not been inoculated [8].

As early as 1986 it was recognized that culture of joint fluid in BCB could increase recovery of pathogens by more than 20% [9]. At that time automated blood culture systems were not widely used for culture of body fluids and detection of growth was performed by manual subculture. Better detection in BCB media is largely due to the greater volume cultured. The drop of specimen planted to solid media is generally 25 to 50 μl, whereas between 0.5 ml and 10 ml (10 to 200×) is placed in BCB. Moreover, newer formulations of blood culture media contain resins that chelate antibiotics and components of the innate immune system, improving yield [10]. Such media are used routinely in most laboratories. BCB are incubated for 5 days in automated blood culture instruments that detect growth without periodic, manual sampling from the bottles. BCB were shown to be especially effective in the recovery of *Kingella kingae* in an early evaluation of children with septic arthritis [11].

As fungal and mycobacterial etiologies are rare, and given the relatively small amount of synovial fluid that may be available, prioritizing bacterial culture is appropriate [3, 12, 13]. If bacterial cultures remain negative, but symptoms persist and cell counts and biomarkers are supportive, fungal and mycobacterial culture may be indicated. Both *M. tuberculosis* and the non-tuberculous mycobacteria (NTM) have been associated with joint infection. Some NTM that may be agents of joint infection, particularly *M. ulcerans*, *M. marinum*, *M. haemophilum, M. chelonae*, and *M. immunogenum*, grow preferentially at about 30 °C. Mycobacteriology laboratories generally culture specimens from skin and soft tissue and any specimen from an extremity, including joints at both 35 °C and 30 °C. Additionally, *M. haemophilum* requires a source of hemin. *M. marinum* infections may be paucibacillary emphasizing the need for adequate specimen. If exposure history suggests any of these pathogens, it is helpful to alert the mycobacteriology laboratory to ensure appropriate culture methods are used [14].

Mycoplasma hominis and *Ureaplasma* species have been associated with joint infection in organ transplant patients and those with hypogammaglobulinemia [15, 16]. These pathogens sometimes grow on anaerobic culture plates after several days of incubation, but characterization can be challenging as these cell wall-deficient species do not appear on the Gram stain. Specialized culture methods available at reference laboratories are recommended if these species are suspected. Molecular methods may be more suitable for these and other rare pathogens that are difficult to grow in vitro. Clinicians should consult with the microbiology laboratory prior to specimen collection to determine required volumes and transport media required for detection of mycoplasma.

Special Considerations for Diagnosis of Prosthetic Joint Infections

Diagnosis of prosthetic joint infections is an area of active study and a number of advancements have been achieved in recent years. The American Academy of Orthopedic Surgeons (AAOS) recommends the use of aerobic and anaerobic cultures of synovial fluid for the diagnosis of PJI using methods such as those described above. However, additional methods have proven useful for intraoperative microbiologic analysis of PJI. Atkins et al. demonstrated that the isolation of the same organism from the culture of ≥3 independent tissue or synovial fluid specimens had the highest posttest probability of correlating to infection. At least 3, and preferably 5 or 6 specimens for culture should be collected when PJI is being assessed [17]. Subsequently, a meta-analysis demonstrated that the same organism in ≥2 tissue cultures was useful to rule-in PJI [5]. Swabs should not be collected for culture because they sample a small amount of material and are more likely to produce false-positive results due to contamination. Tissue and fluid specimens can be obtained and provide higher yield, thus reducing false-negative results [18].

Cutibacterium acnes is a common pathogen, particularly in delayed infections and often associated with shoulder implants. Incubation of cultures for up to 14 days significantly improves recovery of *C. acnes*, coryneforme organisms, and other gram-positive anaerobic organisms [19]. Incubation longer than 14 days tends to increase recovery of contaminating microbes and is not usually considered necessary [20]. The 14-day culture may be accomplished using solid agar plates and/or by incorporating an anaerobic broth such as thioglycolate. Shorter time to positive culture results may be achieved if anaerobic conditions are strictly observed during the specimen transport, processing, and incubation phases and if thioglycolate broth is included [8].

Infection associated with a bacterial biofilm on a prosthetic joint or other hardware can be difficult to detect by standard culture of tissue or synovial fluid. Sonication of prostheses has been shown to remove the bacterial biofilm with resulting improvement in the diagnosis of PJI. Trampuz evaluated total knee and hip prostheses using the sonication method and demonstrated 17.7% greater sensitivity than tissue culture [21]. Sonication of prosthetic joints is a time-consuming process that is challenging to implement in busy microbiology laboratories. However, this diagnostic method can be a useful adjunct to routine culture of synovial fluid and tissue.

Summary As orthopedic procedures have been refined and become more common in an aging population, so too microbiologic culture methods have improved. Gram stain and culture remain essential tools for diagnosis of joint infections and advances in culture methods including the use of blood culture bottles, extending incubation for detection of specific pathogens, and sonication of implants have improved diagnostic capability. Close attention to best practice and communication between orthopedic surgeons, the infectious diseases consult service and the microbiology laboratory will improve outcomes for patients.

References

1. Zimmerli W, Trampuz A, Ochsner PE. Prosthetic-joint infections. N Engl J Med. 2004;351(16):1645–54. https://doi.org/10.1056/NEJMra040181.
2. Partridge DG, Winnard C, Townsend R, Cooper R, Stockley I. Joint aspiration, including culture of reaspirated saline after a 'dry tap', is sensitive and specific for the diagnosis of hip and knee prosthetic joint infection. Bone Joint J. 2018;100-B(6):749–54. https://doi.org/10.1302/0301-620X.100B6.BJJ-2017-970.R2.
3. Ross JJ. Septic arthritis of native joints. Infect Dis Clin N Am. 2017;31(2):203–18. https://doi.org/10.1016/j.idc.2017.01.001.
4. García-Arias M, Balsa A, Martín Mola E. Septic arthritis. Best Pract Res Clin Rheumatol. 2011;25(3):407–21. https://doi.org/10.1016/j.berh.2011.02.001.
5. Tubb CC, Polkowksi GG, Krause B. Diagnosis and prevention of periprosthetic joint infections. J Am Acad Orthop Surg. 2020;28(8):e340–8. https://doi.org/10.5435/JAAOS-D-19-00405.
6. Thomson RB. Body fluid cultures (excluding blood, cerebrospinal fluid, and urine). In: Leber AL, editor. Clinical microbiology procedures handbook. 4th ed. Washington, D.C.: ASM Press; 2016. p. 3.5.1–9. https://doi.org/10.1128/9781555818814.ch3.5.
7. Geller JA, MacCallum KP, Murtaugh TS, Patrick DA Jr, Liabaud B, Jonna VK. Prospective comparison of blood culture bottles and conventional swabs for microbial identification of suspected periprosthetic joint infection. J Arthroplast. 2016;31(8):1779–83. https://doi.org/10.1016/j.arth.2016.02.014.
8. Shannon SK, Mandrekar J, Gustafson DR, Rucinski SL, Dailey A, Segner RE, et al. Anaerobic thioglycolate broth culture for recovery of *Propionibacterium acnes* from shoulder tissue and fluid specimens. J Clin Microbiol. 2013;51(2):731–2. https://doi.org/10.1128/JCM.02695-12.
9. von Essen R, Hölttä A. Improved method of isolating bacteria from joint fluids by the use of blood culture bottles. An Rheum Dis. 1986;45(6):454–7. https://doi.org/10.1136/ard.45.6.454.
10. Hughes JG, Vetter EA, Patel R, Schleck CD, Harmsen S, Turgeant LT, et al. Culture with BACTEC Peds plus/F bottle compared with conventional methods for detection of bacteria in synovial fluid. J Clin Microbiol. 2001;39(12):4468–71. https://doi.org/10.1128/JCM.39.12.4468-4471.2001.
11. Yagupsky P, Dagan R, Howard CW, Einhorn M, Kassis I, Simu A. High prevalence of *Kingella kingae* in joint fluid from children with septic arthritis revealed by the BACTEC blood culture system. J Clin Microbiol. 1992;30(5):1278–81. https://doi.org/10.1128/jcm.30.5.1278-1281.1992.
12. Saha B, Young K, Kahili-Heede M, Lim SY. Septic arthritis of native joints due to *Mycobacteirum avium* complex: a systematic review of case reports. Semin Arthritis Rheum. 2021;51(4):813–8. https://doi.org/10.1016/j.semarthrit.2021.05.012.
13. Eid AJ, Berbari EF, Sia IG, Wengenack NL, Osmon DR, Razonable RR. Prosthetic joint infection due to rapidly growing mycobacteria: report of 8 cases and review of the literature. Clin Infect Dis. 2007;45(6):687–94. https://doi.org/10.1086/520982.
14. Lehman D. Mycobacterium tuberculosis and nontuberculous mycobacteria. In: Mahon C, Lehman D, editors. Textbook of diagnostic microbiology. 6th ed. St. Louis: Elsevier, Inc.; 2019.
15. Furr PM, Taylor-Robinson D, Webster AD. Mycoplasma and ureaplasmas in patients with hypogammaglobulinaemia and their role in arthritis: microbiological observations over twenty years. Ann Rheum Dis. 1994;53(3):183–7. https://doi.org/10.1136/ard.53.3.183.
16. Mian AN, Parney AC, Mendley SR. Mycoplasma hominis septic arthritis in a pediatric renal transplant recipient: case report and review of the literature. Am J Transplant. 2005;5(1):183–8. https://doi.org/10.1111/j.1600-6143.2004.00634.x.
17. Atkins BL, Athanasou N, Deeks JJ, Crook DW, Simpson H, Peto TE, et al. Prospective evaluation of criteria for microbiological diagnosis of prosthetic-joint infection at revision arthroplasaty. The OSIRIS collaborative study group. J Clin Microbiol. 1998;36(10):2932–9. https://doi.org/10.1128/JCM.36.10.2932-2939.1998.

18. Aggarwal VK, Higuera C, Deirmengian G, Parvizi J, Austin MS. Swab cultures are not as effective as tissue cultures for diagnosis of periprosthetic joint infection. Clin Orthop Relat Res. 2013;471(10):3196–203. https://doi.org/10.1007/s11999-013-2974-y.
19. Schäfer P, Fink B, Sandow D, Margull A, Berger I, Frommelt L. Prolonged bacterial culture to identify late periprosthetic joint infection : a promising strategy. Clin Infect Dis. 2008;47(11):1403–9. https://doi.org/10.1086/592973.
20. Butler-Wu SM, Burns EM, Pottinger PS, Magaret AS, Rakeman JL, Matsen FA 3rd, et al. Optimization of periprosthetic culture for diagnosis *of Propionibacterium acnes* prosthetic joint infection. J Clin Microbiol. 2011;49(7):2490–5. https://doi.org/10.1128/JCM.00450-11.
21. Trampuz A, Piper KE, Jacobson MJ, Hanssen AD, Unni KK, Osmon DR, et al. Sonication of removed hip and knee prostheses for diagnosis of infection. N Engl J Med. 2007;357(7):654–63. https://doi.org/10.1056/NEJMoa061588.

Chapter 7
Molecular Microbiology for Diagnosing Infectious Arthritis

Joshua A. Lieberman and Stephen J. Salipante

Introduction to Molecular Microbiology Testing of Synovial Fluid and Joint Specimens

Molecular methods to detect pathogens comprise an important suite of assays for detecting and identifying pathogens that are difficult to cultivate in vitro, and to diagnose specimens that are not suitable for culture. Moreover, recent studies indicate that the use of molecular assays in conjunction with conventional culture increases diagnostic yield compared to the use of either assay alone [1, 2], arguing for their incorporation into initial diagnostic workups. This chapter summarizes the role of molecular methods in evaluating joint-space infections, with particular emphasis on pre-analytical considerations like specimen selection and handling, and to principles of test selection that will maximize detection of important pathogens from these anatomic sites.

Molecular diagnostic techniques rely on purification, amplification, and detection of organism-specific nucleic acid (either DNA or RNA). These tools can be divided into "pathogen-specific" and "broad-range" assays, which have important trade-offs in both sensitivity and turnaround time (TAT). Briefly, broad-range assays can detect a wide array of pathogens but require sequencing to generate results, which increases TAT. This is typically achieved by conventional chain-termination sequencing and subsequent taxonomic classification using a database of known microbial reference sequences. In contrast, species-specific assays typically have higher sensitivity for their intended target organism and may not require sequencing, potentially reducing TAT.

J. A. Lieberman (✉) · S. J. Salipante
Department of Laboratory Medicine and Pathology, University of Washington, School of Medicine, Seattle, WA, USA
e-mail: joshuaal@uw.edu; stevesal@uw.edu

B. F. Mandell (ed.), *Synovial Fluid Analysis and The Evaluation of Patients With Arthritis*, https://doi.org/10.1007/978-3-030-99612-3_7

Molecular-based pathogen identification offers several advantages over conventional microbiological techniques: detection of fastidious organisms, utility following antimicrobial treatment, and applicability to frozen or fixed tissues and fluids.

Multiple studies have examined the clinical utility and performance of molecular diagnostic methods as specifically applied for diagnosis of joint infections. Differences of inclusion criteria and analytical methods lead to a wide range of estimated sensitivities and specificities, ranging from 67.1–95.7% and 12.3–97.8%, respectively, in a recent systematic review [3]. Large, multicenter trials of prosthetic joint infections (PJI) have reported sensitivities over 70% and specificities ~95% for broad-range bacterial PCR [4] while smaller trials have reported 100% sensitivity and 99.5% specificity [5]. When panels of broad-range PCR assays were performed after conventional cultures yielded negative results, synovial fluids had a 16.5% positivity rate with half of results determined to be clinically significant [6]. Among culture-negative specimens submitted for broad-range PCR panels, 30% of specimens had a positive PCR and positivity rate was similar for orthopedic and non-orthopedic specimens [7]. The same study found 25% of results – 11 of 21 positive and 7 of 50 negative – changed clinical management; two test results were determined to be false positives, giving a specificity of 94% [7]. Collectively, these findings indicate that molecular methods are both accurate and useful as primary diagnostic tools to rule in and rule out infectious arthritides.

Nonetheless, molecular assays have several important drawbacks. Because nucleic acid amplification techniques are highly sensitive, exogenous introduction of microbial genetic material can lead to false positives or mask the presence of a true pathogen. In addition, molecular assays alone are usually insufficient to determine microbes' susceptibility to antimicrobial treatments, outside of intrinsic resistance profiles inherent to particular species of microorganisms. Finally, clinically available broad-range assays applicable to joint infections are typically confined to identifying representatives from a single microbial Kingdom. Unbiased, universal, metagenomic next-generation sequencing assays theoretically able to detect pathogens of any kind (viral, eukaryotic, or bacterial) are emerging technologies with applications for joint space infections. Such metagenomic assays can currently be performed on plasma but are in development for synovial fluid; these are briefly discussed at the end of this chapter.

Benefits and Limitations of Available Techniques

The range of available molecular diagnostic assays continues to expand. Optimal assay selection should reflect the clinical context – post-infectious arthritis, PJI or native joint infection, immunosuppression, travel or social history, patient age, and concurrent microbiologic findings – with suspected pathogens. Recommended molecular tests for prevalent and/or important infectious arthritis pathogens [8–13] are summarized in Table 7.1.

Table 7.1 Pathogens frequently implicated in septic arthritis and recommended molecular testing strategies

Pathogen	Most common infection type	Recommended molecular testing strategies
Bacterial		
Staphylococcus aureus and other staphylococci	Native joint infection and PJI	Broad-range
Streptococcus spp	Native joint infection, PJI, and reactive arthritis	Broad-range
Enterobacteriaceae spp	Native joint infection, PJI, and reactive arthritis	Broad-range
Borrelia burgdorferi	Native joint infection and reactive arthritis	Pathogen-specific
Haemophilus influenzae	Native joint infection	Broad-range
Neisseria spp	Native joint infection	Broad-range
Neisseria gonorrhoeae	Native joint infection	Pathogen-specific, broad-range
Tropheryma whippelii	Native joint infection	Pathogen-specific
M. tuberculosis and other *Mycobacteria* spp	Native joint infection	Pathogen-specific
Cutebacterium acnes (formerly *Proprionibacterium acnes*) and other *Cutebacterium* spp	PJI	Broad-range
Corynebacterium spp	PJI	Broad-range
Pseudomonas aeruginosa	Native joint infection and reactive arthritis	Broad-range
Mycoplasma pneumoniae	Reactive arthritis	Pathogen-specific
Ureoplasma urealyticum	Reactive arthritis	Pathogen-specific
Clamydia trachomatis	Reactive arthritis	Pathogen-specific
Campylobacter spp.	Reactive arthritis	Broad-range
Fungal		
Candida spp	Native joint infection and PJI	Broad-range
Aspergillus spp	Native joint infection and PJI	Pathogen-specific, broad-range
Viral		
Parvovirus B19	Viral arthritis	Serology, pathogen-specific (joint fluid or blood)
Hepatitis B	Viral arthritis	Serology, pathogen-specific (blood)
HCV	Viral arthritis	Serology, pathogen-specific (blood)
HIV	Viral arthritis	Serology, pathogen-specific (blood)

(continued)

Table 7.1 (continued)

Pathogen	Most common infection type	Recommended molecular testing strategies
HTLV-I	Viral arthritis	Serology, pathogen-specific (blood)
Alphaviruses	Viral arthritis	Serology, consult Department of Health for additional testing
SARS-CoV-2	Reactive arthritis	Serology, pathogen-specific (respiratory)

Most molecular microbiology assays applicable to infectious arthritis are Laboratory-Developed Tests performed at laboratories certified to conduct high-complexity testing. Sequence-based identification of microbial isolates is relatively widespread, but few laboratories offer such testing directly on patient specimens. Larger "reference laboratories" accept specimens from outside their hospital system or local patient catchment, and typically provide a variety of molecular microbiology testing options, including broad-range and pathogen-specific tests. Since multiple assays can frequently be performed using nucleic extracted from one specimen, selecting a laboratory that offers the widest range of applicable assays may be valuable in conserving sample and minimizing TAT. Many reference laboratories enumerate the tests they perform in an online test guide/directory and include instructions for specimen handling and acceptable specimen types. When in doubt, we recommend consulting the test directory and/or staff of the performing laboratory before ordering molecular assays.

Broad-Range Assays and Next-Generation Sequencing

Broad-range assays that detect bacteria, mycobacteria/acid fast bacilli (AFB), and fungi are available for clinical use [6, 7]. These assays function by amplifying taxonomically informative regions of essential genes that are carried by their targeted organisms, and by subsequently classifying the product by DNA sequencing [14, 15]. The term "universal PCR" appears in the molecular diagnostic literature and frequently is meant to indicate a panel of broad-range assays for fungal, bacterial, and mycobacterial organisms performed concurrently [6, 7]. As their name suggests, broad-range assays are capable of detecting a wide assortment of organisms relevant to infectious arthritis including *Staphylococcus aureus* and *Neisseria gonorrhoeae* [16, 17]. Broad-range assays are particularly important for diagnosing PJI, as pathogen-specific tests are not currently available for *Cutebacterium* spp. (formerly *Proprionibacterium* spp.; see Table 7.1), which are pathogens in this setting and challenging to recover by microbiological culture [18]. The utility of broad-range assays may be limited by polymorphisms at primer-binding sites in certain organisms, like spirochetes [19], or insufficient species-specific sequence

variation to resolve closely related species, such as within Enterobacteriaceae [20]. To date, broad-range assays for viruses in joint-space infection have not been developed, owing to the biological lack of a singular nucleic acid target that is carried by all, or even most, viral taxa.

Polymicrobial infections, processes involving two or more discrete species, cannot be resolved by prevalent, conventional molecular methods like polymerase chain reaction (PCR) with subsequent chain-termination sequencing. These methods produce a single analog signal that, in the presence of multiple microbial templates, result in conflicting, superimposed data that are generally uninterpretable. In contrast, next-generation sequencing (NGS) is a massively parallel approach that allows interrogation of individual DNA fragments. NGS assays can thereby resolve each component of the admixed genetic material [21]. Such NGS-based assays for bacteria may be more sensitive than conventional microbial culture in detecting minor constituents of the infecting population [21]. Currently, clinically validated NGS assays that can resolve polymicrobial joint infections are limited to detection of bacteria, including mycobacteria. Use of NGS assays add cost and TAT, but can identify organisms that are missed by culture because they are difficult or impossible to cultivate in vitro, because their growth has been overwhelmed by more abundant species; or because have been rendered non-viable by prior antibiotic/antifungal treatment [1].

Pathogen-Specific Assays

Pathogen-specific assays are an important tool since they can often detect organisms with a lower limit of detection than their broad-range counterparts, and may better distinguish between closely related species [21]. Pathogen-specific assays may also have faster TAT, since many do not require a sequencing step for interpretation. Since these assays are targeted to particular organisms, they are best deployed either when the clinical context suggests involvement of a particular pathogen, or as an adjunct to broad-range assays to investigate the presence of a suspected organism with greater levels of sensitivity. Viral assays are necessarily limited to this category of molecular testing.

Multiple pathogen-specific assays have been developed for organisms relevant to joint infections and have high utility in organisms that are challenging to recover by conventional methods. Several *Mycoplasma* spp. and *Ureaplasma* spp. have the potential to cause arthritis [22]: molecular testing for these organisms is potentially of high yield, as they do not reliably grow in culture, replicate slowly in vitro, and are invisible to Gram staining due to the absence of a cell wall. Arthritis is also an important manifestation of *Tropheryma whipplei* infection and, like *Mycoplasma* spp. and *Ureaplasma* spp., the organism is difficult to cultivate and to identify by Gram stain [23]. *Borrelia burgdorferi*, the most common causative agent of Lyme disease, can frequently cause joint pain. It, too, is difficult to culture [24], and molecular testing for *B. burgdorferi* in synovial fluid has higher sensitivity than

culture [25]. Clinically available tests for each of these pathogens – *Mycoplasma* spp., *T. whipplei*, and *Borrelia* spp. – are available at reputable reference laboratories.

For viral arthritis, serologic assays and nucleic acid amplification tests (NAAT) performed on peripheral blood are the most common diagnostic assays performed [9]. Some viruses, including DNA viruses like parvovirus B19 and Epstein-Barr virus, have been directly detected in synovial fluid specimens [26]. Molecular assays from sites of primary viral infection, such as respiratory sites in cases of post-COVID-19 infectious arthritis [13] may aid in diagnosis.

Acceptable Specimen Types and Specimen Handling

Specimen Types

Like culture, molecular methods may be used to identify pathogens directly from patient specimens, including body fluids and tissues. We are not aware of contraindications to submission of synovial fluid for molecular testing, provided the performing laboratory has validated this specimen type. Molecular testing can also be used to identify organisms that have been isolated using culture. Yet unlike culture, which requires viable organisms, molecular tests expand the range of possible samples to include previously frozen and refrigerated specimens, ethanol-fixed fluids submitted for cytopathology, and formalin-fixed paraffin-embedded (FFPE) tissues or cytopathology cell blocks. Although formalin exposure damages nucleic acids in a time-, dose-, and pH-dependent manner [27], multiple studies have reported equivalent diagnostic yields from fresh and FFPE specimens [2, 6, 7, 28]. The equivalent positivity of fresh and fixed specimens may be explained by compensatory effects of specimen selection or because the least damaging formulation of 10% neutral buffered formalin [27] is now common in anatomic pathology laboratories.

Specimen Handling

Although molecular diagnostics do not require that organisms are kept viable prior to testing, several pre-analytical variables can influence yield and diagnostic accuracy of test results (Table 7.2). Fresh specimens are preferred for most molecular testing, as they preserve the integrity of nucleic acids. Prolonged time at ambient temperature can lead to degradation of template nucleic acids and subsequent false negatives upon testing. Most laboratories recommend short storage periods at room temperature for fresh specimens (often 4–6 hours): after cultures have been inoculated, fresh specimens should be promptly refrigerated or frozen. If synovial fluid or

Table 7.2 Predicted impact of select clinical and specimen characteristics on recovery of microbial pathogens

Factors associated with lower recovery	Factors associated with higher recovery
Clinical features	
Alternative diagnosis likely History of non-infectious arthritis or auto-immune disease with joint involvement Prolonged symptom duration Native joint without trauma Immunocompetent	Clinical history suggestive of infection History of STI (e.g., *N. gonorrhoeae*) Cold agglutinin (e.g., *Mycoplasma* spp) History of rash, tick bite (e.g., *Borrelia, N. gonorrhoea*) Prosthetic joint deterioration (e.g., *C. acnes*) History of joint trauma (e.g., *S. aureus*) Immunocompromised (e.g., *T. whipplei*) Travel history (e.g., *Coccidioides* spp)
Specimen features	
Pauci-inflammatory or cellular infiltrate consistent with non-infectious cause No organisms directly observed *N.B. Mycoplasma spp*, *T. whipplei* stain poorly Formalin fixation Acid decalcification Poor storage conditions Small specimen volume (e.g., fine needle aspirate) Presence of inhibitors or contaminating microbial DNA Alternative pathogen already detected[a]	Cellular inflammatory pattern consistent with infection Organisms seen in synovial fluid/tissue Concurrent positive culture from another site and suspicion for dissemination Pathologist-selection of FFPE to optimize pre-analytical variables Larger specimen volume Fresh frozen specimen Sterile collection in DNA-free container

[a] For example, the yield of a fungal PCR is likely reduced if a pathogenic bacterium is recovered in culture or alternative molecular test. However, polymicrobial infections do occur

tissue is not submitted for molecular testing at the time of collection but may be requested later (e.g., if cultures yield negative results), then it is prudent to request that the laboratory freeze an aliquot at the earliest possible opportunity. Formalin fixation performed for extended periods or under suboptimal conditions can similarly damage specimen nucleic acids [27].

Collection of specimens into improper vessels can introduce substances that inhibit PCR amplification, such as EDTA or agarose present in gel swabs. DNAses, RNAses, or exonucleases that degrade template nucleic acids may be present in specimen collection vessels unless they are specifically certified to be free of these agents. Viral NAAT testing on peripheral blood, often performed after positive serologic tests, can typically be performed from a variety of peripheral blood collection tubes, including EDTA, serum separator, and plasma separator tubes. For evaluation of synovial fluid or swab specimens, universal transport media (UTM) is usually appropriate. Given these varied requirements, special attention must be paid to specimen collection practices to ensure that they conform with the requested testing. Consultation with the laboratory performing the tests may be warranted to confirm acceptable sample types and collection requirements.

Molecular assays are additionally susceptible to the introduction of exogenous microbes or microbial/viral nucleic acid. Such pre-analytical contamination can not

only result in false-positive results, but also mask legitimate pathogens in the sample and produce false negatives. Therefore, sterile collection technique and use of certified nucleic acid-free sample containers are critical components for specimen handling.

Exogenous microbial DNA can be found in surprising places, and it is important to recognize that "sterility", a lack of viable organisms, does not equate with an absence of microbial nucleic acids, which may persist after the destruction of an organism. Our laboratory has found that broth for microbial cultures and media used to grind patient specimens as part of culture preparation often contain microbial DNA, likely introduced as a byproduct of manufacturing processes. Similarly, we have identified sporadic lots of *Eswabs* that contain DNA from *Saccharomyces cerevisiae* (baker's yeast).

Specimen Storage

Optimal storage and transport conditions avoid overgrowth of contaminating organisms and prevent degradation of nucleic acids and are thereby important considerations to achieve maximal assay sensitivity. Laboratories routinely accept specimens stored for up to 1 week at 4 °C and specimens that have been frozen for at least several months. Fresh specimens should be transported to reference laboratories in insulated crates using cold packs or dry ice, for refrigerated or frozen specimens, respectively. Cold packs should be considered if sending FFPE specimens in hot regions or months to prevent melting of paraffin wax.

Specimen Selection to Maximize Clinical Yield

The ability to detect microbial DNA (or RNA) critically depends on selecting patient specimens with the highest pathogen load [6, 7]. If organisms are not observed – or in the case of viruses, not directly observable – then a pattern of inflammation consistent with infection serves as a reasonable proxy [6, 7]. Direct microscopic examination and/or inflammatory cell counts can aid in specimen selection for both fresh and frozen specimens. Regardless of organism burden, it is also important that nucleic acids undergo minimal damage prior to testing. For fresh specimens, freezing helps preserve nucleic acid in tissue. As noted earlier, FFPE specimens have been shown to have equivalent positivity rates to fresh tissue. One explanation is that selecting FFPE specimens with the most organisms or inflammatory pattern most suggestive of infection increases the pre-test probability of detection with a molecular method, thus "overcoming" the effects of formalin damage in aggregate. Nevertheless, fresh tissue is still generally preferred to formalin-fixed specimens, if it is available.

Special attention must be paid to FFPE specimens containing bone. In the anatomic pathology laboratory, such samples undergo decalcification in order to produce reliable histopathology. Samples decalcified with EDTA are acceptable for molecular methods. However, the faster and more commonly employed process of acid decalcification destroys nucleic acids and renders specimens unsuitable for molecular identification of pathogens. In our laboratory's experience, we have never successfully identified organisms that were visualized on histopathology when testing is performed on acid-decalcified specimens; alternative specimens, including fresh frozen bone, EDTA-decalcified bone, or adjacent soft FFPE tissue that did not undergo decalcification, are strongly recommended.

Additionally, specimen volume and type may impact clinical yield. Some studies have that shown small biopsies and fine-needle aspirates have significantly lower diagnostic yields compared to surgical resections [28]. Other work has reported lower positivity in fluids compared to either FFPE or fresh tissue [6]. These studies have aggregated anatomic sites for testing and conclusions are not necessarily specific to synovial fluid; nonetheless, specimen volume and type (fluid, aspirate, biopsy, resection) are likely to be important general considerations that impact the success diagnosis.

Finally, it is worth noting that optimizing pre-analytical variables and specimen selection is important not only to recover pathogens, but also to maximize confidence if ruling out infection with molecular tests. The impacts of select specimen and clinical factors on the recovery of pathogens by molecular diagnostic testing are summarized in Table 7.2. Clinical and specimen characteristics associated with lower pathogen recovery (Table 7.2) typically favor non-infectious etiologies.

Emerging Technology

Development of novel assays to identify infectious diseases in patient specimens continues to march on, despite identified research gaps in characterizing the use of extant molecular diagnostic tools for joint infections [29]. NGS assays are at the forefront of new test development and are likely to increase the spectrum of clinically available tests over the coming years. NGS assays targeting bacteria are already clinically available [1]. Given the added costs carried by NGS, some clinical laboratories only perform targeted NGS reflexively when initial assays suggest the presence of multiple pathogens, while other reports have suggested the feasibility of direct-from-specimen of NGS testing [30] including for orthopedic samples [31].

Perhaps the most exciting assays under development are unbiased "shotgun" NGS strategies, also termed metagenomic NGS (mNGS), in which bulk sequencing of all nucleic acids in a specimen is performed to detect pathogens from all kingdoms of life, including viruses. Identification of circulating microbial DNA from patient plasma by mNGS testing also has potential to detect PJIs, with positivity reported in ~67% of culture-positive and 57% of culture-negative cases [32]. Metagenomic NGS assays that can be performed directly on synovial fluids are

likely to become clinically available in the near future. Studies of mNGS assays performed on synovial fluid or tissue specimens in suspected joint infections have reported high sensitivities (> 90%) [33–36].

However, available data leave it uncertain whether mNGS is superior to either culture [34, 35] or broad-range PCR [34]. Interrogation of suspected PJIs with mNGS can identify pathogens that have not been detected by other methods, although these cases are typically in the minority (9.6%) [33]. Additional research on test performance and utility, as well as validation by appropriately certified clinical testing laboratories will be necessary for this class of emerging molecular diagnostics. Studies are also needed to determine whether, or for which patients, there is sufficient clinical utility of mNGS in diagnosing infectious arthritis to justify the high costs of the approach.

Conclusions

Molecular assays for infectious arthritis provide important diagnostic capabilities that are complimentary to those offered by conventional microbial culture. Available tests include both broad-range and pathogen-specific assays; the former offer breadth while the latter achieve higher sensitivity when specific organisms are suspected (e.g., Whipple's Disease, Lyme arthritis, mycoplasma-associated arthritis). Specimens submitted for testing should be selected to provide maximal organism burden or inflammatory patterns consistent with infection and adequate sample volumes. Care must be taken to protect nucleic acids from degradation by promptly freezing fresh specimens, optimizing fixation conditions, and avoiding acid treatment of bony specimens. Specimens should be collected and processed in order to prevent the introduction of contaminating microorganisms or their nucleic acids. Despite the negative effects of formalin on DNA quality, FFPE samples are appropriate for testing and provide an important sample reservoir. Although promising new NGS-based assays are on the horizon, research will be needed to critically evaluate their real-world clinical utility, risks of false-positives, and costs.

References

1. Cummings LA, Hoogestraat DR, Rassoulian-Barrett SL, Rosenthal CA, Salipante SJ, Cookson BT, et al. Comprehensive evaluation of complex polymicrobial specimens using next generation sequencing and standard microbiological culture. Sci Rep. 2020;10(1):5446.
2. Lieberman JA, Bryan A, Mays JA, Stephens K, Kurosawa K, Mathias PC, et al. High clinical impact of broad-range fungal PCR in suspected fungal sinusitis. J Clin Microbiol. 2021;59:JCM0095521.
3. Mitchell D, Perez J, Grau L, Summers S, Rosas S, Ong A, et al. Systematic review of novel synovial fluid markers and polymerase chain reaction in the diagnosis of prosthetic joint infection. Am J Orthop (Belle Mead NJ). 2017;46(4):190–8.

4. Bémer P, Plouzeau C, Tande D, Léger J, Giraudeau B, Valentin AS, et al. Evaluation of 16S rRNA gene PCR sensitivity and specificity for diagnosis of prosthetic joint infection: a prospective multicenter cross-sectional study. J Clin Microbiol. 2014;52(10):3583–9.
5. Kuo F-C, Lu Y-D, Wu C-T, You H-L, Lee G-B, Lee MS. Comparison of molecular diagnosis with serum markers and synovial fluid analysis in patients with prosthetic joint infection. Bone Joint J. 2018;100-B(10):1345–51.
6. Kerkhoff AD, Rutishauser RL, Miller S, Babik JM. Clinical utility of universal broad-range PCR amplicon sequencing for pathogen identification: a retrospective cohort study. Clin Infect Dis. 2020;71(6):1554–7.
7. Basein T, Gardiner BJ, Andujar Vazquez GM, Joel Chandranesan AS, Rabson AR, Doron S, et al. Microbial identification using DNA target amplification and sequencing: clinical utility and impact on patient management. Open Forum Infect Dis. 2018;5(11):ofy257.
8. Bariteau JT, Waryasz GR, McDonnell M, Fischer SA, Hayda CRA, Born CT. Fungal osteomyelitis and septic arthritis. JAAOS. 2014;22(6):390–401.
9. Marks M, Marks JL. Viral arthritis. Clin Med (Lond). 2016;16(2):129–34.
10. Li Z, Hou Y, Zhang B, Chen Y, Wang Q, Wang K, et al. Identifying common pathogens in Periprosthetic joint infection and testing drug-resistance rate for different antibiotics: a prospective, single center study in Beijing. Orthop Surg. 2018;10(3):235–40.
11. Geipel U. Pathogenic organisms in hip joint infections. Int J Med Sci. 2009;6(5):234–40.
12. Weston VC, Jones AC, Bradbury N, Fawthrop F, Doherty M. Clinical features and outcome of septic arthritis in a single UK Health District 1982–1991. Ann Rheum Dis. 1999;58(4):214–9.
13. Cincinelli G, Di Taranto R, Orsini F, Rindone A, Murgo A, Caporali R. A case report of monoarthritis in a COVID-19 patient and literature review: simple actions for complex times. Medicine (Baltimore). 2021;100(23):e26089.
14. Clarridge JE. Impact of 16S rRNA gene sequence analysis for identification of bacteria on clinical microbiology and infectious diseases. Clin Microbiol Rev. 2004;17(4):840–62.
15. Khot PD, Ko DL, Fredricks DN. Sequencing and analysis of fungal rRNA operons for development of broad-range fungal PCR assays. Appl Environ Microbiol. 2009;75(6):1559–65.
16. Jensen KH, Dargis R, Christensen JJ, Kemp M. Ribosomal PCR and DNA sequencing for detection and identification of bacteria: experience from 6 years of routine analyses of patient samples. APMIS. 2014;122(3):248–55.
17. Diemert DJ, Libman MD, Lebel P. Confirmation by 16S rRNA PCR of the COBAS AMPLICOR CT/NG test for diagnosis of Neisseria gonorrhoeae infection in a low-prevalence population. J Clin Microbiol. 2002;40(11):4056–9.
18. Levy PY, Fenollar F, Stein A, Borrione F, Cohen E, Lebail B, et al. Propionibacterium acnes postoperative shoulder arthritis: an emerging clinical entity. Clin Infect Dis. 2008;46(12):1884–6.
19. Wilson MR, Naccache SN, Samayoa E, Biagtan M, Bashir H, Yu G, et al. Actionable diagnosis of neuroleptospirosis by next-generation sequencing. N Engl J Med. 2014;370(25):2408–17.
20. McLean K, Rosenthal CA, Sengupta D, Owens J, Cookson BT, Hoffman NG, et al. Improved species-level clinical identification of enterobacteriaceae through Broad-Range dnaJ PCR and sequencing. J Clin Microbiol. 2019;57(11):e00986–19.
21. Cummings LA, Kurosawa K, Hoogestraat DR, SenGupta DJ, Candra F, Doyle M, et al. Clinical next generation sequencing outperforms standard microbiological culture for characterizing Polymicrobial samples. Clin Chem. 2016;62(11):1465–73.
22. Chen Y, Huang Z, Fang X, Li W, Yang B, Zhang W. Diagnosis and treatment of mycoplasmal septic arthritis: a systematic review. Int Orthop. 2020;44(2):199–213.
23. Puéchal X, Fenollar F, Raoult D. Cultivation of Tropheryma whipplei from the synovial fluid in Whipple's arthritis. Arthritis Rheum. 2007;56(5):1713–8.
24. Lochhead RB, Strle K, Arvikar SL, Weis JJ, Steere AC. Lyme arthritis: linking infection, inflammation and autoimmunity. Nat Rev Rheumatol. 2021;17(8):449–61.
25. Nocton JJ, Dressler F, Rutledge BJ, Rys PN, Persing DH, Steere AC. Detection of Borrelia burgdorferi DNA by polymerase chain reaction in synovial fluid from patients with Lyme arthritis. N Engl J Med. 1994;330(4):229–34.

26. Stahl HD, Hubner B, Seidl B, Liebert UG, van der Heijden IM, Wilbrink B, et al. Detection of multiple viral DNA species in synovial tissue and fluid of patients with early arthritis. Ann Rheum Dis. 2000;59(5):342–6.
27. Amemiya K, Hirotsu Y, Oyama T, Omata M. Relationship between formalin reagent and success rate of targeted sequencing analysis using formalin fixed paraffin embedded tissues. Clin Chim Acta. 2019;488:129–34.
28. Gomez CA, Budvytiene I, Zemek AJ, Banaei N. Performance of targeted fungal sequencing for culture-independent diagnosis of invasive fungal disease. Clin Infect Dis. 2017;65(12):2035–41.
29. Osmon DR, Berbari EF, Berendt AR, Lew D, Zimmerli W, Steckelberg JM, et al. Diagnosis and management of prosthetic joint infection: clinical practice guidelines by the Infectious Diseases Society of America. Clin Infect Dis. 2013;56(1):e1–25.
30. Culbreath K, Melanson S, Gale J, Baker J, Li F, Saebo O, et al. Validation and retrospective clinical evaluation of a quantitative 16S rRNA gene metagenomic sequencing assay for bacterial pathogen detection in body fluids. J Mol Diagn. 2019;21(5):913–23.
31. Sabat AJ, van Zanten E, Akkerboom V, Wisselink G, van Slochteren K, de Boer RF, et al. Targeted next-generation sequencing of the 16S-23S rRNA region for culture-independent bacterial identification – increased discrimination of closely related species. Sci Rep. 2017;7(1):3434.
32. Echeverria AP, Cohn IS, Danko DC, Shanaj S, Blair L, Hollemon D, et al. Sequencing of circulating microbial cell-free DNA can identify pathogens in periprosthetic joint infections. J Bone Joint Surg Am. 2021;103(18):1705–12.
33. Thoendel MJ, Jeraldo PR, Greenwood-Quaintance KE, Yao JZ, Chia N, Hanssen AD, et al. Identification of prosthetic joint infection pathogens using a shotgun metagenomics approach. Clin Infect Dis. 2018;67(9):1333–8.
34. Wang C-X, Huang Z, Fang X, Li W, Yang B, Zhang W. Comparison of broad-range polymerase chain reaction and metagenomic next-generation sequencing for the diagnosis of prosthetic joint infection. Int J Infect Dis. 2020;95:8–12.
35. Cai Y, Fang X, Chen Y, Huang Z, Zhang C, Li W, et al. Metagenomic next generation sequencing improves diagnosis of prosthetic joint infection by detecting the presence of bacteria in periprosthetic tissues. Int J Infect Dis. 2020;96:573–8.
36. Fang X, Cai Y, Shi T, Huang Z, Zhang C, Li W, et al. Detecting the presence of bacteria in low-volume preoperative aspirated synovial fluid by metagenomic next-generation sequencing. Int J Infect Dis. 2020;99:108–16.

Chapter 8
Basics of Light Microscopic Analysis of Synovial Fluid

Sharon Cowley and Geraldine McCarthy

Practical Aspects of Light Microscopy

Light microscopy remains an essential tool in the examination of synovial fluid microstructures despite the evolution of electron microscopes. The light microscope must accomplish three tasks: produce a magnified image of the specimen, separate the details in the image, and render the details visible to the human eye or camera. The illumination system for incident light microscopy consists of the lamp, lenses, filters, the condenser and diaphragm which lie along the light path between the light source and the specimen [1]. Generally, the aim is to produce a uniformly illuminated object field exactly the size of the field of view which is desired. The light should be adjustable in intensity, colour and polarization.

The first step in examining a joint fluid sample involves making a slide. The single drop sample is placed on a clean microscope slide and flattened beneath a cover slip. The specimen is then mounted on the stage. There may be a simple clip to hold the slide in place or a slide holder, which may require manual positioning or there may be a mechanical stage with a mechanism to hold and move the microscope slide. The light source should be turned on and adjusted to provide high-intensity illumination at high magnifications and allow comfortable viewing at lower magnifications. The condenser is the apparatus that sits directly below the stage and contains one or more lenses. *The lenses take the scattered microscope light source and "convert" the light rays into a neat, converging beam, or a cone of light which shine up through the stage aperture and specimen*. The condenser will go in between the light source and the specimen and takes the random angles and "converges them". It *condenses* all these different light rays into a single point into an organized cone of light [2]. There are typically two controls to help control the

S. Cowley · G. McCarthy (✉)
Division of Rheumatology, Mater Misericordiae University Hospital, Dublin, Ireland
e-mail: g.mccarthy@ucd.ie

B. F. Mandell (ed.), *Synovial Fluid Analysis and The Evaluation of Patients With Arthritis*, https://doi.org/10.1007/978-3-030-99612-3_8

condenser. There is one knob that moves the entire condenser closer or further from the specimen stage. This helps with fine-tuning the resolution of the image being seen.

The other control is the diaphragm, which controls the amount of light going to the sample. It limits the light travelling through the condenser without the operator changing the brightness of the light source itself. There are a few different varieties of diaphragm to be familiar with. The first is a disc diaphragm. It is a rotating wheel with several differently sized diameter openings. In order to allow additional light shine through to the sample a circle with a larger diameter can be chosen. The more common type of diaphragm is an aperture iris diaphragm. It is more sophisticated in that it mimics the biological function of the iris in self-adjusting to allow the appropriate amount of light through. It opens and closes with a gliding switch that opens the diaphragm to varying degrees. The condenser sits directly on top of the iris diaphragm. The field diaphragm is located closer to the light source of the microscope. This operates in the same way but only affects the width of the bundle of light rays reaching the condenser. This variable aperture does not affect the optical resolution, numerical aperture, or the intensity of illumination. Proper adjustment of the field diaphragm is important for preventing glare that can reduce contrast in the observed image [3].

A low power objective should be selected to begin with, with the slide on the stage. The focus can be turned until the image comes into view. It is important to observe from the side to ensure that the power objective does not touch the slide. While observing through the eyepiece, the correct position can be achieved by adjusting the coarse and fine focus controls. Scan the slide, first at low power and then switch to a higher power objective once the sample is in clear view. When finished examining the slide go back to the low powered lens, remove and safely dispose of the slide, make sure the stage and lenses are clean. Turn off the light bulb and cover the microscope with a dust jacket when not in use.

Sample Handling

It is traditional to examine synovial fluid macroscopically before proceeding to microscopic analysis. The gross examination includes subjective assessment of its colour, clarity and viscosity. The presence of formation of a mucin clot can also be considered. The procedure for mucin clot formation varies among laboratories as evidenced by differing fluid to acid ratios appearing in various texts. Rope's test is an estimation of the integrity of the hyaluronic acid–protein complex (mucin). Normal synovial fluid forms a tight ropy clot upon the addition of acetic acid [4]. Based on this macroscopic information it is possible to distinguish four groups of arthropathies: non-inflammatory, inflammatory, haemorrhagic and purulent [5]. Ropes and Bauer classified these to include non-inflammatory fluid which appears

straw coloured with opalescent clarity, high viscosity and good mucin clot formation [6]. Not all laboratories routinely perform these tests on the physical characteristics of the synovial fluid. Inflammatory fluid is straw, white or yellow coloured with translucent or opaque opacity, low viscosity and fair to poor mucin clot formation. Purulent fluid is white, green or yellow in colour, opaque, has low viscosity and fair to poor mucin clot formation. The fourth category of haemorrhagic fluid is red or dark yellow in colour, can be translucent or opaque, has intermediate viscosity and has poor mucin clot formation.

Synovial fluid, in general, is best assessed with microscopy as soon as possible after collection to give maximal yield. There is some flexibility in the analysis of monosodium urate (MSU) crystals but this does not hold true for calcium pyrophosphate (CPP) crystals which are more fragile. There are a number of studies to show no major difference in the quality and quantity of monosodium urate (MSU) crystals up to 24 hours post collection [7–10] and further studies showed stability of the MSU crystals at 72 hours [7, 8, 11]. However, unlike MSU crystals calcium pyrophosphate (CPP) crystals degrade rapidly with time [7] with this study showing degradation of numbers of crystals identified to diminish over hours with further changed appearance over time to include changed crystal shape, appearance of artefacts and unexplained crystals.

Studies have also compared the effects of storage temperature on MSU and CPP crystal detection. A systemic review by Meyer et al. [12] compared storage at room temperature versus refrigeration at 4 degrees Celsius and found overall there was no major difference in MSU or CPP crystal detection between samples stored at either temperature after 24 hours, 72 hours and 8 weeks.

The initial microscope assessment of synovial fluid is that of examination of a ‘wet prep’ sample which consists of unstained, undiluted synovial fluid. This sample can be assessed for ragocytes, non-cellular particulate and crystalline material. The sample, taken intact from the joint aspirate, is placed on a clean microscope slide and flattened beneath a cover slip and examined by microscopy.

Centrifugation is a technique used for the separation of particles according to their size, shape and density. The number of cells in synovial fluid can greatly vary from sample to sample and centrifugation aims to standardise their number and quality. The synovial fluid aspirate is diluted with normal saline to give an optimum concentration of 400 cells/mm^2 [5]. The centrifuge chamber is loaded with 0.1 ml of the saline cell suspension and centrifuged at 800 rotations/minute for 10–15 minutes. A slow speed is preferred to keep the fragile fluid contents intact.

There has been some debate over the benefit of centrifugation on synovial fluid samples. Some studies have shown marginal benefit in using this technique to identify CPP crystals [13]. CPP crystals were identified in a higher number of smears after centrifugation. As MSU crystals are already quite readily visible there was less benefit in centrifuging samples in this case. Therefore, centrifugation may be of additional value in selected patients with suspected calcium pyrophosphate deposition disease with a negative ‘wet prep’ microscopy. It is useful to a lesser extent for gout.

Gram Stain of Initial Synovial Fluid Sample

The exclusion or confirmation of septic arthritis is a common and critical reason for synovial fluid to be examined. Unfortunately synovial fluid contains inhibitors of bacterial growth which may prevent their detection on culture. Joints can also contain organisms such as mycobacteria which can be easily missed. For these reasons careful examination and staining of synovial fluid is an important adjunct to culture and maximises the chances of detecting an infective organism. The Gram stain test has been in use since 1883 when Hans Christian Gram, a Danish physician, observed differential staining of lung tissue samples following application of reagents, and thus serendipitously discovered the test [14].

The original Gram staining method involves covering the slide completely with crystal violet solutions stain for 3 minutes and pouring it off, not rinsing. The slide is then covered completely with Lugol's solution which is left on for 2 minutes and again poured off. The slide is then completely immersed in decolorization solution (acetone, ethanol or methanol) and gently moved for about 20–60 seconds until no more clouds of stain are released and the smear is grey. It is then rinsed carefully with distilled water for about 5 seconds. The slide is then completely covered with Ziehl-Neelsen carbol fuchsin solution diluted 1:10, stained for 1 minute and poured off. Again, it is rinsed carefully with distilled water for about 5 seconds and allowed to dry. Results can be read as dark violet in the presence of Gram-positive bacteria and red in the presence of Gram-negative bacteria [15].

In some institutions, the initial clinical decision on treatment with antibiotics is still based on the results of Gram stain analysis. This is likely due to the relative rapidity of performing the test with the possibility of results being available in as soon as an hour. Cultures on the other hand will require at least 24–48 hours of processing time for the primary culture, and 3–7 days for the extended cultures.

Despite its widespread use, the sensitivity and specificity of Gram staining of synovial fluid is much less reliable than culture. A recent review of over 800 synovial fluid samples from native joints in the UK compared Gram stain with culture and revealed a Gram stain sensitivity of 17% and specificity of 99.7% [16]. A positive Gram stain was one reported as organisms seen which was accompanied by a description of the structure of the organism and a negative test was one recorded as no organisms seen. Synovial fluid culture was the gold standard technique for detecting infection. Older reviews estimate Gram stain sensitivity at 27% to 45% [17, 18]. The consequences of failed diagnosis or inadequate treatment could result in the mortality rate of up to 11.5%, and a morbidity rate of up to 31.6%, largely due to complications such as osteomyelitis, subchondral joint bone loss and dysfunction, as well as septicaemia [19, 20].

False-positive Gram stain results can also occur as a result of contamination or misinterpretation. Correct interpretation of Gram stains is not always straightforward and to a large extent influenced by experience. Clumping of dye, staining of cellular structures, or cellular debris other than bacteria can mimic Gram-positive

bacteria. Conversely, a thick Gram smear with a strong background counterstain can cloak Gram-negative bacteria. The Gram stain has also been shown to have high intra- and inter-observer variability as a result of an inherent degree of subjectivity [21]. Crystals can also be seen in stained samples. A recent review estimates that 5% of Gram stain positive synovial fluid samples are also positive for crystals [22].

Unusual Cells

Synovial fluid analysis provides a vast amount of clinically relevant information, in particular in cases of an effusion of unknown origin. Aside from crystals and microorganisms, there are other uncommon findings that can guide the clinician to a better understanding of the underlying diagnosis including the presence of fat droplets, large mononuclear cells, cartilaginous fragments, LE cells and sickle cells.

Several types of lipids have been described in synovial fluid. Quantitation of lipids has minimal yield but rather the nature of the lipid is of greater importance. Fats can be differentiated from each other by their morphology. In wet preps lipids appear as both globules and crystals within globules. Their different morphology is a valuable diagnostic tool but also may lead to an erroneous diagnosis of an acute crystal arthropathy. The distinguishing feature is that lipid crystals are always found within a globule. Globules of neutral fat are suggestive of traumatic arthropathy. Globules of neutral fat with associated needle-shaped lipid crystals are suggestive of recent trauma with intra-articular haemorrhage (Fig. 8.1). Cholesterol plates (Fig. 8.2) are usually evidence of long-standing inflammatory arthropathy, most commonly from rheumatoid arthritis.

Large mononuclear cells with fat droplets are also seen in cases of intra-articular fracture. In normal synovial fluid mononuclear cells account for 50–90% of the cell count, of which 80% or more are macrophages or synovial lining cells. Most macrophages are not activated, that is they lack cytoplasmic vacuolation, do not show

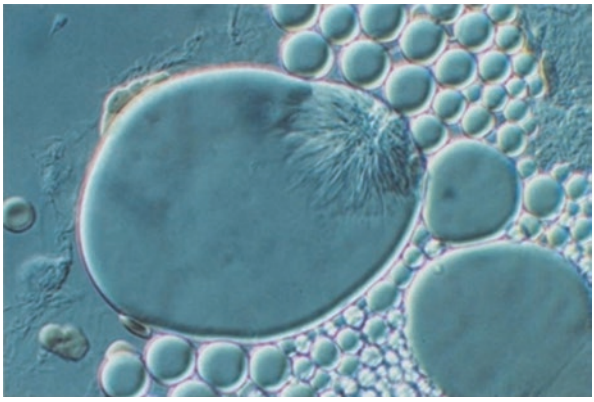

Fig. 8.1 Needle-shaped crystals in a fat globule

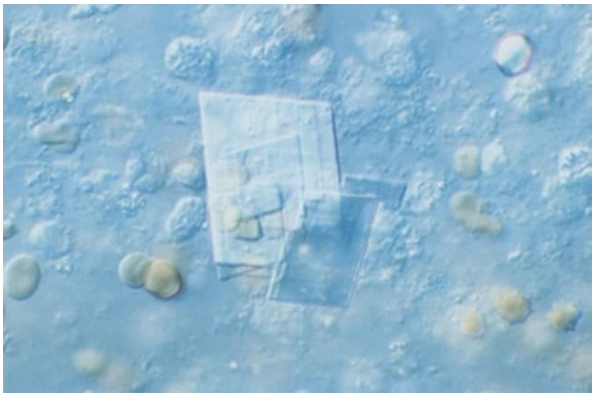

Fig. 8.2 Typical notched corners of a cholesterol plate

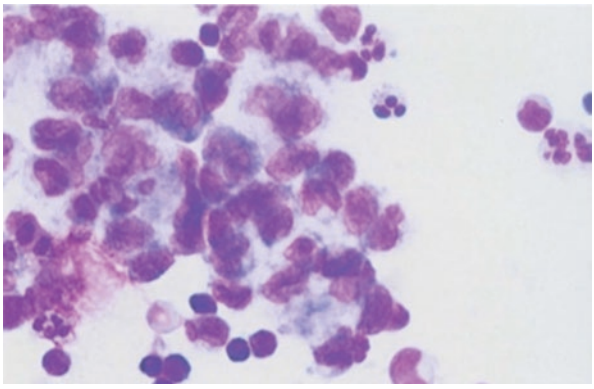

Fig. 8.3 Mononucleated macrophages

phagocytic activity and have round monocytoid nuclei. In trauma and intra-articular fracture there is an increase in the amount of joint fluid and a mild increase in the nucleated cell count, consisting mostly of mononucleated cells which may be macrophages or synoviocytes (Fig. 8.3). The presence of cartilaginous fragments can be identified in patients with severe osteoarthritis (OA) or traumatic arthropathies [23]. Under light microscopy, chondrocytes display a clustered organisation of cells and have clearly visible nuclei (Fig. 8.4).

The presence of lupus erythematosus (LE) cells (Fig. 8.5) can also be identified in synovial fluid. The phenomenon occurs when numerous damaged cells are present and substantial nucleo-phagocytosis has occurred. In systemic lupus erythematosus (SLE), positive LE cells have been shown to indicate active disease with joint involvement. Normal joint fluid and synovium do not contain polymorphs. They enter the synovial fluid from the blood, either as part of the process of intra-articular haemorrhage or diapedesis across the walls of synovial vessels during inflammation. Thus their presence can be considered a feature of intra-articular inflammation. These cells have morphological similarity to the LE cells seen in the peripheral blood in patients with SLE. They have fragmented lymphocyte nuclei, pink or purple in colour and lack any clear nuclear chromatin pattern. If more than 10% of all polymorphs are small or large LE cells then the diagnosis is very probably SLE [5].

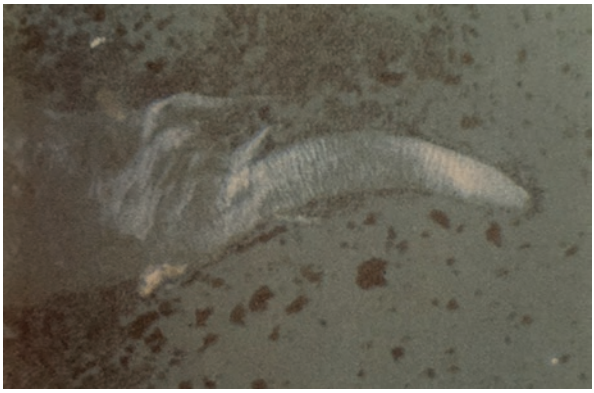

Fig. 8.4 A free fragment of cartilage shed from the articular surface

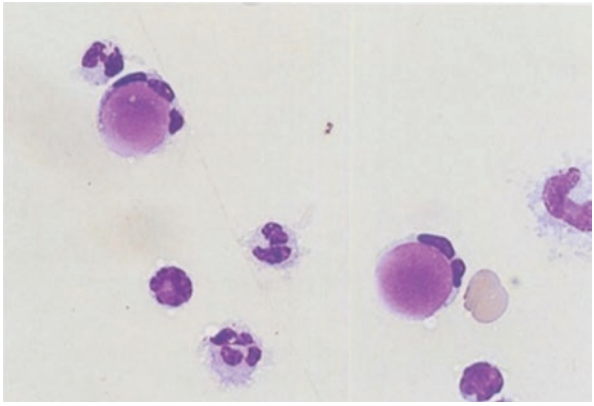

Fig. 8.5 Large LE cells (polymorphs with large cytoplasmic inclusions)

Lower proportions of LE cells are seen in most primary inflammatory arthropathies but are particularly common in rheumatoid disease.

Sickle cells can also be identified in synovial fluid. This is particularly useful as patients with sickle cell disease may present with an acute swollen joint. Aspiration of joint fluid is invaluable to differentiate septic arthritis from sickle cell arthropathy which is postulated to arise from microocclusion of synovial vessels due to sickling resulting in an inflammatory reaction. Such patients are also predisposed to osteonecrosis. The synovial fluid from sickle cell arthropathy typically has a marked leucocytosis. There may also be findings that point to bone necrosis such as superimposed haemorrhage, fragments of cartilage and hydroxyapatite crystals.

References

1. Treating H. Light microscopy subject guide. Metallogr Microstruct Anal 2013;2: 48–52.
2. Murphy DB, Davidson MW. Fundamentals of light microscopy and electronic imaging. Hoboken NJ: Wiley-Blackwell; 2012.

3. Wilson EE, Davidson MW. Education in microscopy and digital imaging. Zeiss. Accessed June 28th, 2021. http://zeiss-campus.magnet.fsu.edu/articles/basics/opticaltrain.html.
4. Shanahan K, Mundt L. Graff's textbook of urinalysis and body fluids. Philadelphia, PA: Lippincott, Williams, Wilkins; 2010.
5. Freemont AJ, Denton J. Atlas of synovial fluid cytopathology. Current histopathology, vol 18. Berlin, Germany: Springer Press; 1991.
6. Ropes MW, Bauer W. Synovial fluid changes in joint diseases. Cambridge, MA: Harvard University Press; 1953.
7. Kerolus G, Clayburne G, Schumacher HR Jr. Is it mandatory to examine synovial fluid promptly after athrocentesis? Arthritis Rheumatol. 1989;32(3):271–8.
8. Tausche AK, Gehrisch S, Panzner I. A 3 day delay in synovial fluid crystal identification did not hinder the reliable detection of monosodium urate and calcium pyrophosphate crystals. Clin Rheumatol. 2017;19:241–5.
9. Bible MW, Pinals RS. Late precipitation of monosodium urate crystals. J Rheumatol. 1982;3(9):480.
10. Robier C, Neubauer M, Settin M, Lunzer R, Rainer F. Dried cytospin preparations of synovial fluid are a stable material for long time storage and delayed crystal analysis. Clin Rheumatol. 2012;31:1115–6.
11. Pastor S, Bernal JA, Cano R, Gomez-Sabater S, Borras F, Andres M. Persistence of crystals in stored synovial fluid samples. J Rheumatol. 2020;47(9):1416–23.
12. Meyer MM, Marks LA, Aslam F. Clinical implications of synovial fluid handling for crystal associated arthridites: a systematic review. Int J Rheum Dis. 2021;24:10–20.
13. Boumans D, Hettema ME, Vonkeman HE, Maatman RG, van de Laar MA. The added value of synovial fluid centrifugation for monosodium urate and calcium pyrophosphate crystal detection. Clin Rheumatol. 2017;36(7):1599–605. https://doi.org/10.1007/s10067-017-3633-6. Epub 2017 Apr 19. PMID: 28424907.
14. Austrian R. The gram stain and the etiology of lobar pneumonia, an historical note. Bacteriol Rev. 1960;24(3):261–5.
15. Merck. Microbiology Manual 12th Edition. 2010. p. 631–2.
16. Gbejuade H, Elsakka M, Cutler L. How well does synovial fluid gram staining correlate with cultures in native joint infections? Orthop Rev (Pavia). 2019;11(4):8156.
17. Morgan PM, Sharkey P, Ghanem E, Parvizi J, Clohisy JC, Burnett RS, Barrack RL. The value of intraoperative Gram stain in revision total knee arthroplasty. J Bone Joint Surg Am. 2009;92(2):442.
18. Faraj AA, Omonbude OD, Godwin P. Gram staining in the diagnosis of acute septic arthritis. Acta Orthop Belg. 2002;68(4):388–91.
19. Weston V, Jones A, Bradbury N, et al. Clinical features and outcome of septicarthritis in a single UK Health District 1982–1991. Ann Rheum Dis. 1999;58:214–9.
20. Horowitz DL, Katzap E, Horowitz S, Barilla-LaBarca M-L. Approach to septic arthritis. Am Fam Phys. 2011;84:653–60.
21. Willcox JR, Adler MW, Belsey EM. Observer variation in the interpretation of Gram-stained urethral smears: implications for the diagnosis of non-specific urethritis. Br J Vener Dis. 1981;57:134–6.
22. Stirling P, Tahir M, Atkinson HD. The limitations of Gram-stain microscopy of synovial fluid in concomitant septic and crystal arthritis. Curr Rheumatol Rev. 2018;14(3):255–7.
23. Evans CH, Mears DC, McKnight J. A preliminary ferrographic survey of the wear particles in human synovial fluid. Arthritis Rheum. 1981;24:912–8.

Chapter 9
Basics of Polarized Light Microscopy

Francesca Oliviero and Leonardo Punzi

Introduction

Crystal search represents a fundamental step in synovial fluid (SF) analysis. The identification of monosodium urate (MSU) and calcium pyrophosphate (CPP) crystals allows an immediate diagnosis of crystal-induced arthritis [1] and, as a consequence, the timely pharmacological management of the patient. This aspect is very important in clinical practice, due to the high prevalence of both these diseases in the population. Indeed, gout is the most frequent arthritis in men and CPP crystal-induced arthritis is the most common mono-arthritis in the elderly [2, 3]. Besides primary crystal-induced arthritis, crystals can occasionally be detected in SF from other different joint diseases. In these cases, SF analysis provides an aid for the diagnosis of possible comorbidities linked to the presence of crystals [4] and may explain an unexpected clinical course.

The presence of pathogenic crystals in SF can be evidenced under ordinary light by an expert view; however, only polarized light associated with compensated light permits establishing with certainty the molecular nature of these crystals [5]. Furthermore, due to their variable size, some crystals can be missed under ordinary light.

F. Oliviero
Rheumatology Unit, Department of Medicine – DIMED, Biomedical Campus "Pietro D'Abano", University of Padova, Padova, Italy
e-mail: francesca.oliviero@unipd.it

L. Punzi (✉)
Centre for Gout and Metabolic Bone and Joint Diseases, Rheumatology, SS Giovanni and Paolo Hospital, Venice, Italy

B. F. Mandell (ed.), *Synovial Fluid Analysis and The Evaluation of Patients With Arthritis*, https://doi.org/10.1007/978-3-030-99612-3_9

Basic Principles

Light propagates in the form of transverse electromagnetic waves that are composed of both an electric field and a magnetic field perpendicular to one another. Natural or unpolarized light originating from an ordinary light source is composed of waves having the electric field vectors oriented in all possible directions with a range of frequencies that depends on the characteristics of the light source. By contrast, in polarized light all the electric field vectors vibrate in only one direction. This light is produced when unpolarized light passes through a polarizing lens whose optical axis is in line with the desired linear polarization [6, 7]. The human eye cannot distinguish between unpolarized and polarized light, unless a second polarizer is used to block (or adsorb) the waves passing through the first polarizing filter. According to this principle, polarized light enhances the degree of sensitivity in the detection of birefringent materials in different biological and non-biological specimens.

The Polarized Light Microscope

A basic polarized light optical microscope as the one depicted in Fig. 9.1 is used for routine examination of SF samples. In order to identify crystals, the microscope must be equipped with two polarizing filters. The first is positioned between the light source and the specimen. The second, called analyzer, is placed above the objectives and can be unmovable or inserted as required (Fig. 9.1) depending upon the style of the microscope.

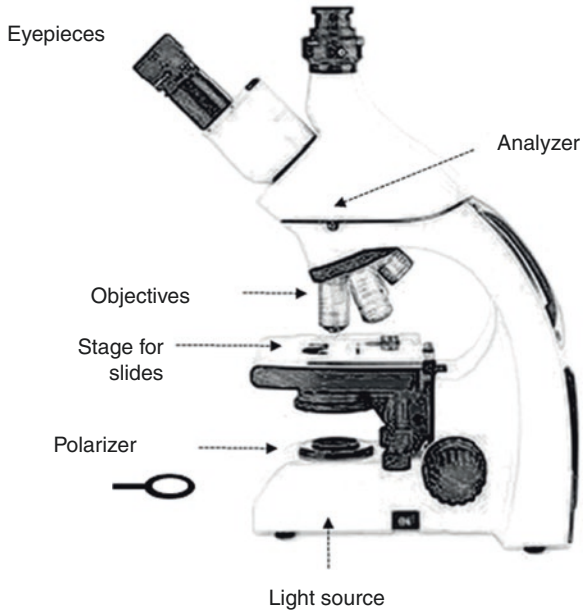

Fig. 9.1 Basic model of optical polarized microscope

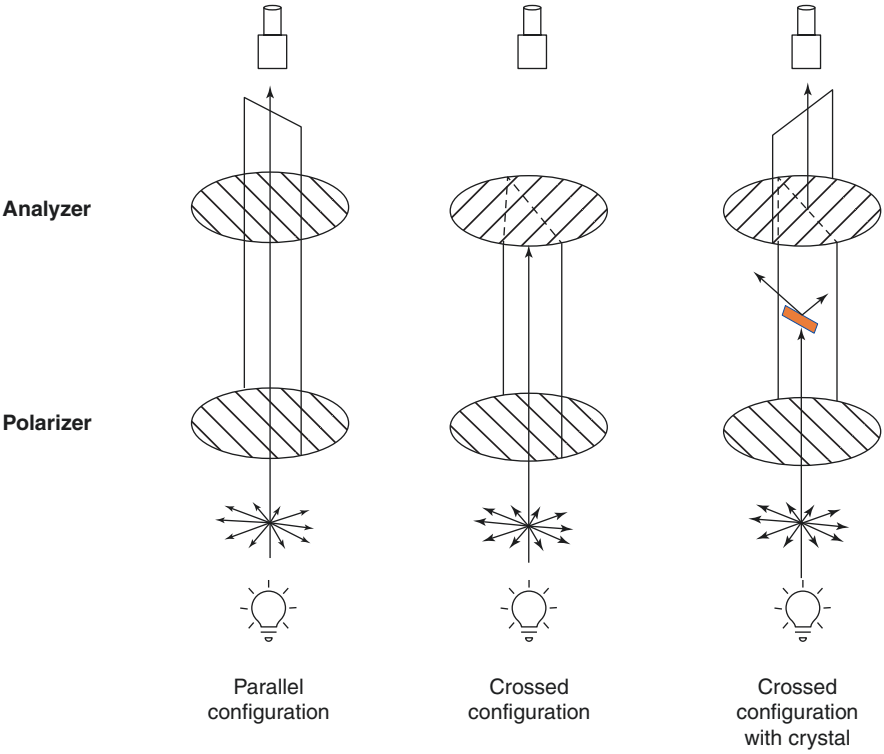

Fig. 9.2 Different configurations of polarized light in the optical microscope. Parallel configuration: polarizer and analyzer parallelly oriented, bright field. Crossed configuration: polarizer and analyzer orthogonally oriented, dark field. Crossed configuration with crystal: polarizer and analyzer orthogonally oriented, dark field with shining material

As illustrated in Fig. 9.2, when the transmission axis of the polarizer and the analyzer are parallel one to the other, the polarized light emerging from the polarizer passes through the analyzer and reaches the eyepieces (parallel configuration), appearing to the human eye as normal light. By contrast, if the two filters are reciprocally oriented at 90 degree, the polarized light emerging from the polarizer is completely blocked (or absorbed) by the analyzer (crossed configuration) (Fig. 9.2) and the background field is dark.

If a birefringent material is present along the optical path, it deviates the polarized light beam originating two separate waves. This phenomenon is known as *birefringence* and the material, i.e., the crystal, appears bright in the dark view field.

The waves created by birefringence travel in the same direction with different velocities and have electric vectors reciprocally perpendicular. They are called ordinary and extraordinary waves depending on, respectively, the perpendicular or parallel position of the electric vector with respect to the optical axis of the crystals (which is the axis down the length of the crystal). The difference between the refractive indices of the two wave components emerging from the crystal establishes the

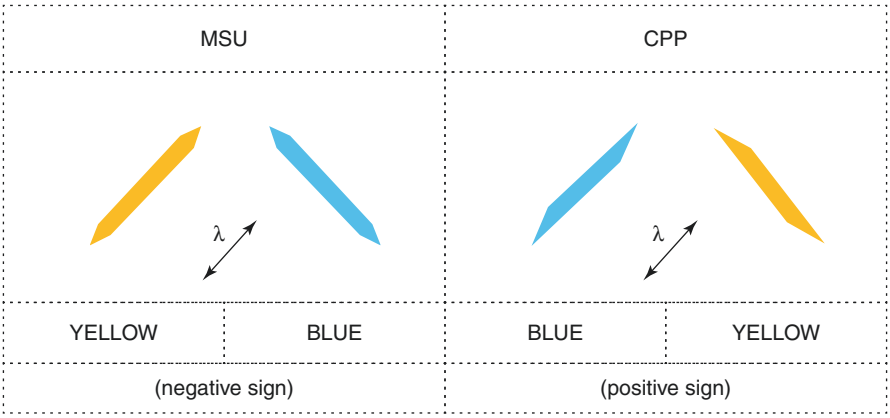

Fig. 9.3 Schematic representation of MSU and CPP crystal colors under polarized compensated light

sign of birefringence. It is positive (by definition) when the refractive index of the extraordinary wave is greater than the refractive index of the ordinary wave and vice versa [6].

The sign of birefringence varies according to the molecular nature of the material and can be determined by the use of a first-order retardation plate (compensator) which, consequently, helps to distinguish MSU crystals, which have a negative sign, from CPP crystals that have a positive sign (see next paragraph).

This additional element, called the *compensator, red plate or lambda (λ) filter*, is inserted between the polarizer and the analyzer and adds a fixed optical path difference between 530 and 560 nanometers to every wavefront in the field. This causes a complete cancellation of green light thus giving the background field of view a red tone.

Besides the determination of the optical sign of birefringent material, the compensator is also useful for enhancing contrast in weakly birefringent crystals.

Practice

Polarized light microscopy is used in daily practice as a routine part of the examination of SF, which also includes the total and differential white blood cell count [8, 9]. Crystal identification requires subjective interpretation and proper training of the observers is very important in obtaining reliable results [10].

As far as the preparation technique is concerned, a single drop of fresh SF is placed into a clean glass slide, covered with a clean cover slip and observed at a 400 or 600× magnification. It is sequentially examined under ordinary, polarized, and compensated light. When the polarizer and analyzer filters are crossed, the birefringent crystal will reach a maximum intensity and will be clearly visible on the black background. In this configuration, the addition of the compensator will allow the

Table 9.1 Characteristics of MSU and CPP crystals viewed under polarized and compensated light

	Sign of birefringence	Characteristics		
		Shape	Polarized light	Polarized compensated light[a]
MSU	–	Needle-shaped, rod-shaped	Very bright	Yellow/orange when parallel Blue when perpendicular
CPP	+	Rectangular, rhomboidal, parallelepiped, rod-shaped	Variably bright	Blue when parallel Yellow/orange when perpendicular

[a] Parallel and perpendicular are referred to the position of the optical axis of the crystal with respect to that of the compensator

crystals to exhibit a color which will gradually change as the compensator (or microscope stage with the crystal) is rotated. As is often also located on the polarizer, an arrow on the compensator indicates the orientation of the transmission axis of the compensator. After positioning this axis of the compensator arrow parallel to the optical axis of the crystal identified in the dark field, the birefringent crystal will appear yellow/orange (negative sign) or blue (positive sign) depending on whether it is a MSU or a CPP crystal, respectively (Fig. 9.3, Table 9.1). This phenomenon is due to the interference generated by the additive or subtractive effects of the crystal and the compensator. The opposite color is observed when the axis of the crystal is perpendicular to the compensator axis.

In some models of polarizing microscope, the compensator is introduced after the specimen but before the analyzer and oriented at 45 degrees to the polarizer and analyzer with no possibility of motion. In this case, a rotating stage allows the change of the orientation of the crystal axis.

Monosodium Urate Crystals

Under polarized light MSU crystals present a strong birefringence that makes them very easy to be identified. Figure 9.4 shows a long needle-shaped crystal entrapped in a fibrin aggregate and depicted according to the three microscope configurations illustrated previously. The crystal exhibits a blue and orange color when its optical axis is oriented, respectively, perpendicular or parallel to the compensator (lamina λ). Numerous tiny crystals are shown in Fig. 9.5 with two crystals found at right angle one to the other and therefore exhibiting opposite colors in that position (Fig. 9.5c).

Calcium Pyrophosphate Crystals

Different than with MSU, the search for CPP crystals often requires more attention by the operator as most of these crystals are weakly birefringent (or not birefringent at all) and can be missed in the dark field [11]. As a result, it is very important to

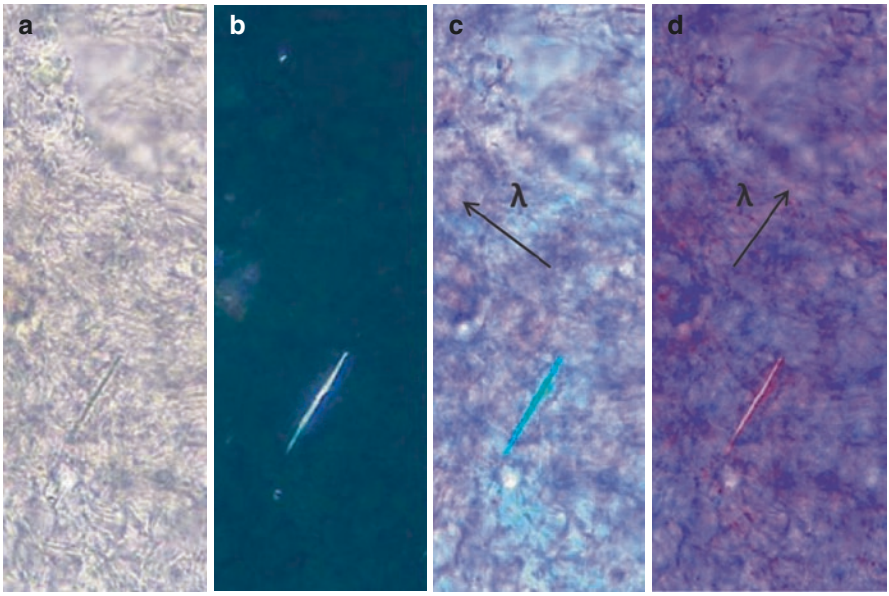

Fig. 9.4 Needle-shaped MSU crystal under ordinary (**a**), polarized (**b**), and compensated polarized light (**c**, **d**), 400×. The arrow indicates the direction of the transmission axis of the lambda filter which is perpendicular (**c**, blue) and parallel (**d**, orange) to the optical axis of the crystal

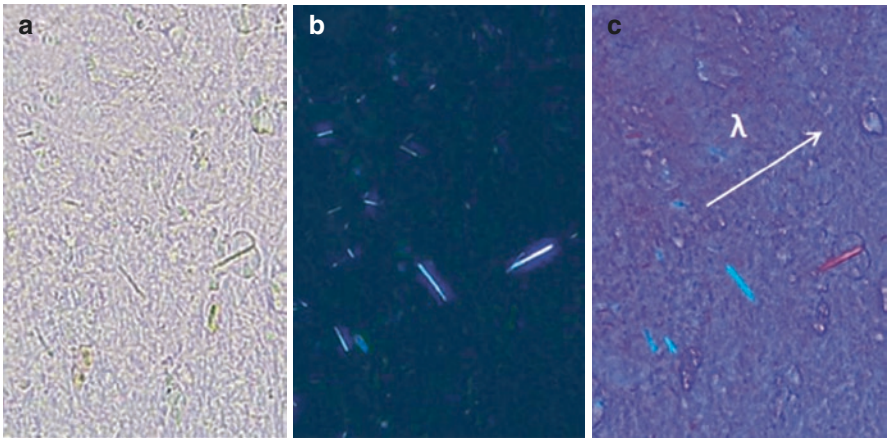

Fig. 9.5 Needle-shaped tiny MSU crystals under ordinary (**a**), polarized (**b**), and compensated polarized light (**c**), 400×. The arrow indicates the direction of the transmission axis of the lambda filter which is perpendicular (blue) and parallel (orange) to the optical axis of the crystal

examine the glass slide under ordinary bright light to put their shape in evidence before the use of the polarizer.

CPP crystal form depends on the arrangement of the atoms of the molecule which lead to monoclinic (more frequent) and triclinic (less frequent) systems.

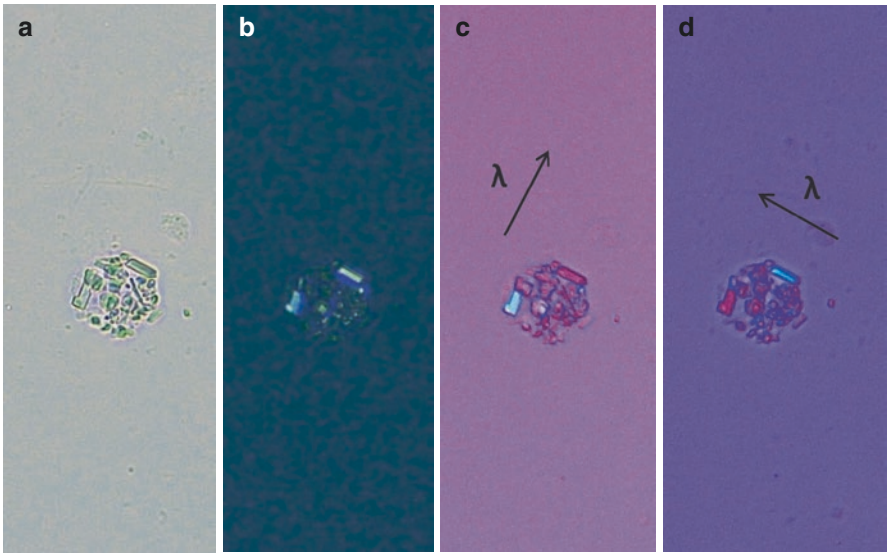

Fig. 9.6 Intracellular parallelepipedic and rectangular CPP crystals observed under ordinary (**a**), polarized (**b**) and compensated polarized light (**c**, **d**), 400×. The arrow indicates the direction of the transmission axis of the lambda filter. Depending on the optical axis of the crystal the crystals appear blu (parallel) or orange (perpendicular)

Parallelepiped, rectangular and rod-shaped forms such as those seen in Figs. 9.6 and 9.7 are classically found in SF positive for CPP crystals. Very small crystals can also be present. As shown in the figures, birefringent CPP crystals exhibit a blue color when their axis is aligned to that of the compensator (Figs. 9.6c, d and 9.7c).

Polarized light microscopy for CPP identification has shown a high level of concordance with that conducted by scanning electron microscopy, underling the utility of a polarized microscope in the clinical setting [12].

Birefringent Artifacts

Several artifacts can be found in SF during routine examination. Some of them can show a certain degree of birefringence and, if not recognized by an expert view, can be mistaken for pathogenic crystals [7]. Artifacts can be endogenous components, including collagen fibrils, tissue fragments (Fig. 9.8), lipids, and unspecified material such as the one shown in Fig. 9.9. The positive birefringence of this artifact might lead to a misdiagnosis. In such situations, it is always useful to conduct a more extensive search throughout the glass slide area for more "classic" crystals.

Metallic fragments and debris after prosthetic arthroplasty can also be found in SF and appear as shining little dots in the dark field. Other crystals such as calcium oxalate, cholesterol, and synthetic crystals such as corticosteroids may be identified

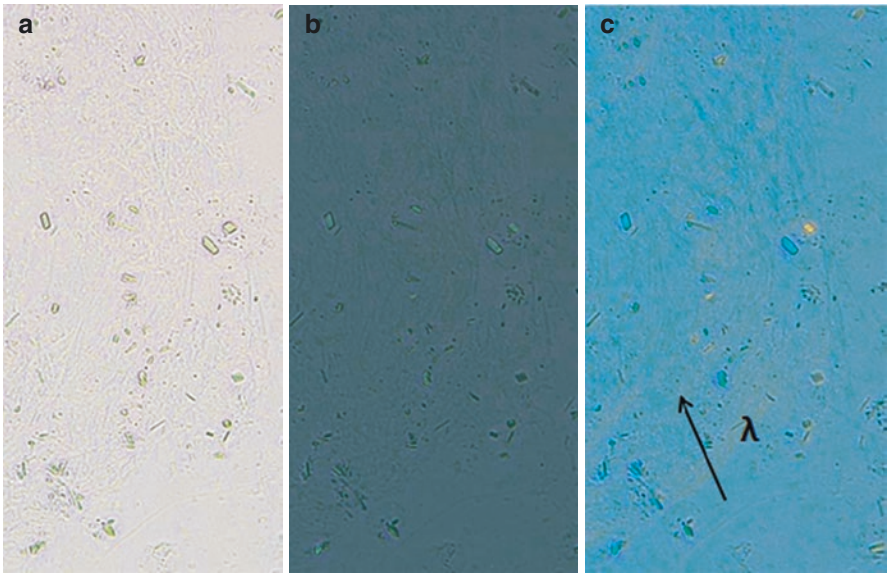

Fig. 9.7 Rectangular and rod-shaped, weakly birefringent CPP crystals under ordinary (**a**), polarized (**b**), and compensated polarized light (**c**), 400×. The arrow indicates the direction of the transmission axis of the lambda filter

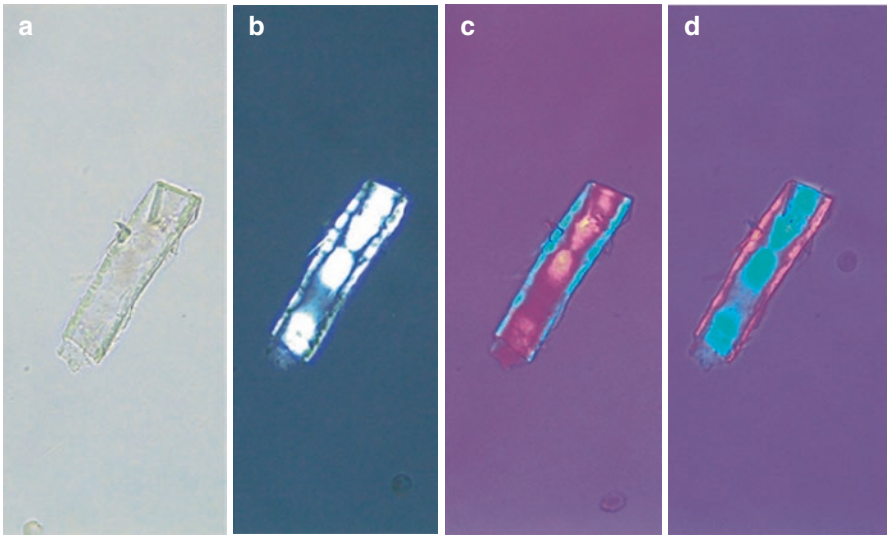

Fig. 9.8 A birefringent tissue fragment observed in SF sample under ordinary (**a**), polarized (**b**), and compensated polarized light (**c**, **d**), 400×

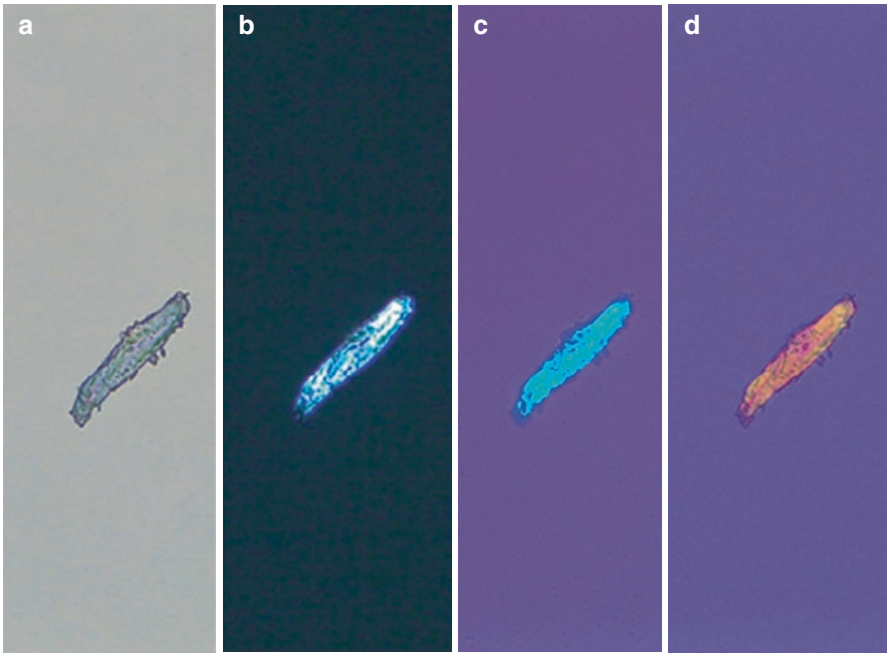

Fig. 9.9 A birefringent unspecified fragment found in a non-inflammatory SF examined under ordinary (**a**), polarized (**b**), and compensated polarized light (**c**, **d**), 400×

in SF. The latter include triamcinolone acetonide/hexacetonide and methylprednisolone acetate, and are among the most common artifacts in SF as they persist a long time after intra-articular injections [13]. These crystals may present different sizes and shapes, and due to their strong birefringence can be confused with MSU or, more easily, with CPP crystals (Fig. 9.10) [14].

At times, artifacts can be introduced from the outside. They include contaminants such as dust from dirty slides (Fig. 9.11) and paper fibers released on the glass slide surface after cleaning. At times, air bubbles entrapped during specimen handling or after slide drying can form some artifacts resembling MSU crystals (Fig. 9.12).

Conclusion

Polarized light microscopy is fundamental for the identification of pathogenic crystals in SF. While MSU crystals are easily recognizable often search requires more time and attention by the analyst. The addition of a red compensator along the optical path of the microscope allows for establishing the sign of birefringence of the crystals.

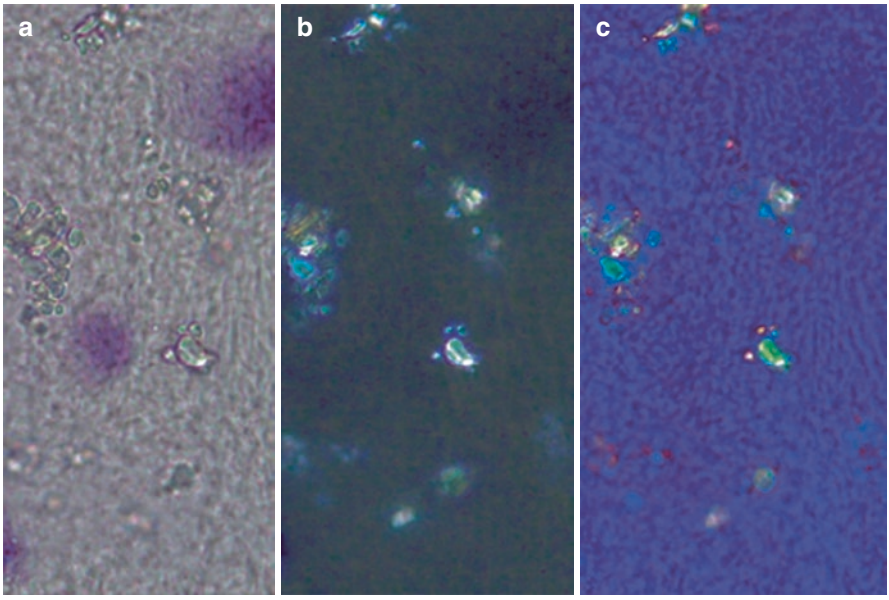

Fig. 9.10 Polymorphic irregular corticosteroids crystals found in SF of a patient who received a previous intra-articular injection of triamcinolone hexacetonide. Ordinary (**a**), polarized (**b**), and compensated polarized light (**c**), 1000×

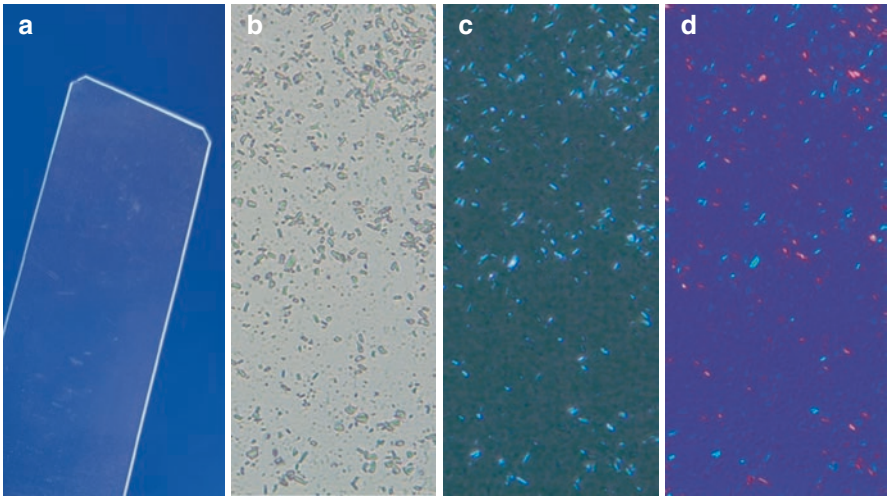

Fig. 9.11 Birefringent particles observed from a dirty glass slide (**a**) under ordinary (**b**), polarized (**c**), and compensated polarized light (**d**), 400×

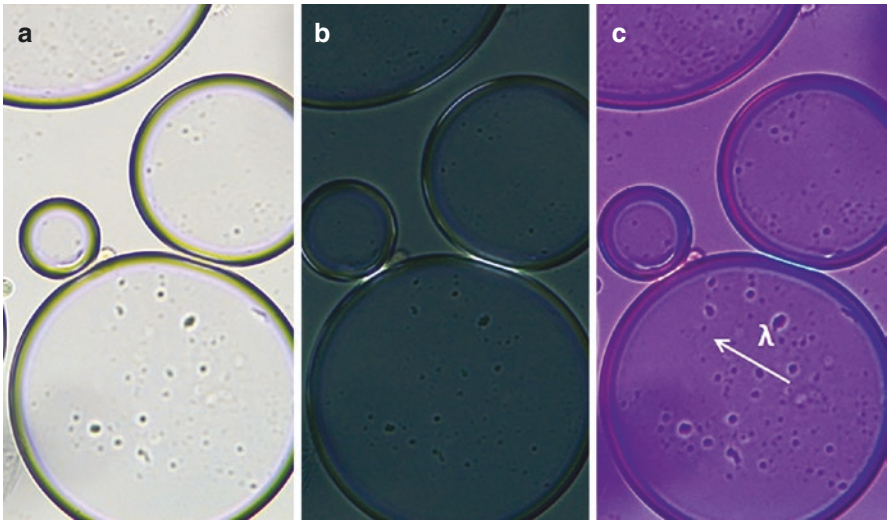

Fig. 9.12 Birefringent artifacts from the touching of air bubbles observed under ordinary (**a**), polarized (**b**), and compensated polarized light (**c**), 400×

References

1. Pascual E, Jovaní V. Synovial fluid analysis. Best Pract Res Clin Rheumatol. 2005;19:371–86. https://doi.org/10.1016/j.berh.2005.01.004.
2. Punzi L, Scanu A, Galozzi P, Luisetto R, Spinella P, Scirè CA, Oliviero F. One year in review 2020: gout. Clin Exp Rheumatol. 2020;38:807–21.
3. Abhishek A, Doherty M. Update on calcium pyrophosphate deposition. Clin Exp Rheumatol. 2016;34(4 Suppl 98):32–8.
4. Oliviero F, Scanu A, Galozzi P, Gava A, Frallonardo P, Ramonda R, Punzi L. Prevalence of calcium pyrophosphate and monosodium urate crystals in synovial fluid of patients with previously diagnosed joint diseases. Joint Bone Spine. 2013;80:287–90. https://doi.org/10.1016/j.jbspin.2012.08.006.
5. Pascual E, Tovar J, Ruiz MT. The ordinary light microscope: an appropriate tool for provisional detection and identification of crystals in synovial fluid. Ann Rheum Dis. 1989;48:983–5. https://doi.org/10.1136/ard.48.12.983.
6. Bagnell R. Light microscope alignment methods. Methods Mol Biol. 2014;1180:45–80. https://doi.org/10.1007/978-1-4939-1050-2_4.
7. Schumacher HR, Reginato AJ. Atlas of synovial fluid analysis and crystal identification. Philadelphia: Lea & Febiger; 1991.
8. Oliviero F, Pascual E, Punzi L. Detection and identification of crystals in synovial fluid. Reumatismo. 2005;57:208–11.
9. Punzi L, Oliviero F. Arthrocentesis and synovial fluid analysis in clinical practice: value of sonography in difficult cases. Ann N Y Acad Sci. 2009;1154:152–8. https://doi.org/10.1111/j.1749-6632.2009.04389.x.
10. Lumbreras B, Pascual E, Frasquet J, González-Salinas J, Rodríguez E, Hernández-Aguado I. Analysis for crystals in synovial fluid: training of the analysts results in high consistency. Ann Rheum Dis. 2005;64:612–5. https://doi.org/10.1136/ard.2004.027268.

11. Ivorra J, Rosas J, Pascual E. Most calcium pyrophosphate crystals appear as non-birefringent. Ann Rheum Dis. 1999;58:582–4. https://doi.org/10.1136/ard.58.9.582.
12. Frallonardo P, Oliviero F, Peruzzo L, Tauro L, Scanu A, Galozzi P, Ramonda R, Punzi L. Detection of calcium crystals in knee osteoarthritis synovial fluid: a comparison between polarized light and scanning electron microscopy. J Clin Rheumatol. 2016;22:369–71. https://doi.org/10.1097/RHU.0000000000000416.
13. Gordon GV, Schumacher HR. Electron microscopic study of depot corticosteroid crystals with clinical studies after intra-articular injection. J Rheumatol. 1979;6:7–14.
14. Kahn CB, Hollander JL, Schumacher HR. Corticosteroid crystals in synovial fluid. JAMA. 1970;211:807–9.

Chapter 10
Crystal-Associated Arthritis: Gout

Fernando Perez-Ruiz and Maria C. Modesto-Caballero

The most frequent crystal-associated arthritides, gout and calcium pyrophosphate disease (CPPD), are derived from the inflammatory responses elicited by the shedding into the joint of crystals previously formed in the surface (gout) or within (CPPD) the hyaline cartilage.

Although modern imaging techniques such as ultrasonography (US) or dual-energy computed-tomography (DECT) may demonstrate and identify tissue deposition of both crystals, deposition is not recognized to be enough for diagnosis unless symptoms are present [1]. Chondrocalcinosis and hyperuricemia are quite common in elderly patients, but the presence of phagocytosed crystals within the white cells of synovial fluid (SF) samples remains the gold-standard for diagnosis of crystal-induced arthritis [2].

Daniel J McCarty was the first to describe in detail the morphology, refringence characteristics, and pathogenic significance of urate crystals in SF. At the time, he was still a trainee [3].

The present text has not been ever published. All images ©FPerezRuiz. With permission for this publication.

F. Perez-Ruiz (✉)
Osakidetza, OSI EE-Cruces, Cruces University Hospital, Barakaldo, Spain

Biocruces-Bizkaia Health Research Institute, Barakaldo, Spain

Medicine Department of the Medicine and Nursing School, University of the Basque Country, Barakaldo, Spain
e-mail: fernando.perezruiz@osakidetza.eus

M. C. Modesto-Caballero
Osakidetza, OSI EE-Cruces, Cruces University Hospital, Barakaldo, Spain
e-mail: mariadelconsuelo.modestocaballero@osakidetza.eus

B. F. Mandell (ed.), *Synovial Fluid Analysis and The Evaluation of Patients With Arthritis*, https://doi.org/10.1007/978-3-030-99612-3_10

Characteristic of SF Samples in Gout

Gout may involve acute and chronic inflammation of different musculoskeletal, articular, and periarticular structures, clinically expressed as gout flares and chronic joint swelling respectively. Therefore, the characteristics of the SF samples obtained from synovial-lined structures (joints, tendon sheaths, and bursae) may differ depending on specific clinical setting at the moment the SF samples are obtained.

SF samples in patients with gout may then range macroscopically from almost normal (chronic or persistent effusion) to highly opalescent (gout flare) appearance mimicking purulent samples. White cell counts may also range from almost normal (<1000 cells per μL) to that seen in bacterial (septic) arthritis (>50,000 cells per μL). Some chronic effusions in joints or bursa may have so many crystals that they appear milky.

The pathognomonic characteristic of SF samples in gout is the presence of monosodium monohydrate urate (MSU) crystals [3].

Microscopy Characteristics of MSU Crystals

MSU crystals may be characterized by shape, using light microscopy, but readily by their birefringence and elongation properties using polarized microscopy.

MSU crystals, contrary to calcium pyrophosphate crystals, are not subject to rapid ex-vivo degradation. At room temperature MSU crystals may be detected days after joint aspiration, weeks if the samples are refrigerated from 4 to 10 ° C (refrigerated). MSU crystals may be recovered from frozen samples even longer (months or years) [4]. To avoid the blurring effect of cell debris that occurs with passing time or after defreezing samples, especially those with high white cell counts, the addition of dimethyl sulfoxide 5–10% to the SF samples before freezing will keep cells alive and intact for a short period of time (less than 30 min) after defreezing [5]. Also, dried cytospin (centrifuged) preparations have been reported to be useful to store samples yielding reproducible results [6].

Ordinary Light Microscopy (OLM)

The length of MSU crystals may vary from 5 to 25 μm, and show from the frequent small narrow parallelepiped-like shape (rod-shape) to a long sting shape (needle-shape), the last most commonly observed in the presence of tophaceous deposits [3]. MSU crystals may be easily detected and identified by ordinary light microscopy (OLM) if abundant and typical, that is long and needle-shaped crystals as commonly observed in gout flares (Fig. 10.1).

Nevertheless, some issues may jeopardize the detection and identification of MSU crystals using OLM: scarce number (difficult to detect) or presence of small

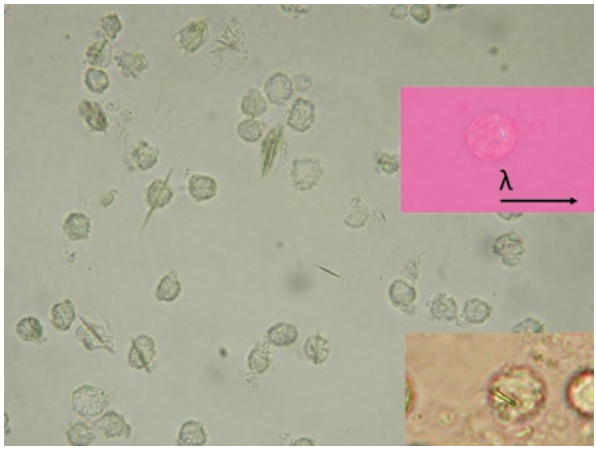

Fig. 10.1 OLM, 400x, MSU crystals. Long needle-shape crystals are quite apparent, but also small rod-shape crystals lay within the cells and may be difficult to detect. In the upper right corner PLM 1000x, in the lower right corner 1000x contrast phase microscopy enhancing both the presence of small rod-shaped MSU crystals

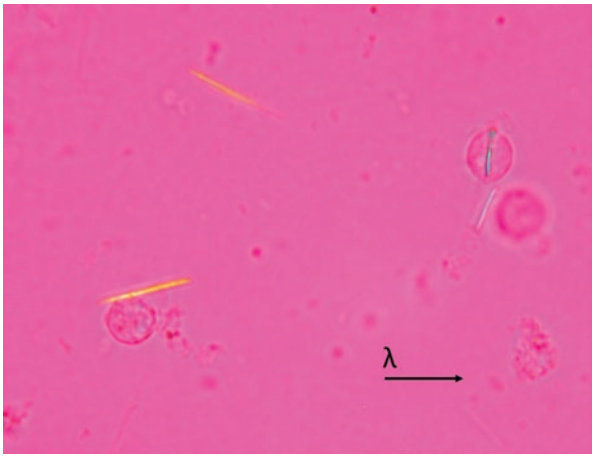

Fig. 10.2 PLM, 400x magnified. All crystals shine bright and yellow when parallel to the extinction axis (lambda)

rod-shaped crystals difficult to distinguish from monoclinic calcium pyrophosphate crystals, as may be seen in chronic effusions (Fig. 10.1). If such is the case, contrast-phase microscopy and polarized light microscopy (PLM) will be useful to both, detect, and then identify MSU crystals.

Polarized Light Microscopy (PLM)

MSU crystals are more easily detected and identified using PLM than with OLM, as they all show intense birefringence with negative elongation properties. MSU crystals all shine intensely under PLM microscopy when appropriately aligned, contrary to calcium pyrophosphate monoclinic (rod-shaped) crystals (Fig. 10.2), which are mostly non-birefringent. A systematic review concluded that PLM is to be considered the standard method for crystal detection and identification [4].

In addition to being almost unanimously birefringent, MSU crystals show negative elongation properties, that is, shine yellow when parallel to the polarizing axis and blue when perpendicular to the extinction axis (Fig. 10.2). In contrast, calcium pyrophosphate crystals will mostly be non-birefringent or mildly birefringent and their elongation will be positive: blue if parallel and yellow if perpendicular to the polarizing axis.

Avoiding False-Negative Results

False-negative results for MSU crystals in SF samples may derive from different causes: delayed joint aspiration, scarce presence of crystals, and delayed observation in high white cell count samples causing cell debris.

Joint aspiration could be delayed due to a number of different causes. In such cases, the clearance of crystals from the joint by polymorphonuclear white cells and synoviocytes may render a reduction in the crystals present in SF. If clinical suspicion is high, consider a second diagnostic arthrocentesis [7].

A scarce number of crystals may be present in SF in patients with persistent or chronic effusions or delayed aspiration after an episode of acute arthritis. A rapid scanning of multiple optic fields crossing the polarizer and the analyzer filters may help detect birefringent MSU crystals. Centrifugation of the SF and examining a sample of the pellet may also help detection [6].

Delayed observation with OLM of SF samples with high white cell counts may hinder the detection of crystals due to the presence of cell debris or clumping of the sample due to fibrin content, as it happens when centrifuged aliquots are used. The use of PLM is helpful in most cases.

Avoiding False-Positive Results

Other crystals or crystalloid structures may mimic the microscopic appearance of birefringent MSU crystals and induce a false-positive report, including glass, corticosteroid, and cholesterol microcrystals. None of these crystals are phagocytized by white blood cells, so just considering the presence of intracellular crystals as pathogenic will help to avoid false-positive results.

Glass microcrystals may derive from the glass slides or coverslips. Such crystals usually show intense birefringence, but erratic elongation (same sample showing positive, negative, or no elongation for different crystals) (Fig. 10.3). Such glass crystals are not phagocytosed by SF cells, so absence of cells and intracellular crystals is distinctive.

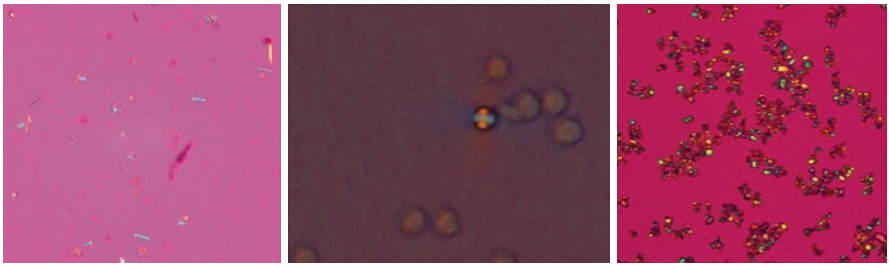

Fig. 10.3 PLM, 400x. Artefacts that may mimic MSU crystals. Glass crystals to the left, lipidic beach ball/malta cross centrally, triamcinolone acetonide to the right

Previous cleaning of the slides and coverslips or discarding the last units in the box may help avoiding misdiagnosis. If in doubt, preparing a new sample with clean slides and coverslips from a new box can be considered.

Cholesterol crystals may be found in chronic effusions, showing a kind of envelope, birefringent shape. Fragments of cholesterol crystals may mimic MSU crystals and cause false-positive results. The presence of other intact cholesterol crystals and absence of intracellular crystals are distinctive. Lipidic spherules figuring malta crosses or beach balls may also mimic two MSU crystals crossed within a cell (Fig. 10.3).

Corticosteroid preparations (phosphate, acetate, acetonide) are crystalloid preparations. Aspirating a joint previously injected with crystalloid corticosteroids preparations may render a false-positive detection (Fig. 10.3). The absence of intracellular crystals and asking the patient if they had received recent intra-articular injection may help to avoid confusion.

MSU Crystals in SF Samples From Asymptomatic Joints

"Never Symptomatic" Joints in Patients with Hyperuricemia

Decades ago, aspiration of the metatarsophalangeal joint of patients with either hyperuricemia or gout showed MSU crystals [8]. Today it is well known that patients with long-lasting hyperuricemia but without symptoms of gout may show ⁼urate deposition around the joints when examined with US or DECT [9, 10]. Aspiration of such deposits may confirm that they contain MSU crystals [10]. From an academic perspective, this is a demonstration that MSU deposition precedes the clinical manifestations of gout [1] and that the crystallization does not occur suddenly before the flare. It has been suggested to call this asymptomatic hyperuricemia with MSU crystal deposits [1], distinct from gout in the absence of clinical manifestations.

Asymptomatic Joints Previously Affected by Gout Flares

SF samples are most easily aspirated from a swollen joint during a gout flare and from joints with persistent (chronic) effusion. SF samples may also be obtained in the interval between flares: small amounts or droplets of SF may be obtained in half to three out of four previously symptomatic joints (joints in which a flare had taken place) and over two-thirds of the samples may show MSU crystals [11, 12].

Coexistence of MSU Crystals in Patients with Other Causes of Arthritis

Diagnosis of gout does not preclude the co-occurrence of other articular diseases. Osteoarthritis, psoriatic arthritis, rheumatoid arthritis, ankylosing spondylitis, and CPPD may precede gout in patients who afterward develop long-lasting hyperuricemia. Conversely, other articular diseases may develop in patients who have had gout flares in the past. In such cases, the microscopic demonstration of MSU crystals in SF samples will allow us, as clinicians, to make a correct diagnosis of true coexistent gout, as MSU crystals have been observed in SF of patients with hyperuricemia and different arthritides [13].

Two clinical settings are of special importance: coexistence of gout and infection and gout with CPPD.

Coexistent Gout and Infection

The presence of MSU crystals in a SF sample does not exclude an ongoing bacterial infection. Previous joint inflammation or injury is a risk factor for joint infection, and MSU crystals have been found in 1.5% of patients with septic arthritis [14]. Bacterial arthritis is characterized by sudden joint swelling, fever, high blood leukocyte counts, and high levels of acute-phase reactants. Gout flares share some of these clinical characteristics and may mimic septic arthritis but also predispose to bacterial infection. Indeed, in the series of patients used for the 1974 preliminary criteria for the classification of gout, 4/112 patients with septic arthritis had crystal proven tophi, although none of the 84 infected SF samples showed MSU crystals [15].

A careful analysis of clinical settings, risk factors, and general symptoms should be made in every patient with acute arthritis, and SF samples should be sent to the microbiology lab for culture even when the SF contains crystals. High serum procalcitonin levels have been suggested to be potentially useful to detect concomitant bacterial infection.

Coexistent CPP and MSU Crystals

Acute pyrophosphate arthritis (CPPA) in CPPD has been previously known as "pseudogout" [16]. That is because it close mimics gout flares. Chondrocalcinosis and hyperuricemia frequently coexist in elderly people, thus gout and CPPA frequently coexist. The demonstration of which crystal is responsible for the development of acute arthritis remains crucial, as urate-lowering medications may be indicated for gout, but nor for patients with hyperuricemia and CPPA or asymptomatic chondrocalcinosis.

In addition, some patients may infrequently show both crystals in SF samples. It is important to highlight that careful SF exam should be made even though MSU bright-shining crystals are found in SF in patients with radiographic chondrocalcinosis, as rod-shaped, non-birefringent monoclinic CPP crystals may not be apparent among the MSU crystals with ordinary light microscopy among small rod-shaped MSU crystals. The finding of wide parallelepiped-shaped rhomboid crystals of triclinic CPPD may also and non-birefringent crystals with PLM may help (Fig. 10.4). This is important because after years of urate lowering therapy, a flare in CPPA could be misconstrued as a gout flare indicating treatment failure.

Diagnosis of Gout in Tissue Sample

MSU crystals may also be found in tissues. Bone, skin, and synovial membrane are common sources for histopathologic study in patients with present or past hyperuricemia and infrequent symptoms or uncommon locations for gout, although deposits in other many organs have been described [17]. MSU crystals are soluble to

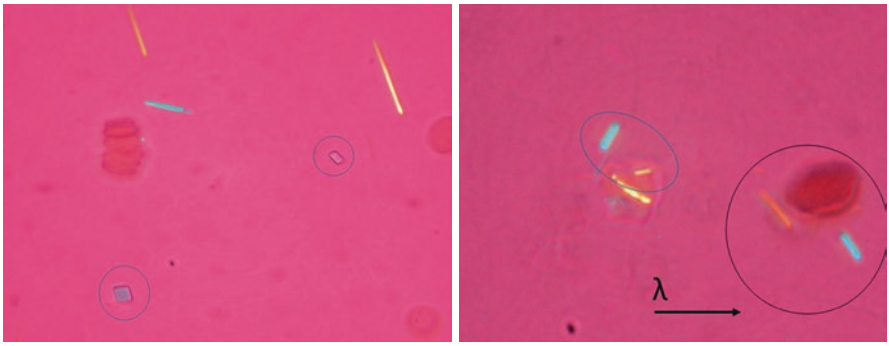

Fig. 10.4 PLM, 400x. To the left, needle-shaped MSU crystals coexist with rhomboidal CPP crystals (within circles). To the right, rod-shaped crystals show different elongation despite they are parallel: the "cousins, but not brothers" image

formalin but not to ethanol. Therefore, to avoid disappearance of MSU crystals during the fixation procedure of biopsy samples, absolute ethanol should be used [18] when possible, and the pathologist alerted to the plausible diagnosis of gout if ethanol fixation is not available.

Histopathology of Synovial Membrane

The histopathology of synovial membrane depends on the presence of either acute and chronic inflammatory response [19]. Both findings, acute inflammation and a chronically inflamed synovial membrane, may coexist.

Acute neutrophilic synovitis is the paradigm of gout flares. Intense neutrophil infiltration cannot be differentiated from acute bacterial (septic) arthritis (Fig. 10.5). Chronic synovitis in gout is characterized by a granulomatous, foreign body-like infiltration (Fig. 10.5).

Histopathology of Subcutaneous Tophi

The most common finding is an amorphous central area where MSU aggregates develop, surrounded by a foreign body-like granulomatous reaction with an epithelioid palisade with surrounding giant multinucleate cells and mononuclear cells (Fig. 10.6). As previously mentioned, ethanol fixation is necessary to preserve MSU crystals.

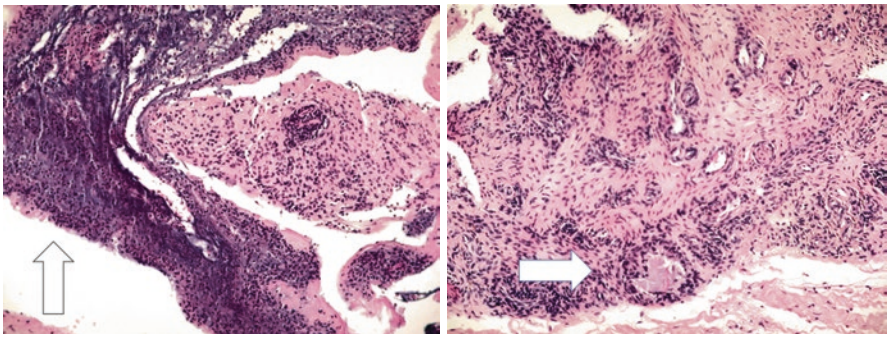

Fig. 10.5 Hematoxylin eosin stain. Left image showing acute, intensely neutrophilic infiltration and hypertrophy of the synovial membrane (arrow). Right image, chronic inflammation of the synovial membrane showing a central matrix (no crystal present due to formalin fixation) surrounded by a foreign body granulomatous reaction

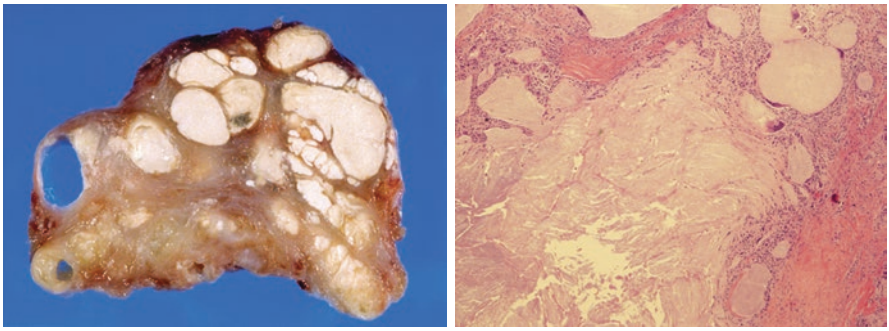

Fig. 10.6 Macroscopic (left) and hematoxylin eosin stain microscopy of a subcutaneous tophus, with central amorphous matrix (MSU deposits not present due to formalin fixation) and peripheral fibrosis and chronic inflammation

References

1. Bursill D, Taylor WJ, Terkeltaub R, Abhishek A, So AK, et al. Gout, hyperuricaemia and crystal-associated disease network (G-CAN) consensus statement regarding labels and definitions of disease states of gout. Ann Rheum Dis. 2019;0:1–8. https://doi.org/10.1136/annrheumdis-2019-215933.
2. Pascual E, Doherty M. Aspiration of normal or asymptomatic pathological joints for diagnosis and research - indications, technique and success rate. Ann Rheum Dis. 2009;68(1):3–7. https://doi.org/10.1136/ard.2008.088328.
3. McCarty DJ, Hollander JL. Identification of urate crystals in gouty synovial fluid. Ann Intern Med. 1961;43:452–9. https://doi.org/10.7326/0003-4819-54-3-452.
4. Graf SW, Buchbinder R, Zochling J, Whittle SL. The accuracy of methods for urate crystal detection in synovial fluid and the effect of sample handling: a systematic review. Clin Rheumatol. 2013;32:225–32. https://doi.org/10.1007/s10067-012-2107-0.
5. Perez-Ruiz F, Castillo E, Chinchilla SP, Herrero-Beites AM. Clinical manifestations and diagnosis of gout. Rheum Dis Clin N Am. 2014;40(2):193–206. https://doi.org/10.1016/j.rdc.2014.01.003.
6. Robier C, Neubauer M, Stettin M, Lunzer R, Rainer F. Dried cytospin preparations of synovial fluid are a stable material for long-time storage and delayed crystal analysis. Clin Rheumatol. 2012;31:1115–6. https://doi.org/10.1007/s10067-012-1967-7.
7. Schumacher HR, Jimenez SA, Gibson T, Pascual E, Traycoff R, et al. Acute gouty arthritis without urate crystals identified on initial examination of synovial fluid. Arthritis Rheum. 1975;18(6):603–12.
8. Rouault T, Caldwell DS, Holmes EW. Aspiration of the asymptomatic metatarsophalangeal joint in gout patients and hyperuricemic controls. Arthritis Rheum. 1982;25(2):209–12. https://doi.org/10.1002/art.1780250215.
9. Wang P, Smith SE, Garg R, Lu F, Wohlfahrt A, Campos A, et al. Identification of monosodium urate crystal deposits in patients with asymptomatic hyperuricemia using dual-energy CT. MRD Open. 2018;4:e000593. https://doi.org/10.1136/rmdopen-2017-000593.
10. De Miguel E, Puig JG, Castillo C, Peiteado D, Torres RJ, Martin-Mola E. Diagnosis of gout in patients with asymptomatic hyperuricaemia: a pilot ultrasound study. Ann Rheum Dis. 2011;71(1):157–8. https://doi.org/10.1136/ard.2011.154997.

11. Bomalaski JS, Lluberas G, Schumacher HR. Monosodium urate crystals in the knee joints of patients with asymptomatic nontophaceous gout. Arthritis Rheum. 1986;29(12):1480–4. https://doi.org/10.1002/art.1780291209.
12. Pascual E, Batlle-Gualda E, Martinez A, Rosas J, Vela P. Synovial fluid analysis for diagnosis of intercritical gout. Ann Intern Med. 1999;131:756–9. https://doi.org/10.7326/0003-4819-131-10-199911160-00007.
13. Oliviero F, Scanu A, Galozzi P, Gava A, Frallonardo P, et al. Prevalence of calcium pyrophosphate and monosodium urate crystals in synovial fluid of patients with previously diagnosed joint diseases. Joint Bone Spine. 2013;80(3):287–90. https://doi.org/10.1016/j.jbspin.2012.08.006.
14. Shah K, Spear J, Nathanson LA, McCauley J, Edlow JA. Does the presence of crystal arthritis rule out septic arthritis? J Emerg Med. 2007;32(1):23–6. https://doi.org/10.1016/j.jemermed.2006.07.019.
15. Wallace SL, Robinson H, Masi AT, Decker JL, McCarty DJ, Yü. Preliminary criteria for the classification of the acute arthritis of primary gout. TF. Arthritis Rheum. 1977;20(3):895–900. https://doi.org/10.1002/art.1780200320.
16. Zhang W, Doherty M, Bardin T, Barskova V, Guerne PA, et al. European league against rheumatism recommendations for calcium pyrophosphate deposition. Part I: terminology and diagnosis. Ann Rheum Dis. 2011;70(4):563–70. https://doi.org/10.1136/ard.2010.139105.
17. Lichtenstein L, Scott W, Levin MH. Pathologic changes in gout. Survey of eleven autopsies. Am J Pathol. 1956;32(5):871–95. PMCID: PMC1942635.
18. Schumacher HR. Pathology of the synovial membrane in gout. Arthritis Rheuma. 1975;18(Suppl):771–82. https://doi.org/10.1002/art.1780180722.
19. Towiwat P, Chhana A, Dalbeth N. The anatomical pathology of gout: a systematic literature review. BMC Musculoskelet Disord. 2019;20:140. https://doi.org/10.1186/s12891-019-2519-y.

Chapter 11
Crystal-Associated Arthritis: Calcium Pyrophosphate Arthritis

Eliseo Pascual and Mariano Andrés

CPP Crystal Detection and Identification

Bright Field Microscopy This allows detection and identification of CPP and MSU crystals by morphology. Our experience is that CPP crystals are most frequently identified this way [1]. Although large parallelepipeds, rhombuses, and large thick bars are considered the characteristic CPP crystals on which identification is based, very thin bars are frequent, even more common in some synovial fluids (SF) than the characteristic CPP crystals, and may be confused with MSU by morphology (Fig. 11.1). Tiny crystals are very common, either little very thin needles, parallelepipeds or rhombuses, or quite refringent (not to be confused with *birefringent*) little chunks with a couple of linear borders making an angle. When these are seen, we consider it wise to continue looking until seeing more characteristic crystals for definitive identification. As it will be described below, these thin needle-like bars are at most only slightly birefringent under (uncompensated) polarized microscopy allowing clear distinction from the highly birefringent – very brilliant – MSU crystals. Characteristic crystals with different degrees of irregularity are frequently seen. In the fresh preparation, where crystals frequently move, it is instructive to look at them moving to appreciate how their apparent shape differs with different crystal orientation. CPP crystals are very often intracellular, and that is there where they should be sought, especially in SF with few cells. They are often found inside vacuoles (Fig. 11.2), and tiny crystals may be found inside very large vacuoles; this appearance, if it happens, is very rare with MSU crystals. Finding

E. Pascual (✉) · M. Andrés
Rheumatology Unit, Dr. Balmis General University Hospital-Institute of Sanitary and Biomedical Research (ISABIAL), Alicante, Spain

Clinical Medicine Department, Miguel Hernandez University, San Juan de Alicante, Spain
e-mail: pascual_eli@gva.es; mariano.andresc@umh.es

B. F. Mandell (ed.), *Synovial Fluid Analysis and The Evaluation of Patients With Arthritis*, https://doi.org/10.1007/978-3-030-99612-3_11

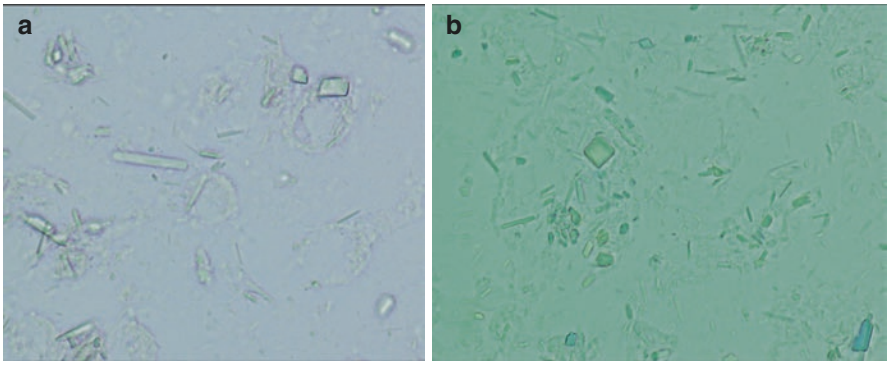

Fig. 11.1 (**a**, **b**) Bright field microscopy 600X, fresh SF preparation, demonstrating different shapes of CPP crystals, from large characteristic rhombuses and parallelepipeds, to bars of different width, to very thin ones that could be taken as MSU crystals. Note the large number of tiny crystals, especially in (**b**). (**a**, **b**) Slight background light color differences depend on whether one of the polarized filters is in place (**a**) or no filter (**b**). Only one polarized filter has no other effect on the image. Consider that any of these crystals may appear isolated in the field you are examining. Definitive identification of CPP crystals relies on identifying ones with characteristic morphology

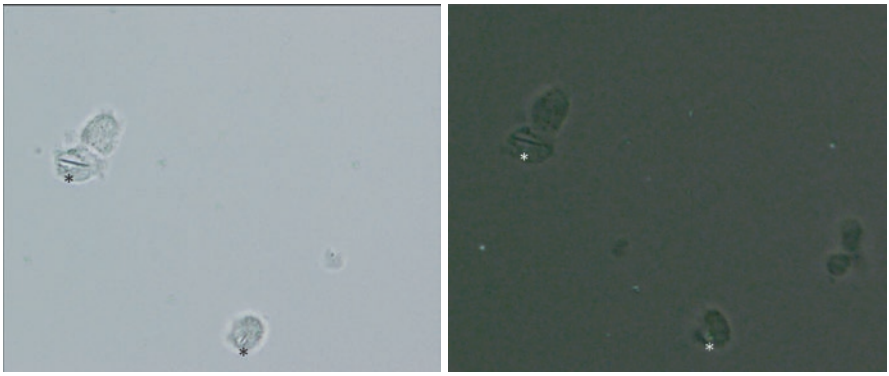

Fig. 11.2 Fresh preparation, 400X. Left: clear field microscopy, right: same field, polarized microscopy uncompensated [polarized filters are slightly uncrossed (rotated) to allow some background detail]. Two CPP thin needle-like crystals (*) associated with an intracellular vacuole. Note that they lack birefringence (right). These two features help to identify them as CPP crystals. Identification should be supported by identifying crystals of characteristic shape – large rhombuses, parallelepipeds, or thick bars

only these very small intracellular bars should prompt a continued search for larger parallelepipeds, rhombuses, or large thick bars, the appearance of more characteristic CPP crystals. Crystals with some irregularity – or appearing so because of their three-dimensional orientation on the slide are frequently seen. The shape of tiny crystals is best seen at 600X or 1000X (the higher magnification is particularly useful during the training period to appreciate the heterogeneity of CPP crystals). At

many emergency rooms and clinics, there is an available light microscope. Paying attention to identifying crystals in SF by bright light microscopy may allow a rapid diagnosis of many patients if crystals are detected, attaining an immediate, unequivocal diagnosis of crystal arthritis and avoiding additional unnecessary workup. With experience, MSU can quite often be distinguished from CPP crystals by using light microscopy [1].

Polarized Microscopy (Uncompensated) The polarized filters only permit the light vibrating parallel to their axis to pass through the microscope to the oculars and the analyst's eyes, so when a second polarizing filter is placed in the path of this polarized beam with its axis perpendicular to the one of the first filter, no light will pass through because the light that went through the initial filter is perpendicular to the axis of the second and so blocked by it; This results in a dark microscope field; a birefringent crystal sitting in it splits the light beam in two perpendicular polarized components which add to each other in all directions permitting one of the split beams to now pass through the second filter. Perpendicular split beam will not pass through. These not passing beams, perpendicular to each other, mark the dark cross in the "Maltese cross" form by fat globules under polarized microscopy (Fig. 11.3). Birefringent crystals are seen as bright images in the dark background; the brighter the microscope lighting, the brighter the crystals will show. A strong light is desirable for this, so it is valuable to adjust the height of the condenser, for optimal birefringence (adjusting the condenser for maximal birefringence while looking at an MSU crystal preparation – by changing the height of the condenser with an open diaphragm). Slightly uncrossing (rotating) one of the polarized filters will allow some light to pass, retaining the brilliance of the birefringent crystal while permitting the analyst to see background detail, something especially useful while acquiring microscopic skills.

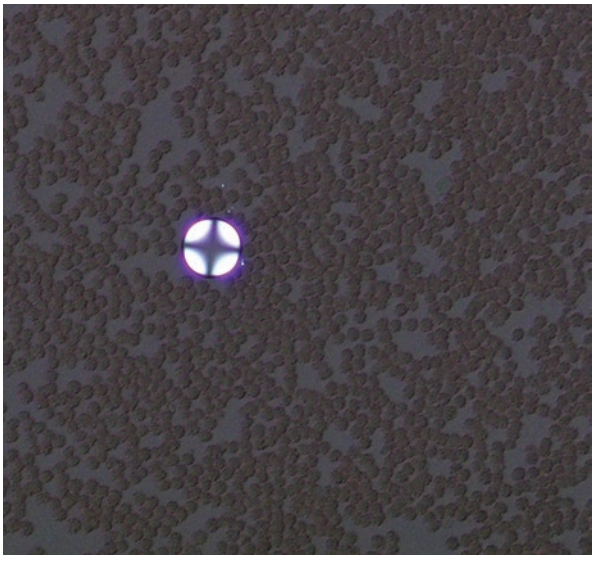

Fig. 11.3 Fat globule as seen with (uncompensated) polarized light, 200X. The dark perpendicular branches of the "Maltese Cross" are perpendicular to the axes of the crossed polarizing filters

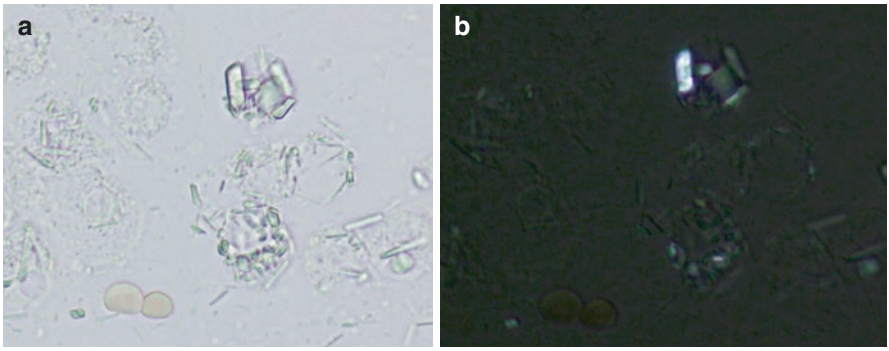

Fig. 11.4 Fresh SF preparation 600X. (**a**): Ordinary light, (**b**): Same microscope field with crossed polarized filters – slightly uncrossed to allow background detail. CPP crystals, note that few of them seen under ordinary light do not show brilliance under polarized light, one of the large parallelepiped crystals is highly birefringent, others are modestly so, and many not at all

Only a small proportion of CPP crystals show brilliant birefringence (Figs. 11.4 and 11.5). Daniel McCarty appreciated this in the report in which these crystals were described "The birefringence of most [CPP] crystals was weak and the sign was positive; some appeared to be isotropic (non-refractile)" [2] and Paul Dieppe and Angela Swann made a similar comment "CPPD crystals are only weakly birefringent, and are probably better identified by non-polarized light and characterized by morphology, than by their polarization properties" [3]; we fully agree with these comments. In reports from our unit, we found that only 18% of CPP crystals had any birefringence [4]. In studying the birefringence of acicular-looking CPP crystals, the ones that by morphology could be taken for MSU, we found that a majority of CPP crystals (76–82%) are non- or weakly birefringent. And only about 1/3 of needle (or thin bars) CPP crystals showed birefringence that was considered weak or moderate. No needle crystals were found to be as birefringent – with uncompensated polarized microscopy – as are MSU crystals used as a reference for strong birefringence [5]. So, the absence of birefringence helps us to consider that acicular or long bar may be CPP; but no firm diagnosis should be based on the observation of a single one of these crystals. Frequently novices are halted in their exam by a single crystal that they cannot properly identify. It is often prudent to initially leave this crystal aside, if unique, and continue looking for ones allowing identification. It should be remembered that MSU crystals parallel to the axis of either of the polarized filters (not the compensator) are in the position of "extinction" and will not appear as birefringent, unless the crystal is rotating on the slide, this makes the availability of a rotating stage invaluable to permit reorienting the crystal, although this stage is not necessary. When MSU crystals are abundant it is possible to see occasional ones that seem not to show birefringence.

Compensated Polarized Microscopy This is a more complex technique and beginners should abstain from it until they can recognize CPP and MSU crystal with ordinary light and simple polarized microscopy, preferably looking with compen-

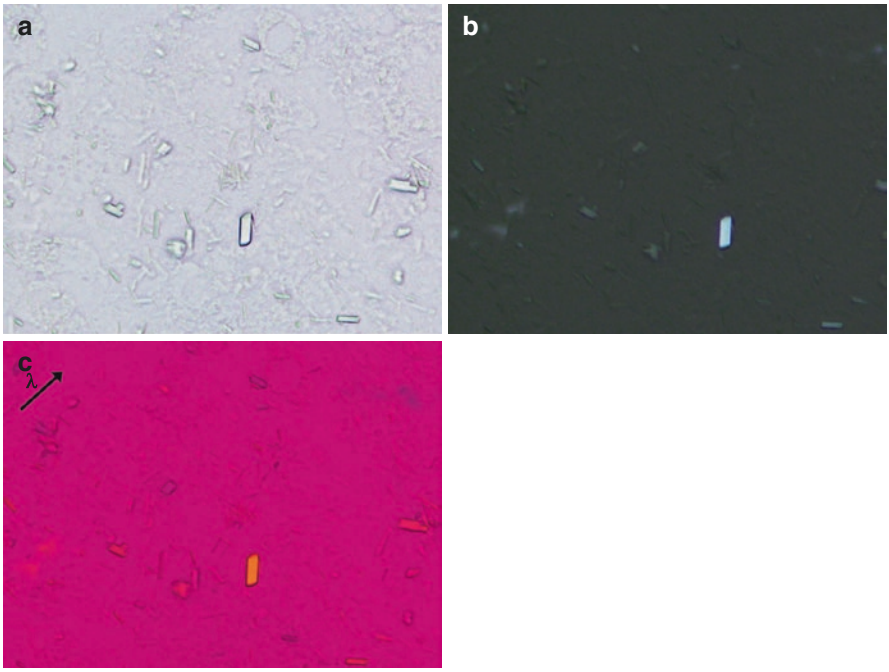

Fig. 11.5 (**a**, **b**, **c**) Abundant CPP crystals as seen by (**a**): bright field; (**b**): uncompensated polarized microscopy; and (**c**): compensated polarized microscopy. Note the almost absence of birefringence under the polarized microscope, and the less brilliant and faint to absent colors taken by the crystals. 600X, that are much better distinguished under the bright field microscope. The arrow and λ indicate the axis of the compensator

sated polarized microscopy at crystals previously identified by the other means, as a training exercise. It adds to the previous optical system a first-order red compensator ("retardation plate"; its axis marked by a λ and an arrow) placed between the polarizing filters. This helps to determine whether the long axis of the birefringent crystal is parallel to the slower or faster wavelength of the compound beam emerging from the crystal in this system, the direction in relation to this axis on the compensator of the slow and fast beams generated when the polarized light strikes it, defines the positive or negative birefringence (elongation) of a specific crystal. The slow and fast beams will appear as different colors when the red compensator is in the optical circuit. Most modern clinical microscopes can be equipped with reasonably priced polarization filters appropriate for SF crystal analysis.

CPP crystals show a weak positive birefringence (weak because they are weakly birefringent and many crystals may not change color at all as they rotate in relation to the axis of the red compensator). Positive birefringence means that when the long axis of the crystal is parallel to the compensator axis (marked with an arrow and a λ) it shows pale blue, and pale yellow when perpendicular to it (opposite to the color pattern of MSU crystals) (Figs. 11.5 and 11.6); it is important to compare this color

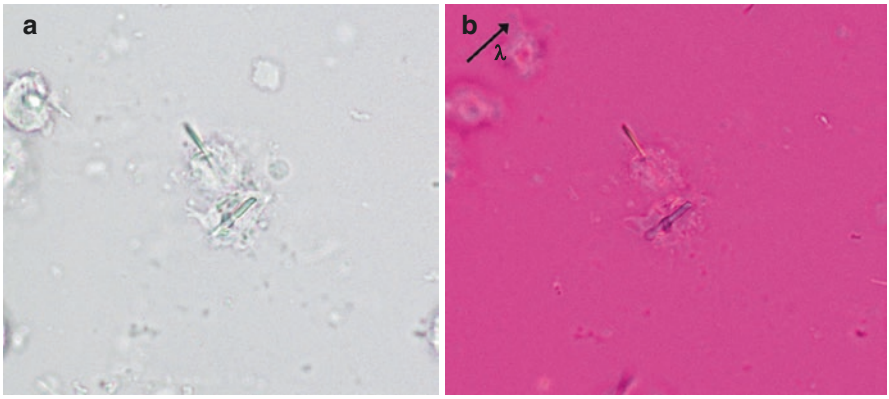

Fig. 11.6 (**a**, **b**) Two quite thin CPP bars. (**a**): bright light and (**b**): compensated light microscopies, 600X. The crystals are clearly seen in (**a**), and too thick for classic MSU but could be confused with MSU. Here compensated light microscopy helps in their proper identification. Additional characteristic crystals seen in other fields confirmed the identification as CPP. To find nice CPP crystals properly positioned and birefringent as those here may take time and patience. By contrast, almost any microscope field showing MSU crystals provides a proper example and this is why they are more readily identified. The arrow and λ indicate the axis of the compensator

change with the brilliance of the yellow (parallel) and blue (perpendicular) to the compensator axis given by the MSU crystals; Daniel McCarty, noted in the report where CPPD crystals were described that "CCPD crystals are much more difficult to see by polarized microscopy than are MSU crystals…" [2]. A not minor difference is that the yellow and blue coloration of MSU crystals is quite intense and for CPP crystals the intensity of the color appears to relate to intensity of birefringence under the (uncompensated) polarized microscope, and is quite variable but rarely reaching that of MSU crystals. In the learning process it is useful to repeatedly look under this filter combination to crystals clearly seen as birefringent with simple polarized microscopy (removing the red compensator from the optical circuit), and also to those not appearing as birefringent with the same polarization setting. Change in color of many crystals can be very subtle, and particularly for weakly birefringent crystals may seem to change with adjustment of the fine focusing knob.

Why CPP Crystals Are the Troublesome Ones to Identify? Likely factors influencing the proper identification of CPP crystals include (1) The historical teaching that rhombuses and parallelepipeds are the characteristic CPP crystals when long thin bars and needle-like crystals (that may be mistaken for MSU crystals) are often more common. (2) The teaching that CPP crystals show weakly positive elongation, although even large crystals may not show any birefringence, and this may depend on proper setting of the microscope. (3) We find that most often CPP crystals can be found phagocytized and especially when cellularity is low, they should be searched inside cells. (4) Frequently CPP crystals can be found inside vacuoles – even very small ones – and this finding should prompt the search for larger rhombuses or parallelepipeds to confirm their presence.

Notes for Beginners Be patient and assure that the microscope lenses ocular and slides are clean. Become familiar with the appearance of red cells and white blood cells in the fluid with different settings of the polarizing filters, compensator, and condenser. When looking at fluids from known gouty or CPP arthritis patients, you will be surprised by seeing crystals in or outside the cells that you will recognize by morphology. Take time and effort to appreciate the different appearances of CPP crystals and the more uniform needle shape of MSU. Rotate one of polarized filters, done differently in different microscope brands. Note the brilliance of MSU and the very faint or absent shine of most CPP crystals under different optical conditions. Become familiar with the many shapes of CPP crystals. Expert analysts most often recognize crystals as MSU or CPP crystals at first glance even with bright light microscopy.

Mimics of CPP Crystals

There is a variety of crystals that occasionally are found in SF samples that might be mistaken for CPP crystals. When the observer becomes familiar with the different shapes that CPP crystals may display, along with their birefringence characteristics, the confusion is less likely to occur.

Calcium oxalate crystals may show their typical bipyramidal "envelope"-like shape, but others are irregular or rod-shaped. Calcium oxalate crystals were detected in end-stage renal patients getting hemodialysis [6], but now are a rarity, limited to patients with primary hyperoxaluria, as current hemodialysis membranes efficiently clear oxalate. *Cholesterol* crystals can form in longstanding effusions in joints or bursae in patients with osteoarthritis, tophaceous gout, or rheumatoid arthritis (now exceptional due to advances in management), but with no definite pathogenic role. They are classically large crystal plates (8–100 μm) of a squared shape with a typical notched margin, and an intense birefringence. *Steroids* used for intra-articular injections are formulated as crystalline solutions to allow local and sustained agent delivery, achieving more prolonged anti-inflammatory results. Innate immune cells occasionally may react to them, leading to a flare-like phenomenon occurring hours or a few days after the injection [7]. In this context, the principal differential diagnosis is septic arthritis, so SF analysis is mandatory, and steroid crystals can be seen. The shape and birefringence vary among the steroidal agents, though usually are intense, positively birefringent, and often polymorphous. Occasional isolated steroid crystals may mimic CPP crystals. Becoming familiar with the microscopy appearance of the steroid used in your own clinic is advisable to help avoid misdiagnoses. *Hematoidin* crystals may mimic CPP as they often display polygonal shapes of varying sizes. However, the reddish color shown under ordinary light gives a clue for the diagnosis, as well as characteristic light green after polarization [8]. Hematoidin is a derivation product of hemoglobin and is occasionally seen in synovial effusions with prior recurrent hemarthrosis. They are presumed to have no arthritogenic role.

Many attendees to SF crystal analysis workshops report difficulties in distinguishing CPP crystals from *artifacts*. Artifacts occur from different sources (dirty glasses, gloves powder, and fibers, among others) and depict variable shapes and birefringence, but most often different from CPP crystals. Some may resemble "Maltese cross" lipid crystals but are larger and non-symmetrical. Using powder-free gloves and cleaning the glass slide with alcohol 70° before placing the sample reduces the presence of these artifacts. In addition, in case of doubt about a certain crystal, we recommend searching the preparation for more typical pathogenic crystals. It has been reported that another source of artifacts may be the presence of lithium heparin in the containing tube as an anticoagulant [9]. *Lithium heparin* crystals seem to be polymorphic (even polygonal) and pose positive birefringence, so should be distinguished from CPP crystals. No crystals were seen using sodium heparin. This data is important if the SF analysis is delayed or sent to the laboratory in heparinized tubes for crystal identification.

Effects of Delays Prior to Observation, Transportation, and Processing Issues

Slide Preparation and SF Examination The preparation to be examined by ordinary light and polarized microscopies is the same. Neither fixation nor staining is required, but note that crystals may still be recognized even in gram-stained SF. The glass slide and cover slide should be carefully cleaned to minimize artifacts. A single drop of SF sample should be placed from the syringe on the glass slide, gently laying the cover slip on it. The smaller the drop the thinner the layer of SF obtained, and thin ones are desirable if SF samples are highly inflammatory to obtain a clear view of individual cells. Learning the technique described here has been consistent after a short training period [10].

Cytocentrifugation Its main advantage is to theoretically increase the detection of crystals, especially if sparse because the process concentrates cells and crystals. Centrifugation does not add much in the detection of MSU crystals, usually recognized easily, but substantially increased recognition of CPP crystals by about 20% of the total number of CPP-positive smears [11]. But centrifugation, especially cytocentrifugation is a more complex technique needing additional equipment. Another study showed superiority for detecting MSU crystals by cytospin compared with dry smears [12], but a limitation of this study is the use of stained dry slides for crystal identification as the comparator, a technique that has received little attention and has not been compared with examination of fresh SF.

Delay on Examination Many trainees and rheumatologists often inquire during SF workshops about delays in performing the analysis. This question is indeed essential for colleagues with no immediate access to the polarized microscope, as it might result in avoiding the testing and establishing the diagnosis of crystal arthritis

solely on clinical terms with the risk of misdiagnosis [13]. Several studies have assessed this question with discrepant results [14–22]. In summary, MSU remained in the stored samples regardless of the temperature of storage and the preservation method, while CPP crystals would dissolve or be more difficult to identify; their evaluation largely depends on the crystal shape under ordinary light [5], which can be complicated by cell degradation, clots formation, and appearance of artifacts, common in stored samples over time [15]. On the other hand, the intense birefringence on a polarized field will reveal MSU crystals' presence, occasionally even for those not seen on initial analysis. It has been reported that no new crystals form [17]. Samples stored refrigerated (~4 °C/39 °F) and within lithium heparin-containing tubes allowed a delay identification until a week after extraction [21]. Heparin may limit the clotting of highly inflammatory SF samples, but as noted above lithium heparin may cause some confusion due to artifactual crystal formation. The quick access to a polarized microscope is the ideal situation to perform SF analysis for crystals. This allows a quick, firm diagnosis of gout or CPP crystal disease, avoids unnecessary workups, and ensures the appropriate management in the same visit, making the polarized light microscopy a key bedside procedure for the rheumatologist. However, not having the microscope nearby should not impede performing joint aspiration for crystal assessment.

Alizarin Red Stain Alizarin red S staining was proposed as a useful method to detect calcium-containing crystals in the SF, such as CPP, basic calcium phosphates (BCP), or calcium oxalates [23, 24]. The procedure requires mixing a drop of fresh SF and freshly filtered 2% alizarin red S solution using a Pasteur pipette, analyzing the sample under the ordinary light microscope within 3 minutes. The calcium crystals that are visible with the light microscope will appear colored in red, while amorphous, red-colored clumps will be seen for BCP. However, in our practice, the alizarin red staining entails no significant advantage for detecting CPP crystals, which are successfully identified by their polymorphic shape with normal light and moderate birefringence under polarized microscopy. Hence, the main utility of alizarin red would be identifying BCP-containing SFs, as they are not visible under light microscopy and require electron microscopy [25], but the clinical significance of identifying BCP crystals in SF is often uncertain [26].

Quality Control Between Different Observers for CPP Identification

Since Hollander and McCarty's initial description of MSU and CPP crystals [2, 27], the works assessing the performance of SF analysis for crystal identification have yielded contradictory results [10, 28–34]. This controversy has been used to argue against the procedure. However, the methodology followed in those papers varied notably in terms of the origin of crystals (natural or synthetic), vehicle (dry slides or

wet preparations), type of microscope (ordinary, simple polarized, or compensated polarized light microscopes), or analysts (rheumatologists, pathologists, or laboratory technicians). In addition, other factors, such as storing and preserving conditions, were not considered and may also influence the results. Globally, the identification of CPP crystals tends to be less reliable than more easily recognized MSU crystals. The dedication and training of the observers are significant factors to be considered. For instance, in the paper by Schumacher et al. [28], the authors compared performance by technicians from three laboratories, two of them mainly concentrated on hematological analyses. Our group reported that laboratory fellows could acquire full competence in crystal detection and identification following a short training period [10]. Similar findings have been reported recently in a French study with rheumatologists [34]. As long as they regularly assess obtained SF samples, rheumatologists have remained competent [35].

CPP Crystals in Synovial Tissue and in Cartilage at Time of Joint Replacement

CPP and Osteoarthritis There is a close relationship between CPP crystal disease (CPPD) and osteoarthritis. Daniel McCarty included osteoarthritis as part of the CPPD clinical spectrum, particularly in cases when involved joints are atypical for primary osteoarthritis, exhibit rapid progression, or have marked osteophytosis and bone fragmentation [36, 37]. Radiological chondrocalcinosis increases in prevalence with age [36, 38], in close relation to osteoarthritis [39]. CPP crystals can be found in osteoarthritic knees at the time of joint replacement, with a prevalence of deposition ranging from 8.8% to 56.6% according to the method employed for the identification – SF analysis [40–43], conventional radiography [40–43], ultrasound [44], magnetic resonance [45], dual-energy computed tomography [41], or histology [44–46]. CPP has been scantly evaluated in other joints and all cases by histopathology: in hips, presence was noted in 3–10% [46, 47], while in 12.8% of shoulders [46]. CPP crystals can anecdotally be seen in effusions from asymptomatic hyperuricemic subjects [48]. BCP crystals frequently accompany CPP deposition in osteoarthritis [43, 49]. Interestingly, some reports confirmed that osteoarthritic joints with CPP deposition tend to occur in older patients [42, 43, 46], possibly with a longer disease duration. In fact, new deposition of crystals during the follow-up of osteoarthritis with an initial negative evaluation has been noted [40].

Significance of CPP Crystals Contrary to MSU crystals, whose presence in SF defines gout, CPP arthritis is a disease of hazy limits. It is presently uncertain whether CPP crystal deposition in an osteoarthritic joint plays a major role in the progression of joint damage. This appears to be the case of CPPD with inflammatory manifestations, as these patients seem to require a joint replacement more often [39]. However, it remains uncertain for non-inflammatory CPPD demonstrated by

radiology or SF. Chondrocalcinosis predicted further cartilage degeneration and subchondral cyst formation by magnetic resonance – a very sensitive technique [50], while having no significant impact on clinical or radiographic worsening or the ultimate need for joint replacement [51].

Perhaps CPP crystal formation, not leading to inflammatory symptoms, is part of the natural aging process of the joint cartilage, as has been found in joints previously damaged or mechanically stressed: post-meniscectomy [52], self-reported knee malalignment in early adult life [53], localized chondrocalcinosis in traumatized joints [54], unstable joints [55], joints previously affected by juvenile arthritis [56], joint dysplasia [57, 58], or in the Milwaukee shoulder [59]. Interestingly, CPP crystals have been found by cytocentrifugation in seropositive RA, being mostly older that those without crystals and with more frequent knee prostheses [60, 61]. Older patients with symmetrical seronegative RA-like synovitis, showing CPP crystals in their inflammatory SFs and having responded to methotrexate, may have indeed seronegative RA but developed CPP crystals in their inflammation damaged joints; we have seen a number of such patients [62]. The authors of another study that found CPP crystals in SF of seronegative RA noted that CPP arthritis can be misdiagnosed as seronegative RA [63]. Finally, gouty SF has been reported to occasionally contain CPP crystals. In the initial report in which Daniel McCarty described CPP crystals one of the patients also had MSU crystals in his SF [2]; for this coincidence the term mixed crystal disease has been coined [64], although no particular clinical features have been described. Different studies have shown this coincidence in 6/80 (7.5%) gouty SF analyzed by cytocentrifugation [65] and in 2/303 (0.66%) [61], 57/794 (7.18%), and 171/6983 (2.5%) [66] analyzed on fresh preparations. The differences in percentages in these studies and in clinical practice are likely related to the scarce attention paid to occasional CPP crystals found along with abundant MSU ones in analysis carried out for diagnostic purposes.

References

1. Pascual E, Tovar J, Ruiz MT. The ordinary light microscope: an appropriate tool for provisional detection and identification of crystals in synovial fluid. Ann Rheum Dis. 1989;48(12):983–5.
2. Kohn NN, Hughes RE, McCarty DJ, Faires JS. The significance of calcium phosphate crystals in the synovial fluid of arthritic patients: the “pseudogout syndrome”. II. Identification of crystals. Ann Intern Med. 1962;56:738–45.
3. Dieppe P, Swan A. Identification of crystals in synovial fluid. Ann Rheum Dis. 1999;58(5):261–3.
4. Ivorra J, Rosas J, Pascual E. Most calcium pyrophosphate crystals appear as non-birefringent. Ann Rheum Dis. 1999;58(9):582–4.
5. Andrés M, Vela P, Jovaní V, Pascual E. Most needle-shaped calcium pyrophosphate crystals lack birefringence. Rheumatology (Oxford). 2019;58(6):1095–8.
6. Hoffman GS, Schumacher HR, Paul H, Cherian V, Reed R, Ramsay AG, et al. Calcium oxalate microcrystalline-associated arthritis in end-stage renal disease. Ann Intern Med. 1982;97(1):36–42.

7. White D, Munroe S. Clinical image: crystal arthritis induced by intraarticular corticosteroid. Arthritis Rheum. 2011;63(8):2539.
8. Tate GA, Schumacher HR, Reginato AJ, Algeo SB, Gratwick GM, Di Battista WT. Synovial fluid crystals derived from erythrocyte degradation products. J Rheumatol. 1992;19(7):1111–4.
9. Tanphaichitr K, Spilberg I, Hahn BH. Letter: lithium heparin crystals simulating CPPD crystals. Arthritis Rheum. 1976;19(5):966–8.
10. Lumbreras B, Pascual E, Frasquet J, González-Salinas J, Rodríguez E, Hernández-Aguado I. Analysis for crystals in synovial fluid: training of the analysts results in high consistency. Ann Rheum Dis. 2005;64(4):612–5.
11. Boumans D, Hettema ME, Vonkeman HE, Maatman RG, van de Laar MA. The added value of synovial fluid centrifugation for monosodium urate and calcium pyrophosphate crystal detection. Clin Rheumatol. 2017;36(7):1599–605.
12. Robier C, Stettin M, Quehenberger F, Neubauer M. Cytospin preparations are superior to common smears in the detection of monosodium urate crystals in low-cellular synovial fluids. Clin Rheumatol. 2014;33(12):1797–800.
13. Malik A, Schumacher HR, Dinnella JE, Clayburne GM. Clinical diagnostic criteria for gout: comparison with the gold standard of synovial fluid crystal analysis. J Clin Rheumatol. 2009;15(1):22–4.
14. Bible MW, Pinals RS. Late precipitation of monosodium urate crystals. J Rheumatol. 1982;9(3):480.
15. Kerolus G, Clayburne G, Schumacher HR. Is it mandatory to examine synovial fluids promptly after arthrocentesis? Arthritis Rheum. 1989;32(3):271–8.
16. McKnight KM, Agudelo C. Comment on the article by Kerolus et al. Arthritis Rheum. 1991;34(1):118–20.
17. McGill NW, Swan A, Dieppe PA. Survival of calcium pyrophosphate crystals in stored synovial fluids. Ann Rheum Dis. 1991;50(12):939–41.
18. Gálvez J, Sáiz E, Linares LF, Climent A, Marras C, Pina MF, et al. Delayed examination of synovial fluid by ordinary and polarised light microscopy to detect and identify crystals. Ann Rheum Dis. 2002;61(5):444–7.
19. Tausche A-K, Gehrisch S, Panzner I, Winzer M, Range U, Bornstein SR, et al. A 3-day delay in synovial fluid crystal identification did not hinder the reliable detection of monosodium urate and calcium pyrophosphate crystals. J Clin Rheumatol. 2013;19(5):241–5.
20. Kienhorst LBE, Janssens HJEM, Eijgelaar RS, Radstake TRDJ, van Riel PLCM, Janssen M. The detection of monosodium urate crystals in synovial fluid after long-term and varying storage conditions. Joint Bone Spine. 2015;82(6):470–1.
21. Pastor S, Bernal J-A, Caño R, Gómez-Sabater S, Borras F, Andrés M. Persistence of crystals in stored synovial fluid samples. J Rheumatol. 2020;47(9):1416–23.
22. Graf SW, Buchbinder R, Zochling J, Whittle SL. The accuracy of methods for urate crystal detection in synovial fluid and the effect of sample handling: a systematic review. Clin Rheumatol. 2013;32(2):225–32.
23. Paul H, Reginato AJ, Schumacher HR. Alizarin red S staining as a screening test to detect calcium compounds in synovial fluid. Arthritis Rheum. 1983;26(2):191–200.
24. Bardin T, Bucki B, Lansaman J, Bravo EO, Ryckewaert A, Dryll A. Alizarin red staining of articular fluids. Comparison of the results with electron microscopy and clinical data. Rev Rhum Mal Osteoartic. 1987;54(2):149–54.
25. Schumacher HR, Smolyo AP, Tse RL, Maurer K. Arthritis associated with apatite crystals. Ann Intern Med. 1977;87(4):411–6.
26. Conway R, McCarthy GM. Calcium-containing crystals and osteoarthritis: an unhealthy Alliance. Curr Rheumatol Rep. 2018;20(3):13.
27. Mccarty DJ, Hollander JL. Identification of urate crystals in gouty synovial fluid. Ann Intern Med. 1961;54:452–60.
28. Schumacher HR, Sieck MS, Rothfuss S, Clayburne GM, Baumgarten DF, Mochan BS, et al. Reproducibility of synovial fluid analyses. A study among four laboratories. Arthritis Rheum. 1986;29(6):770–4.

29. Gordon C, Swan A, Dieppe P. Detection of crystals in synovial fluids by light microscopy: sensitivity and reliability. Ann Rheum Dis. 1989;48(9):737–42.
30. McGill NW, York HF. Reproducibility of synovial fluid examination for crystals. Aust NZ J Med. 1991;21(5):710–3.
31. Hasselbacher P. Variation in synovial fluid analysis by hospital laboratories. Arthritis Rheum. 1987;30(6):637–42.
32. Von Essen R, Hölttä AM. Quality control of the laboratory diagnosis of gout by synovial fluid microscopy. Scand J Rheumatol. 1990;19(3):232–4.
33. von Essen R, Hölttä AM, Pikkarainen R. Quality control of synovial fluid crystal identification. Ann Rheum Dis. 1998;57(2):107–9.
34. Pollet S, Coiffier G, Albert J-D, Chales G, Guggenbuhl P, Perdriger A. Concordance between fresh joint fluid analysis by the rheumatologist and joint fluid analysis at the laboratory: prospective single-center study of 180 samples. Joint Bone Spine. 2015;82(3):161–5.
35. Bernal JA, Andrés M, López-Salguero S, Jovaní V, Vela P, Pascual E. Compensated polarized microscopy for crystal identification shows high reliability among multiple observers [abstract]. In 2017. p. 1132.
36. Neame RL, Carr AJ, Muir K, Doherty M. UK community prevalence of knee chondrocalcinosis: evidence that correlation with osteoarthritis is through a shared association with osteophyte. Ann Rheum Dis. 2003;62(6):513–8.
37. Riestra JL, Sánchez A, Rodríques-Valverde V, Castillo E, Calderón J. Roentgenographic features of the arthropathy associated with CPPD crystal deposition disease. A comparative study with primary osteoarthritis. J Rheumatol. 1985;12(6):1154–8.
38. Wilkins E, Dieppe P, Maddison P, Evison G. Osteoarthritis and articular chondrocalcinosis in the elderly. Ann Rheum Dis. 1983;42(3):280–4.
39. Kleiber Balderrama C, Rosenthal AK, Lans D, Singh JA, Bartels CM. Calcium pyrophosphate deposition disease and associated medical comorbidities: a National Cross-Sectional Study of US veterans. Arthritis Care Res (Hoboken). 2017;69(9):1400–6.
40. Reuge L, Van Linthoudt D, Gerster JC. Local deposition of calcium pyrophosphate crystals in evolution of knee osteoarthritis. Clin Rheumatol. 2001;20(6):428–31.
41. Tanikawa H, Ogawa R, Okuma K, Harato K, Niki Y, Kobayashi S, et al. Detection of calcium pyrophosphate dihydrate crystals in knee meniscus by dual-energy computed tomography. J Orthop Surg Res. 2018;13(1):73.
42. Viriyavejkul P, Wilairatana V, Tanavalee A, Jaovisidha K. Comparison of characteristics of patients with and without calcium pyrophosphate dihydrate crystal deposition disease who underwent total knee replacement surgery for osteoarthritis. Osteoarthr Cartil. 2007;15(2):232–5.
43. Derfus BA, Kurian JB, Butler JJ, Daft LJ, Carrera GF, Ryan LM, et al. The high prevalence of pathologic calcium crystals in pre-operative knees. J Rheumatol. 2002;29(3):570–4.
44. Filippou G, Bozios P, Gambera D, Lorenzini S, Bertoldi I, Adinolfi A, et al. Ultrasound detection of calcium pyrophosphate dihydrate crystal deposits in menisci: a pilot in vivo and ex vivo study. Ann Rheum Dis. 2012;71(8):1426–7.
45. Abreu M, Johnson K, Chung CB, De Lima JE, Trudell D, Terkeltaub R, et al. Calcification in calcium pyrophosphate dihydrate (CPPD) crystalline deposits in the knee: anatomic, radiographic, MR imaging, and histologic study in cadavers. Skelet Radiol. 2004;33(7):392–8.
46. Dermawan JK, Goldblum A, Reith JD, Kilpatrick SE. The incidence and significance of calcium pyrophosphate dihydrate deposits in histologic examinations of total hip, knee, and shoulder joint arthroplasties. Arch Pathol Lab Med. 2021.
47. Niggemeyer O, Steinhagen J, Zustin J, Rüther W. The value of routine histopathology during hip arthroplasty in patients with degenerative and inflammatory arthritis. Hip Int. 2011;21(1):98–106.
48. Andrés M, Bernal J-A, Arenas M-D, Pascual E. Synovial fluid leukocyte count in asymptomatic hyperuricaemia with crystal deposition: a proof-of-concept study. Rheumatology (Oxford). 2019;58(6):1104–5.

49. Nguyen C, Ea HK, Thiaudiere D, Reguer S, Hannouche D, Daudon M, et al. Calcifications in human osteoarthritic articular cartilage: ex vivo assessment of calcium compounds using XANES spectroscopy. J Synchrotron Radiat. 2011;18(Pt 3):475–80.
50. Foreman SC, Gersing AS, von Schacky CE, Joseph GB, Neumann J, Lane NE, et al. Chondrocalcinosis is associated with increased knee joint degeneration over 4 years: data from the osteoarthritis initiative. Osteoarthr Cartil. 2020;28(2):201–7.
51. Latourte A, Rat A-C, Ngueyon Sime W, Ea H-K, Bardin T, Mazières B, et al. Chondrocalcinosis of the knee and the risk of osteoarthritis progression: data from the knee and hip osteoarthritis long-term assessment cohort. Arthritis Rheumatol. 2020;72(5):726–32.
52. Doherty M, Watt I, Dieppe PA. Localised chondrocalcinosis in post-meniscectomy knees. Lancet. 1982;1(8283):1207–10.
53. Abhishek A, Doherty S, Maciewicz RA, Muir KR, Zhang W, Doherty M. Self-reported knee malalignment in early adult life as an independent risk for knee chondrocalcinosis. Arthritis Care Res (Hoboken). 2011;63(11):1550–7.
54. de Lange EE, Keats TE. Localized chondrocalcinosis in traumatized joints. Skelet Radiol. 1985;14(4):249–56.
55. Settas L, Doherty M, Dieppe P. Localised chondrocalcinosis in unstable joints. Br Med J (Clin Res Ed). 1982;285(6336):175–6.
56. Doherty M, Dieppe PA. Pyrophosphate arthropathy as a late complication of juvenile chronic arthritis. J Rheumatol. 1984;11(2):219–21.
57. Sambrook PN, de Jager JP, Champion GD, Doust BD, McGirr EE, Kozlowski KS, et al. Synovial complications of spondylepiphyseal dysplasia of late onset. Arthritis Rheum. 1988;31(2):282–7.
58. Hamza M, Bardin T. Camptodactyly, polyepiphyseal dysplasia and mixed crystal deposition disease. J Rheumatol. 1989;16(8):1153–8.
59. Halverson PB, Cheung HS, McCarty DJ. Enzymatic release of microspheroids containing hydroxyapatite crystals from synovium and of calcium pyrophosphate dihydrate crystals from cartilage. Ann Rheum Dis. 1982;41(5):527–31.
60. Gerster JC, Varisco PA, Kern J, Dudler J, So AKL. CPPD crystal deposition disease in patients with rheumatoid arthritis. Clin Rheumatol. 2006;25(4):468–9.
61. Oliviero F, Scanu A, Galozzi P, Gava A, Frallonardo P, Ramonda R, et al. Prevalence of calcium pyrophosphate and monosodium urate crystals in synovial fluid of patients with previously diagnosed joint diseases. Joint Bone Spine. 2013;80(3):287–90.
62. Pascual E, Andrés M, Sivera F. Methotrexate: should it still be considered for chronic calcium pyrophosphate crystal disease? Arthritis Res Ther. 2015;17:89.
63. Paalanen K, Rannio K, Rannio T, Asikainen J, Hannonen P, Sokka T. Prevalence of calcium pyrophosphate deposition disease in a cohort of patients diagnosed with seronegative rheumatoid arthritis. Clin Exp Rheumatol. 2020;38(1):99–106.
64. Pascual E, Sivera F, Andres M. Mixed crystal disease: a tale of 2 crystals. J Rheumatol. 2020;47(8):1158–9.
65. Robier C, Neubauer M, Quehenberger F, Rainer F. Coincidence of calcium pyrophosphate and monosodium urate crystals in the synovial fluid of patients with gout determined by the cytocentrifugation technique. Ann Rheum Dis. 2011;70(6):1163–4.
66. Heselden EL, Freemont AJ. Synovial fluid findings and demographic analysis of patients with coexistent intra-articular monosodium urate and calcium pyrophosphate crystals. J Clin Rheumatol. 2016;22(2):68–70.

Chapter 12
Lipid Crystals

Tim L. Jansen

Crystals are bodies formed by solidification of chemical elements, compounds, or mixtures. They have regularly repeating internal arrangements with commonly external plane surfaces. The formation of crystalline conglomerates may occur once saturation levels are exceeded. The current concept is that on top of a matrix a solid as well as liquid lipid may form a crystalline or crystalline-look-alike structure in local compartments such as a joint with supersaturated conditions. Whether these cause or result from synovitis in specific individual cases is uncertain.

Within synovial fluid several lipids have been described: cholesterol hydrates, cholesterol esters, triglycerides, and phospholipids. Interestingly, several of these may be identified as a conglomerate using polarized light microscopy. Non-birefringent lipid circular structures, so-called lipid globules or spherules, are common in synovial fluid. These lipid structures are sometimes birefringent and may appear as solitary microspherules, or may be quite numerous with strong positive elongation properties (birefringence) and are described according to their Maltese cross appearance. These may vary widely in size.

Incidentally one may find typical cholesterol plates that are birefringent; often it is difficult to determine a plate's birefringence as one is unable to find a dendrite for reference. In this chapter, we will focus on these lipid liquid phenomena and their potential clinical significance.

T. L. Jansen (✉)
Department of Rheumatology VieCuri MC, Venlo, The Netherlands

Department Med Cell Biophysics (MCB), University of Twente, Enschede, The Netherlands
e-mail: tjansen@VieCuri.nl

B. F. Mandell (ed.), *Synovial Fluid Analysis and The Evaluation of Patients With Arthritis*, https://doi.org/10.1007/978-3-030-99612-3_12

Cholesterol Crystals

Clinical Settings

Cholesterol plates, solitary or stacked, may be identified in punctates from a bursitis, arthritis, or nodule, i.e., patients with rheumatoid arthritis [1–5]. They have also been identified in osteoarthrosis [6], chronic tophaceous gout [1, 7, 8], lupus [2, 9], tumoral calcinosis in dermatomyositis [10], scleroderma [11], and pericardial effusions [1, 9, 12, 13]. Cholesterol may be deposited in the arterial wall, the skull, breast, and spermatocele [14–16].

Synovial fluids from hyperlipoproteinemic patients have not contained crystalline lipids [2, 4]. Even though deposits such as Xanthomas commonly develop in Achilles tendons and extensor tendon sheaths in hyperlipidemic patients [17]. Rod-like crystals have been identified in a hyperbetalipoproteinemic patient with an Achilles tendonitis [17]. Intra-arterial migration of cholesterol emboli is a recognized syndrome with sequelae of deposited cholesterol inducing "blue toe syndrome", with plate deposits present in biopsied tissue [18].

Punctates

Synovial fluids containing cholesterol lipids are initially colloidal in appearance, and may be milky white, golden-honey, or yellow-brown colored (Fig. 12.1). After standing for several days the heavier lipids will produce a sediment.

Fig. 12.1 Milky white colloidal synovial punctate from a swollen arthritic knee: note colloidal aspect herein is due to noncellular content

Microscopy

Cholesterol conglomerates may present as birefringent, large, flat rectangular stacked plates with notched corners (Fig. 12.2). The plates range from 5 to 100 μm. A second morphologic form may be present as single or numerous dendrites (small comma-like particles) which are considered the *forme fruste* of ultimately accumulated plates. A microscopist may see a small plate from their silhouette, sideways (Fig. 12.3). Occasionally even a third morphologic form may present as dendrites with a yellow or blue color revealing a negative or positive birefringence. Confusion may occur with these negatively birefringent dendrites. But when slightly curved these objects are typical for cholesterol dendrites (Fig. 12.4); when only straight needles are found these objects are to be considered typical for monosodium urate (MSU) but beware of combination specimens of cholesterol plus MSU. Confusion may also occur with dendrites in a short tubular presentation that may suggest calcium pyrophosphate (CPP) or MSU. Note leukocyte count in cholesterol synovitis is low when compared with high leukocyte counts in CPP-associated/MSU-induced arthritis flares. To increase certainty additional imaging techniques may be useful, see Chap. 14.

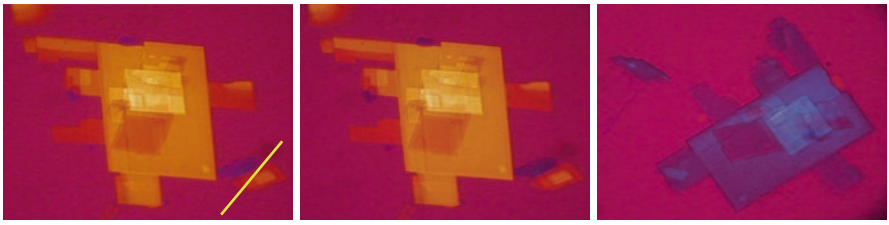

Fig. 12.2 Cholesterol monohydrate plates with birefringence, without a definite axis to the plate, one cannot identify positive or negative elongation; from a patient with rheumatoid shoulder synovitis

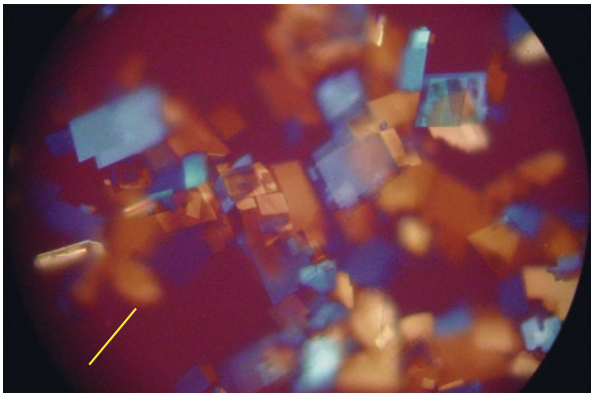

Fig. 12.3 A punctate loaded with rectangular geometric cholesterol plates and a tangential view shows yellow or blue color; from a shoulder in chronic rheumatoid arthritis

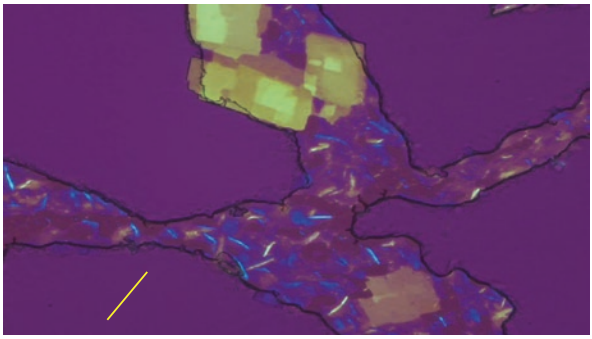

Fig. 12.4 Cholesterol dendrites and plates: beware for confusion with MSU needles; from a monoarthritis of shoulder in a chronic low-grade arthritic shoulder

Clinical Significance

Cholesterol crystal deposition has been described in structures with a synovial layer and has been rarely found in tendon sheaths [19, 20]. There are several factors supposedly involved in the formation of cholesterol crystals in inflamed synovial joints. Causal may be: increased cholesterol synthesis due to synovial hyperperfusion, lipid release from damaged cell membranes and/or organelles, and abnormal intracellular transport of lipids due to chronic inflammation. Injected synthetic cholesterol plates can induce a moderate inflammation in skin, subcutaneous tissue, and rabbit knee joints. In humans a rheumatoid arthritis patient has been described with a cholesterol synovitis which did not respond to csDMARD regimes and worsened after an intra-articular depomedrol injection. The cholesterol synovitis promptly stopped when a statin was started [19].

Cholesterol monohydrate plates have not been observed inside human phagocytes; a phagocytic finding we regularly recognize with MSU, CPP, or basic calcium phosphate (BCP) crystals. Some minor lipid parts may be found in punctates within apoptotic cells. The ongoing inflammation with cholesterol crystals has not been demonstrated to aggravate joint destruction in RA nor in osteoarthritis. The accumulation of cholesterol intra-articularly may induce chronic stiffness due to synovitis.

Do we have evidence for pharmacotherapy with statins? A Trial of Atorvastatin in RA (TARA) has drawn attention to the pivotal role statins may play in chronic rheumatoid inflammation as disease activity decreased [21]. Statins have some immunomodulatory and anti-inflammatory properties [22–26]. As these cholesterol plates are stable yet not easily cleared by phagocytes from the joint, it has been hypothesized that regional monohydrate cholesterol production or other mechanisms may play a role in the pathogenesis of persistent cholesterol synovitis [19]. Clinical studies into appropriateness of statins as pharmacotherapy in chronic cholesterol crystal deposition disease are needed, but the sporadic occurrence of cholesterol synovitis is a significant barrier for such studies.

Liquid Lipid Crystals, i.e., Maltese Crosses

Clinical Settings

Liquid lipid crystalline droplets may be found in synovial or bursal punctates from patients with longstanding rheumatoid arthritis (RA) [1, 2], or rarely in any acute monoarthritis [27–30]. Liquid lipids have been detected in patients with acute bursitis [1], or pigmented villonodular synovitis [31]. These liquid lipids may be identified in punctates from synovial fluid derived from any acute or chronic mono−/polyarthritis [32] including RA [33]. The clinical significance of neutral fat and lipid liquid microspherules is obscure. They may well be an innocent epiphenomenon of arthritis, originating from synovial fat released into the joint or from membrane lipids of lysed cells. Alternatively, liquid lipids may escalate or even initiate arthritis in some patients.

Punctates

These lipid liquid microspherules represent both a liquid and solid state, and are presumably formed by phospholipids and other polar lipid molecules as is stereochemically needed to be arranged as a liquid crystal.

Microscopy

Birefringence is often intense, particularly with the bigger (micro)spherules (Fig. 12.5). Darkening of the surroundings is often needed for a clearer perspective. Sizes range from 2 to 10 μm, and there may be few or many spherulites in specimens (Fig. 12.6). The smaller spherulites often exhibit weaker birefringence. Classically these spherulites are called Maltese crosses and have a positive elongation, but must be differentiated from negative elongation as might be seen with urate microspherules or talc powder contamination, i.e., magnesium silicate or starch granules. These latter have an outline that is more irregular than the circular lipid microspherules. Microscopy for liquid lipid crystals should be done on fresh specimens, as over time (weeks) they will vanish. Some are intracellular and they may be numerous.

Previous analyses included electron microscopy and this revealed that these crystals were multilayered membranous arrays. Such structures have been reported following intra-articular blood injections experimentally, suggesting membrane lipids of lysed cells as the source [7].

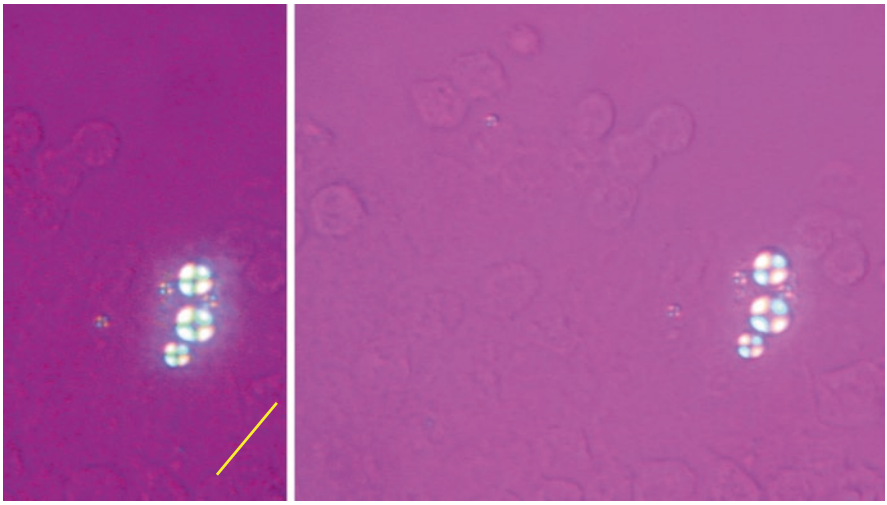

Fig. 12.5 Numerous fresh lipid microspherules: smaller and bigger spherulites, from an acute arthritis from a knee

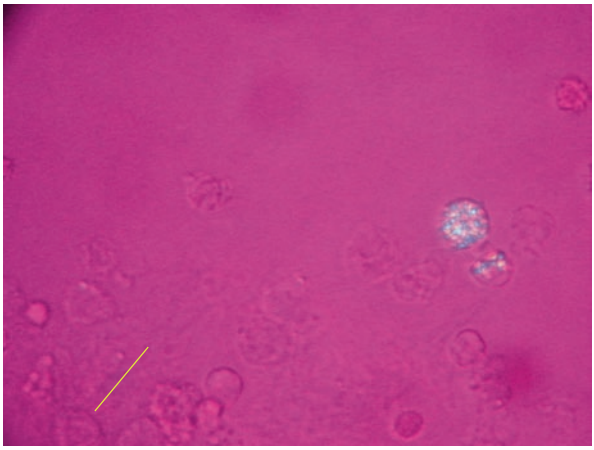

Fig. 12.6 Intracellular Maltese crosses from a fresh sample: enlargement 400 in a recurrent gonarthritis patient

Clinical Significance

Liquid lipid crystalline droplets have predominantly been described in acute knee monoarthritis; but once a wrist [27] and once an ankle were involved [30]. It is not certain whether large joints are most affected, or most likely to be aspirated arthritis may subside after one week with either NSAIDs or glucocorticoid injection.

A biopsy of the synovium was obtained in two patients revealing mild inflammatory changes with sporadic lymphocytic, mononuclear, or polymorphonuclear cell infiltrates [32, 34]. Microspherules were identified, including intracellularly within mononuclear cells [32]. Sometimes a huge liquid lipid crystalline droplet can be found and the elongation axis may remain unclear: the refractive index is high and/or the birefringence may be very strong.

Experimentally, synthetic lipid liquid crystals injected into a rabbit knee joint induced a synovitis [33]. Injection of autologous blood into rabbit knees was associated with similar Maltese crosses [35]. Choi et al. suggested that the source of these birefringent Maltese cross-like spherulites may well be the red blood cells they experimentally injected [35]. They also suggested that cholesterol-rich erythrocyte membrane might be taken up by the synovial cells, and they may elicit a synovitis.

The presence of fat droplets in synovial fluid signifies major or minor joint trauma with damage to the bones with release of marrow fat. Synovial fluids aspirated after traumatic hemorrhage usually have a low white blood cell count. Two patients with hemorrhagic effusions had synovial fluid leukocytosis, presumably secondary to lipid droplet phagocytosis [34]. Lipid globules, intra- and extracellularly in the synovial fluid, and a top fatty layer following centrifugation of the hemorrhagic synovial fluid suggest a traumatic etiology of the arthritis [36, 37].

Other Crystalline Lipids and Lookalikes

Other synovial fluid lipids are thought to consist of fatty acids and have been described in pancreatic disease according to older literature, or in skin fat necrosis of newborns [34, 38]. Intra-articular high concentrations of free fatty acids were demonstrated in the rare pancreatic arthritis syndrome with fat necrosis of affected tissues as the hallmark of the partly understood syndrome [38, 39]. Identical structures have been observed in synovial fluid of patients with osteoarthrosis (OA) with large bone cysts, in hemarthrosis, and in synovial fluids drawn several days post a possibly traumatic arthrocentesis [1, 2, 34]. Also, intra-articular cortical fracture should be considered if lipid globules are found. Such crystals may be positive or negative elongating and may appear as needles, plates or rods, or even rosettes or clumps. These occasionally can be confused with calcium pyrophosphate or monosodium urate or even variously sized rice bodies (Fig. 12.7). The latter being debris with surrounding birefringent materials. One has to carefully differentiate these from artifacts.

For specificity one may use staining techniques such as Alizarin Red for calcium-containing crystals including basic calcium phosphates (BCP) or Sudan Black in liquid lipids; these may be of help to the clinician, but these are hardly used these days due to complexity of use and interpretation.

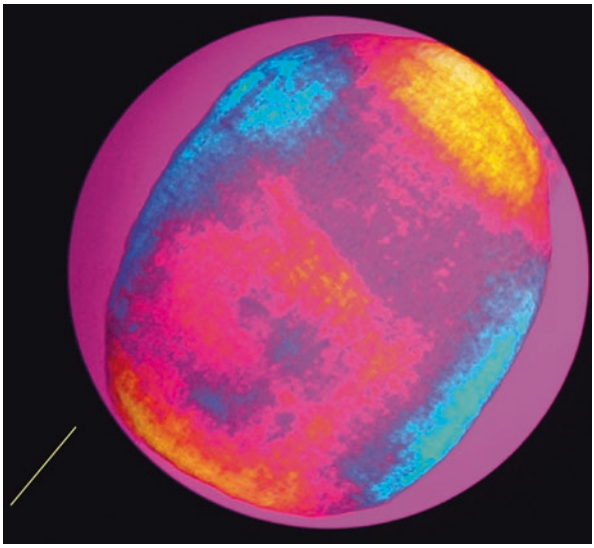

Fig. 12.7 Rice body from a fresh sample (400x) in a chronic gonarthritis patient with a previously diagnosed rheumatoid arthritis (RA)

Discussion

Using polarized light microscopy of synovial fluids, several lipid structures can be identified. Pathognomonic pictures come from cholesterol monohydrate plates or anhydrate dendrites in punctates harvested from patients with non-hyperlipidemic rheumatoid arthritis (RA), osteoarthritis, and chronic bursal effusions. One should be cautious as non-birefringent lipid globules have been reported in traumatic arthritis, and in aseptic necrosis as well as in RA. Small, positively birefringent spherulites are called Maltese crosses, and identification as such helps to prevent misinterpretation. In cases with persistent diagnostic doubt, we may be in need of additional techniques of which electron microscopy or Raman spectrography may be of additional value, see Chap. 14. A spectrograph via Raman technique produces a crystal- and bond-specific spectrograph applicable for identification once a database with all potential spectrograms is present. Such additional techniques may be the future for centers with a focus on crystal expertise.

Acknowledgement I wish to acknowledge Dr. Matthijs Janssen for the critical reading of the manuscript.

References

1. Reginato AJ, Falasca GR, Usmani Q. Do we really need to pay attention to the less common crystals? Curr Opin Rheumatol. 1999;11(5):446–552.

2. Reginato AJ, Falsaca GF. Calcium oxalate and other miscellaneous crystal related arthropathies in gout, hyperuricemia and other crystal-associated arthropathies. In: Holers VM, editor. Smyth CJ. New York: Marcel Dekker; 1999. p. 369–93.
3. Zuckner J, Uddin J, Ganter GE, Dorner RW. Cholesterol crystals in synovial fluid. Ann Intern Med. 1964;60:436–46.
4. Jansen TL, Rasker JJ. Therapeutic consequences of crystals in the synovial fluid: a review for clinicans. Clin Exp Rheumatol. 2011;29(6):1032–9.
5. Jansen TL, Spoorenberg A. Medical mystery: arthritis – the answer. NEJM. 2006;355:421–2. https://doi.org/10.1056/NEJMc066303.
6. Fam AG, Pritzker KP, Cheng PT, et al. Cholesterol crystals in osteoarthritic effusions. J Rheumatol. 1981;8(2):273–80.
7. Kelley JT III, Agudelo C. Subcutaeneous tophaceous nodule formation due to deposition of cholesterol crystals. J Rheumatol. 2002;29(8):1798–9.
8. Fam AG. Cholesterol crystals in gouty bursitis. J Rheumatol. 2001;28(8):1928–9.
9. Wise CM, White RE, Agudelo CA. Synovial fluid lipid abnormalities in various disease states: review and classification. Semin Arthritis Rheum. 1987;16(3):222–30.
10. Corts J, Castellanos J, Reginato AJ, Schumacher HR. Tumoral calcinosis containing hydroxyapatite and cholesterol crystals associated with dermatomyositis. A&R. 1992;35:S76.
11. Saxe PA, Altman RD. Subcutaneous cholesterol crystals mimicking calcinosis cutis in systemic sclerosis. J Rheumatol. 1991;18(5):743–5.
12. Knobel B, Rosman P. Cholesterol pericarditis associated with rheumatoid arthritis. Harefuah. 2001;140(1):10–12,87.
13. Jimenez Elorza A, et al. Cholesterol crystal pericarditis. Rev Esp Cardiol. 2001;54(9):1119–20.
14. Sze CI, et al. Intracalvarial cholesterol granulomas – clinicopathologic correlates of three cases. Clin Neuropathol. 2003;22(1):41–6.
15. Osada T, Kitayama J, Nagawa H. Cholesterol granuloma of the breast mimicking carcinoma: report of a case. Surg Today. 2002;32(11):981–4.
16. Soga N, Sugimura Y. Spermatocele associated with cholesterol crystals. Hinyokika Kiyo. 2003;49(4):229–30.
17. Schumacher HR Jr, Michaels R. Recurrent tendinitis and Achilles tendon nodule with posetively birefringent crystals in a patient with hyperlipoproteinemia. J Rheumatol. 1989;16(10):1387–9.
18. Kronzon I, Saric M. Cholesterol embolization syndrome. Circulation. 2010;122:631–41. https://doi.org/10.1161/CIRCULATIONAHA.109.886465.
19. Jansen TL. Atorvastatin for chronic synovitis due to massive intra-articular cholesterol monohydrate deposition in longstanding rheumatoid arthritis. Rheumatology. 2006;45:1577–8.
20. Balint PV, Kane D, Sturrock RD. Massive cholesterol crystal deposition: unusual location in rheumatoid arthritis. ARD. 2003;62:512.
21. Mc Carey DW, McInnes IB, Madhok R, et al. Trial of atorvastatin in rheumatoid arthritis (TARA): double blind, randomised placebo-controlled trial. Lancet. 2004;363:2015–21.
22. Kwak B, Mulhaupt F, Myit S, Mach F. Stains a newly recognized type of immunomodulator. Nat Med. 2000;6:1399–402.
23. Weitz-Schmidt G, Welzenbach K, Brinkman V, et al. Statins selectively inhibit leukocyte function antigen-1 by binding to a novel regulatory integrin site. Nat Med. 2001;7:687–92.
24. Youssef S, Stuve O, Patarroyo JC, et al. The HMG-CoA reductase inhibitor, atorvastatin, promotes a Th2 bias and reserves paralysis in central nervous system autoimmune disease. Nature. 2002;420:78–84.
25. Mulhaupt F, Matter CM, Kwak, et al. Statins reduce CD40 expression in human vascular cells. Cardiovasc Res. 2003;59:755–66.
26. Nagashima T, Okazaki H, Yudoh K, et al. Apoptosis of rheumatoid synovial cells by statins through blocking of protein geranylgeranylation: a potential therapeutic approach to rheumatoid arthritis. A%R. 2006;54:579–86.

27. Reginato AJ, Schumacher HR, Allan DA, Rabinowitz JL. Acute monoarthritis associated with lipid liquid crystals. Ann Rheum Dis. 1985;44:537–43.
28. Trostle DC. Schumacher HR. Kapoor WM. Microspherule associated acute monoarticular arthritis. Arthritis & Rheum: Medsger TA; 1986.
29. Gardner GC, Terkeltaub RA. Acute monoarthritis associated with intracellular positively birefringent Maltese cross appearing spherules. J Rheumatol. 1989;16(3):394–6.
30. Jansen TL. Clinical Image Clin Rheumatol. 2020;39:2235–6.
31. Ugai K, Kurosaka M, Hirohata K. Lipid microspherules in synovial fluid of patients with pigmented villonodular synovitis. A&R. 1988;31(11):1442–6.
32. Schlesinger PA, Stillman MT, Peterson L. Polyarthritis with birefringent lipid within synovial fluid macrophages: case report and ultrastructural study. Arthritis & Rheum. 1982;25:1365–8.
33. Rivest C, et al. Acute polyarthritis associated with birefringent lipid microspherules accurring in a patient with longstanding RA. J Rheumatol. 1992;19(4):617–20.
34. Reginato AJ, Kurnik B. Calcium oxalate and other crystals associated with kidney diseases and arthritis. Semin Arthritis Rheum. 1989;18(3):198–224.
35. Choi S-J, Schumacher HR, Clayburne G. Experimental haemarthrosis produces mild inflammation associated with intracellular Maltese crosses. Ann Rheum Dis. 1986;45:1025–8.
36. Graham J, Goldman JA. Fat droplets and synovial leukocytosis in traumatic arthritis. A&R. 1978;21:76–80. https://doi.org/10.1002/art.1780210113.
37. Weinstein J. Synovial fluid leukocytosis associates with intracellular lipid inclusions. Arch Int Med. 1980;140:560–1.
38. Simkin PA, Brunzell JD, Wisner D, et al. Free fatty acids in the pancreatitic arthritis syndrome. A&R. 1983;26:127–32.
39. Betrains A, Rosseels W, Van Mieghem E, et al. Clinical characteristics, treatment, and outcome of pancreatitis, panniculitis, and polyarthritis syndrome: a case-based review. Clin Rheumatology. 2020;40:1625–33.

Chapter 13
Analytic Methods to Detect Articular Basic Calcium Phosphate Crystals

Ann K. Rosenthal

Introduction

The term "basic calcium phosphate (BCP) crystals" refers to the trio of calcium phosphate crystals found in musculoskeletal tissues. BCP crystals include tricalcium phosphate, octacalcium phosphate, and carbonate-substituted hydroxyapatite. They are less accurately referred to as "hydroxyapatite" or "apatite". In soft tissues such as tendons, ligaments, and muscles, BCP crystals are associated with acute inflammatory syndromes such as calcific tendonitis or calcific periarthritis. BCP crystals are also common components of osteoarthritic joint fluid [1] and are present in almost 100% of tissues from large joints with end-stage osteoarthritis (OA) [2, 3]. BCP crystals are pathognomonic of Milwaukee shoulder syndrome (MSS). This highly destructive non-inflammatory type of arthritis causes large effusions of the shoulder and joint instability in elderly patients [4]. Similar involvement of the knee can occur.

In contrast to other types of crystalline arthritis, such as gout and calcium pyrophosphate deposition disease (CPDD), polarizing light microscopy of synovial fluid samples cannot be used to identify BCP crystals. Alizarin red S staining of fluids is often used clinically but lacks evidence-based validation. Thus, there are no existing techniques which have been conclusively demonstrated to accurately identify BCP crystal at the bedside. I will discuss below the challenges of BCP crystal identification, strengths and weaknesses of the Alizarin Red S staining method, crystal identification techniques typically relegated to the research realm, and some new technologies on the horizon.

A. K. Rosenthal (✉)
The Division of Rheumatology, Department of Medicine, Medical College of Wisconsin and The Zablocki VA Medical Center, Milwaukee, WI, USA
e-mail: arosenthal@mcw.edu

B. F. Mandell (ed.), *Synovial Fluid Analysis and The Evaluation of Patients With Arthritis*, https://doi.org/10.1007/978-3-030-99612-3_13

Challenges of BCP Crystal Identification

BCP crystals are extremely small, typically measuring 75–250 nanometers in length which is below the detection levels for most light microscopes. Indeed, the first descriptions of BCP crystals in synovial fluid required imaging by electron microscopy [5, 6]. Large aggregates of crystals are visible under light microscopy but without staining, they cannot be distinguished from debris. The lack of birefringence of BCP crystals presents an additional challenge. There is also some concern that in stored fluids, particularly those stored in the cold, a natural loss of CO_2 may produce artifactual BCP crystals. Thus, fluids may require special handling to accurately measure pathogenic crystals in stored synovial fluid samples. While Halverson suggested layering fluids under oil if storage is necessary [7], this is not commonly done, and fluids should be probably be examined fresh without refrigeration.

Alizarin Red S Staining

Alizarin Red S staining is currently the only clinically available method for detecting BCP crystals in synovial fluid. It was described by Paul et al. in 1983 [8]. Alizarin Red S binds to calcium but is relatively agnostic in regard to the accompanying anion. In their seminal paper, Paul and colleagues showed that clumps of BCP crystals stained red with Alizarin Red S and had a somewhat distinctive appearance. Alizarin Red S also stains calcium pyrophosphate (CPP) crystals. Interestingly, staining was also positive in synovial fluids from patients with rheumatoid arthritis, those on dialysis, and in gout patients. While BCP crystals might be present in these other conditions, this observation begs the question of the specificity of this stain.

This test can be done at the bedside with minimal equipment. To stain synovial fluids, a fresh solution of 2% Alizarin Red S is made in distilled H_2O. The pH is adjusted to 4. 2, and then the solution is filtered through a 0.45 μ filter. This solution can be stored in a light-resistant container but should be filtered again through a 0.22 μ filter immediately prior to each use. A drop of synovial fluid is obtained from the bottom of tubes of unspun fresh synovial fluid and added on a slide to a drop of Alizarin Red S stain. The presence of deep orange/red clumps in "fibrous clots" of stained synovial fluids examined with regular light microscopy correlated with the presence of BCP crystals (Fig. 13.1). Polarizing light renders the clumps deep red or orange but provides few advantages and the pink background can render the crystal aggregates more difficult to identify.

The Alizarin Red S stain has not been carefully validated in clinical practice. Interestingly, Paul et al. 's initial description of this assay used the term "apatite arthritis" to define the clinical setting in which fluid was expected to contain BCP crystals [8]. This condition was defined by the presence of calcific deposits in synovium, which is not specific to any one disease. In the Paul study, they further validated Alizarin Red S positivity using transmission electron microscopy (TEM). They showed that for strongly positive fluids containing BCP crystals with and

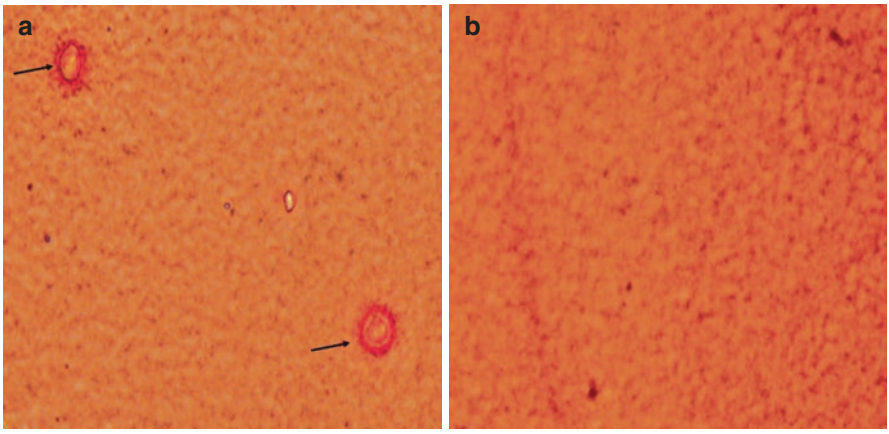

Fig. 13.1 Alizarin Red S staining of BCP crystals in synovial fluid. Panel (**a**) illustrates the typical appearance of synovial fluid BCP crystals stained with Alizarin Red S under light microscopy. The arrows represent aggregates of BCP crystals. Panel (**b**) represents staining of a negative control slide

without CPP crystals, 89% were positive for BCP crystals by TEM [8]. In contrast, of the 16 that were weakly positive, 44% were positive by TEM [8]. More recently, Eggelmeijer et al. used Alizarin Red S to stain 207 synovial fluid samples from patients with inflammatory joint disorders [9]. They found a 16% positivity rate. In this heterogeneous group, there was 65% concordance with 2 observations, and 92% of strongly positive samples had TEM evidence of CPP or BCP crystals. Weak positivity showed calcium-containing crystals in 27% by TEM [9]. Other studies have also questioned the accuracy of Alizarin Red S staining [10, 11]. Without a consistent standard control slide, it is doubtful that this test would perform well in the clinical setting and additional validation is needed [12, 13]. If it were to be used, positive and negative controls would be advisable, and only strong positivity should be considered significant.

Other Chemical Methods for Identifying BCP Crystals in Synovial Fluid

EHDP Binding

A radiometric assay based on the ability of BCP crystals to bind to the bisphosphonate class of drugs has been used for research purposes [7]. This assay requires a radiolabeled form of ethane 1, hydroxy 1.1 diphosphonate (EHDP), which is an etidronate-like bisphosphonate. It appeared to be considerably more specific for BCP crystals than Alizarin Red and did not bind to CPP crystals [7]. There are major obstacles to the widespread use of this assay. Firstly, the reagent is radioactive and requires an industrial partner for synthesis. It also necessitates significant

synovial fluid preparation prior to the assay. If done in whole fluids exposed to air or freeze-thawing, artifactual positivity was noted [7]. It is possible that similar compounds with non-radioactive tracers could be used in the future to develop accurate and accessible assays for BCP crystals.

Tetracycline Binding
A single report in 2008 described a BCP assay based on tetracycline's ability to bind to the mineral in bone and teeth [14]. This assay uses a solution of oxytetracycline composed of 3.5 mg/ml oxytetracycline dihydrate and 1.5 mg/ml oxytetracycline hydrochloride in 0.1 N NaOH titrated to a pH of 7.0 with 6 M HCl. This was mixed with synovial fluid, incubated for 15 minutes at room temperature and then a drop was examined under a light microscope fitted with an exogenous source of UV light. BCP crystal aggregates appeared as fluorescent green amorphous structures (Fig. 13.2). A semi-quantitative method for BCP using a fluorimeter was also described in this paper [14]. There was some attempt at validation using FTIR spectroscopy. It did not appear as if monosodium urate (MSU) or CPP crystals were stained with tetracycline. Shortcomings of this work include the very small number of native synovial fluids examined and the cumbersome set up using a UV penlight attached to the microscope. Clinical use of this method will require further refinement and validation.

Imaging Methods

Electron Microscopy (EM) Both scanning EM (SEM) and TEM are used in research settings to detect BCP crystals. Both can detect quantities as small as 0.003 mg/ml. EM provides morphologic information on tiny structures, but used alone, many small objects have similar appearances. When EM is used for pathologic crystal identification, it is typically used in conjunction with another method that provides chemical analysis. Indeed the first description of apatite arthropathy by Dieppe et al. in 1976 used SEM and energy dispersive analysis (EDA) [6]. Electron probe analysis can also be used in conjunction with EM to determine the ratio of calcium to phosphate which for BCP crystals is 1.6:1 [15]. Frallonardo et al.

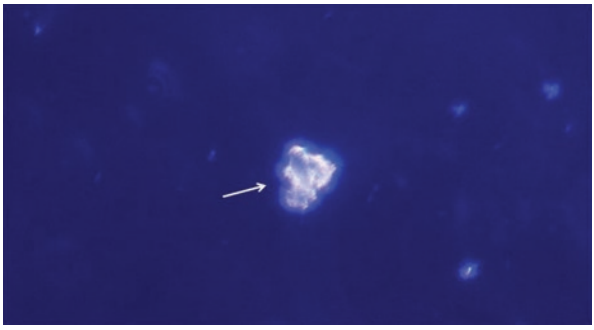

Fig. 13.2 Oxytetracycline staining of BCP crystals in synovial fluid. The arrow connotes a BCP crystal aggregate stained with oxytetracycline

used the combination of SEM and EDA in 110 knee fluids from patients with OA [16]. Only 2–3 ml of fluid was necessary, and the sample was prepped with centrifugation. The pellet required extensive washing and was then oven-dried and carbon-coated. EM in association with a microanalytic method is expensive and not widely available. It requires a moderate amount of fluid preparation to remove organic material, but these techniques remain one of the gold standard methods to conclusively identify BCP crystals in biologic settings.

Chemical Identification Methods

X-ray diffraction is a well-established highly accurate methodology to determine crystal composition and structure. Each crystal type has a unique signature and samples as small as 0.01 mg can yield conclusive results. Mixtures of crystals can also be distinguished from pure samples. Samples must be dried and ground but there is little interference from protein and other biologic material. X-ray diffraction does require dried samples and is problematic when crystals are sparse [17].

Spectroscopy Several spectroscopic methods are used to identify BCP crystals.

FTIR Spectroscopy FTIR spectroscopy has been widely used in the research realm to conclusively identify BCP crystals. This technique has advantages of providing rapid results, requiring minimal preparation, and yielding highly accurate information. However, it requires some expertise and expensive machinery. It can differentiate BCP crystals from CPP crystals using characteristic spectra. FTIR spectroscopy has been used in conjunction with a synchrotron imaging system which allowed analysis of single crystals [18]. However, difficulties with spectra may arise when objects have similar chemical compositions, and this technique may not be ideal to differentiate crystals from amorphous material. The sample must be thoroughly dried before analysis.

Raman Spectroscopy Raman spectroscopy is also useful for crystal identification [19]. There is no interference with water and relatively small samples sizes can be used. However, the required analysis is more complex than other spectroscopic methods. A portable version of the Raman spectroscope was described several years ago but, to date, has only been used for MSU and CPP crystals [20].

Atomic Force Microscopy (AFM) AFM can be used for indirect topographic modeling as well as to generate spectroscopic data on an object. It has been used to identify BCP crystals [21]. This imaging method is highly sensitive to small particles. It requires only a small amount of fluid and samples can be air-dried directly on a slide. Crystal Identification is based on distinct lattice patterns for different types of crystals. Limitations include the highly specialized machinery and expertise necessary for these studies and the expense. There is a very sparse literature on this technique.

Clinical Imaging Modalities

Digital Contact Radiography [2] This technique is borrowed from mammography and can identify areas of calcification in fixed tissue specimens. It has not, to my knowledge, been used in joint specimens in situ or in unfixed tissue, and alone was not sufficient to distinguish between BCP and CPP crystal deposition. These studies required the use of SEM with energy dispersive analysis to accurately determine the chemical composition of these deposits [2].

Dual-Energy CT Scanning There is increasing interest in using dual-energy CT scanning (DeCT) in crystal arthritis [22]. In a study using synthetic MSU, CPP, and BCP crystals embedded in resin, DeCT was able to accurately distinguish these crystals [23]. This method is becoming more widely available and provides imaging as well as information about chemical composition for macroscopic structures in vivo. Challenges to identify crystal composition in synovial fluid or even in intra-articular crystal deposits in settings near bone tissue may represent major hurdles. A similar technology known as multienergy spectral photon-counting CT scanning has been shown to have the ability to distinguish between calcium hydroxyapatite and calcium oxalate and may enter the clinical arena shortly [24].

Other Imaging Methodology Ultrasonography can be an important adjunctive diagnostic modality for gout and CPDD but is rarely used for BCP crystal-associated musculoskeletal syndromes. It can be useful in determining the location and morphology of calcified deposits in periarthritis and in calcific tendinitis, but it is likely that even BCP crystal aggregates are too small to detect in synovial fluid [25].

Conclusions and Future Directions

Understanding the role of BCP crystals in arthritis as well as how these crystals contribute to the destructive arthropathy known as MSS is hampered by the lack of widely available and accurate diagnostic tests for these tiny crystals. The Alizarin Red S staining technique is widely available but needs further validation and refinement before it can be used with confidence in clinical practice. Other promising emerging technologies will likely be based on the ability of BCP crystals to bind to chemical reagents labeled with fluorescent or other types of tags. These types of assays are not likely to be bedside tests, and will require sample preparation, laboratory-grade reagents, and equipment. Spectroscopy and X-ray diffraction are important tools which may be scaled down and automated so as to be widely available. Interestingly, much of the work with new technologies have used synthetic BCP crystals rather than native crystals [26] and the differences in morphology, protein coating, and behavior of the synthetic crystals compared to native crystals will require further study. Techniques such as lens-free crystal identification are in development and have been used successfully for MSU and CPP crystals [27]. More work in this critical area is warranted.

Acknowledgements This work was partially supported by the *Department of Veterans Affairs, Veterans Health Administration, Office of Research and Development* from the Department of Veteran's Affairs (Merit Review Grant I01 BX 004454). *The views expressed in this article are those of the author and do not necessarily reflect the position or policy of the Department of Veterans Affairs or the United States government.*

References

1. Derfus BA, Kurian JB, Butler JJ, Daft LJ, Carrera GF, Ryan LM, et al. The high prevalence of pathologic calcium crystals in pre-operative knees. J Rheumatol. 2002;29(3):570–4.
2. Fuerst M, Bertrand J, Lammers L, Dreier R, Echtermeyer F, Nitschke Y, et al. Calcification of articular cartilage in human osteoarthritis. Arthritis Rheum. 2009;60(9):2694–703.
3. Fuerst M, Niggemeyer O, Lammers L, Schafer F, Lohmann C, Ruther W. Articular cartilage mineralization in osteoarthritis of the hip. BMC Musculoskelet Disord. 2009;10:166.
4. Halverson PB, Cheung HS, McCarty DJ, Garancis J, Mandel N. "Milwaukee shoulder"--association of microspheroids containing hydroxyapatite crystals, active collagenase, and neutral protease with rotator cuff defects. II Synovial Fluid Studies Arthritis and Rheumatism. 1981;24(3):474–83.
5. Schumacher HR, Smolyo AP, Tse RL, Maurer K. Arthritis associated with apatite crystals. Ann Intern Med. 1977;87(4):411–6.
6. Dieppe PA, Crocker P, Huskisson EC, Willoughby DA. Apatite deposition disease. A new arthropathy. Lancet. 1976;1(7954):266–9.
7. Halverson PB, McCarty DJ. Identification of hydroxyapatite crystals in synovial fluid. Arthritis Rheum. 1979;22(4):389–95.
8. Paul H, Reginato AJ, Schumacher HR. Alizarin red S staining as a screening test to detect calcium compounds in synovial fluid. Arthritis Rheum. 1983;26(2):191–200.
9. Eggelmeijer F, Dijkmans BA, Macfarlane JD, Cats A. Alizarin red S staining of synovial fluid in inflammatory joint disorders. Clin Exp Rheumatol. 1991;9(1):11–6.
10. Lazcano O, Li CY, Pierre RV, O'Duffy JD, Beissner RS, Abell-Aleff PC. Clinical utility of the alizarin red S stain on permanent preparations to detect calcium-containing compounds in synovial fluid. Am J Clin Pathol. 1993;99(1):90–6.
11. Gordon C, Swan A, Dieppe P. Detection of crystals in synovial fluids by light microscopy: sensitivity and reliability. Ann Rheum Dis. 1989;48(9):737–42.
12. Swan AJ, Heywood BR, Dieppe PA. Extraction of calcium containing crystals from synovial fluids and articular cartilage. J Rheumatol. 1992;19(11):1764–73.
13. Halverson PB. Arthropathies associated with basic calcium phosphate crystals. Scanning Microsc. 1992;6(3):791–6; discussion 6-7.
14. Rosenthal AK, Fahey M, Gohr C, Burner T, Konon I, Daft L, et al. Feasibility of a tetracycline-binding method for detecting synovial fluid basic calcium phosphate crystals. Arthritis Rheum. 2008;58(10):3270–4.
15. Halverson PB, McCarty DJ, Cheung HS, Ryan LM. Milwaukee shoulder syndrome: eleven additional cases with involvement of the knee in seven (basic calcium phosphate crystal deposition disease). Semin Arthritis Rheum. 1984;14(1):36–44.
16. Frallonardo P, Oliviero F, Peruzzo L, Tauro L, Scanu A, Galozzi P, et al. Detection of calcium crystals in knee osteoarthritis synovial fluid: a comparison between polarized light and scanning electron microscopy. Journal of Clinical Rheumatology: Practical Reports on Rheumatic & Musculoskeletal Diseases. 2016;22(7):369–71.
17. Rosenthal AK, Mandel N. Identification of crystals in synovial fluids and joint tissues. Curr Rheumatol Rep. 2001;3(1):11–6.

18. Rosenthal AK, Mattson E, Gohr CM, Hirschmugl CJ. Characterization of articular calcium-containing crystals by synchrotron FTIR. Osteoarthritis and Cartilage/OARS, Osteoarthritis Research Society. 2008;16(11):1395–402.
19. McGill N, Dieppe PA, Bowden M, Gardiner DJ, Hall M. Identification of pathological mineral deposits by Raman microscopy. Lancet. 1991;337(8733):77–8.
20. Li B, Yang S, Akkus O. A customized Raman system for point-of-care detection of arthropathic crystals in the synovial fluid. Analyst. 2014;139(4):823–30.
21. Blair JM, Sorensen LB, Arnsdorf MF, Lal R. The application of atomic force microscopy for the detection of microcrystals in synovial fluid from patients with recurrent synovitis. Semin Arthritis Rheum. 1995;24(5):359–69.
22. Pascart T, Falgayrac G, Norberciak L, Lalanne C, Legrand J, Houvenagel E, et al. Dual-energy computed-tomography-based discrimination between basic calcium phosphate and calcium pyrophosphate crystal deposition in vivo. Ther Adv Musculoskelet Dis. 2020;12:1759720x20936060.
23. Døssing A, Müller FC, Becce F, Stamp L, Bliddal H, Boesen M. Dual-energy computed tomography for detection and characterization of monosodium urate, calcium pyrophosphate, and hydroxyapatite: a phantom study on diagnostic performance. Investig Radiol. 2021;56(7):417–24.
24. Kirkbride TE, Raja AY, Müller K, Bateman CJ, Becce F, Anderson NG. Discrimination between calcium hydroxyapatite and calcium oxalate using multienergy spectral photon-counting CT. AJR Am J Roentgenol. 2017;209(5):1088–92.
25. Filippucci E, Reginato AM, Thiele RG. Imaging of crystalline arthropathy in 2020. Best Pract Res Clin Rheumatol. 2020;34(6):101595.
26. Yavorskyy A, Hernandez-Santana A, McCarthy G, McMahon G. Detection of calcium phosphate crystals in the joint fluid of patients with osteoarthritis - analytical approaches and challenges. Analyst. 2008;133(3):302–18.
27. Zell M, Zhang D, FitzGerald J. Diagnostic advances in synovial fluid analysis and radiographic identification for crystalline arthritis. Curr Opin Rheumatol. 2019;31(2):134–43.

Chapter 14
Novel Techniques for Synovial Fluid Crystal Analysis

John D. FitzGerald

Introduction

Since 1961, compensated polarized light microscopy (CPLM) has been the gold standard for crystal identification in synovial fluid [17]. However, small and weakly or non-birefringent crystals [14], particularly for calcium pyrophosphate (CPP) crystals [5, 27] are difficult to visualize. Therefore, CPLM can be labor-intensive, requiring examination of many low- and high-power fields to properly detect and identify crystals. Inter-rater reliability has been drawn into question [8, 9, 11, 18, 24–26] and even experienced Rheumatologists with interest in crystal research have been found to be inaccurate [4]. Furthermore, basic calcium phosphate (BCP) crystals are not visible without special staining.

CPLM reporting is limited to clinical labs compliant with Clinical Laboratory Improvement Amendments of 1988 (CLIA based labs). CPLM reports provide qualitative descriptions (present vs. absent) and whether crystals may be intra- or extra-cellular. As a result, little is known about the clinical importance of variation in crystal counts, morphology, or crystals not detected by CPLM such as ultra-small crystals (<1 μm) or BCP crystals. Dependent upon conventional microscopes, CPLM is generally not available as a point of care test and may not be available in remote or low-resource locations in the world.

Newer methodologies are being developed that have the potential to overcome several of these potential shortcomings to provide greater insight into the clinical importance of or greater access to synovial fluid crystal analysis.

J. D. FitzGerald (✉)
Department of Medicine, Division of Rheumatology, University of California, Los Angeles, David Geffen School of Medicine, Los Angeles, CA, USA
e-mail: Jfitzgerald@mednet.ucla.edu

B. F. Mandell (ed.), *Synovial Fluid Analysis and The Evaluation of Patients With Arthritis*, https://doi.org/10.1007/978-3-030-99612-3_14

Enhanced Microscopic Imaging

Application of different engineering advances to polarized light microscopy has been developed by several investigators to enhance detection. All of the enhanced imaging techniques may benefit from either realized (already reported) or potential future benefits. Digital imaging with data acquisition can provide a wealth of information on crystal content, morphology, and relation to inflammatory cells for clinical correlation. Digital imaging paired with computational analysis may provide techniques for automated scanning, crystal detection, identification, and reporting.

Different techniques and the potential benefits specific to each of those methodologies are described below.

Single-Shot Computational Polarized Light Microscopy

Single-shot computational polarized light microscopy (SCPLM) modifies a standard clinical microscope to pass (left-handed circular) polarized light through synovial fluid directly onto a complementary metal-oxide semiconductor (CMOS) digital chip with 4 orthogonally oriented polarized filters across each pixel creating digital images for the field of view [3] (See Fig.14.1, Panel 1). CPLM is dependent on crystal orientation for the classic blue and yellow images associated with positive and negative birefringence. CPLM birefringence is optimized when the crystal is aligned either parallel or perpendicular to the short axis of polarization. Manual rotation of the crystal (or microscope stage) is often required for optimal orientation and imaging. Inadequate orientation can result in poor image quality making small, weakly birefringent crystals more difficult to detect when scanning a slide. The SCPLM orthogonally oriented polarizers eliminate the need for precise crystal orientation for optimal detection.

Using standard microscope objectives, SCPLM provides familiar, traditional high- and low-power fields of view. Examples of dark-field and bright-field images are provided for MSU (Fig. 14.1). Through the use of motorized stage and computer processing, a synovial sample slide can be scanned at low power for birefringent samples then examined at high power (e.g., 40x or 100x objective) as would a clinical rater.

In addition to the benefits of enhanced crystal imaging and digital detection described above, specific benefits of SCPLM include (1) relative ease of adaption to existing clinical laboratory equipment, (2) same optical resolution of images as standard CPLM, and (3) multiple orthogonal polarized views that relax the requirement for crystal orientation for optimal imaging.

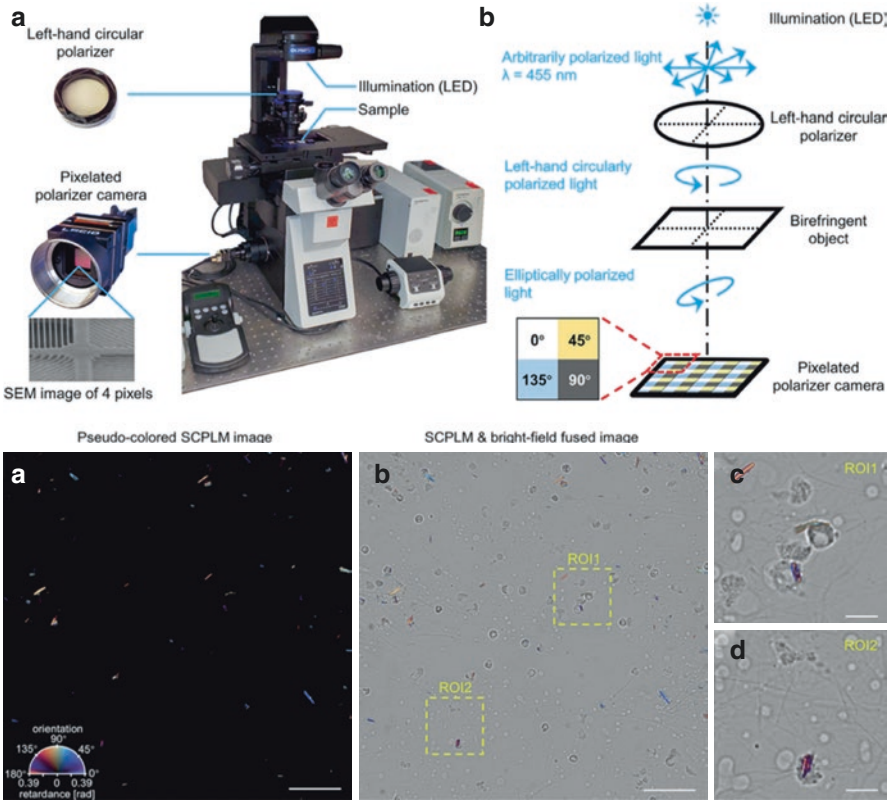

Fig. 14.1 Single-shot computational polarized light microscope (SCPLM) of MSU crystals. Panel 1: A, Single-shot computational polarized light microscope set up. B, Schematic diagram of SCPL setup. Panel 2: Experimentally captured SCPLM images showing MSU crystals engulfed by white blood cells. A, Pseudo-colored SCPLM image. B, Overlay of the pseudo-colored SCPLM image with the bright-field transmittance image. C, D, Two regions of interest (ROIs) showing the digitally fused SCPLM images with MSU in the white blood cells. Scale bar in (A, B) represents 50 μm and scale bar in (C, D) represents 10 μm

Optical Diffraction Tomography

Optical diffraction tomography (ODT) is a three-dimensional (3D) holotomographic microscope technique that uses the 3D-specific refractive index and morphology to identify crystals and other synovial fluid content (with or without polarization). Over 200 sequential beams of polarized light (collected at slightly different angles) are passed through a slide-mounted synovial sample and subsequently collected by digital camera (see Fig. 14.2, Panel 1). Then either planes or 3D images are reconstructed from the digital image data. The authors [20] nicely demonstrate images from synthetic and patient derived MSU crystals (Fig. 14.2,

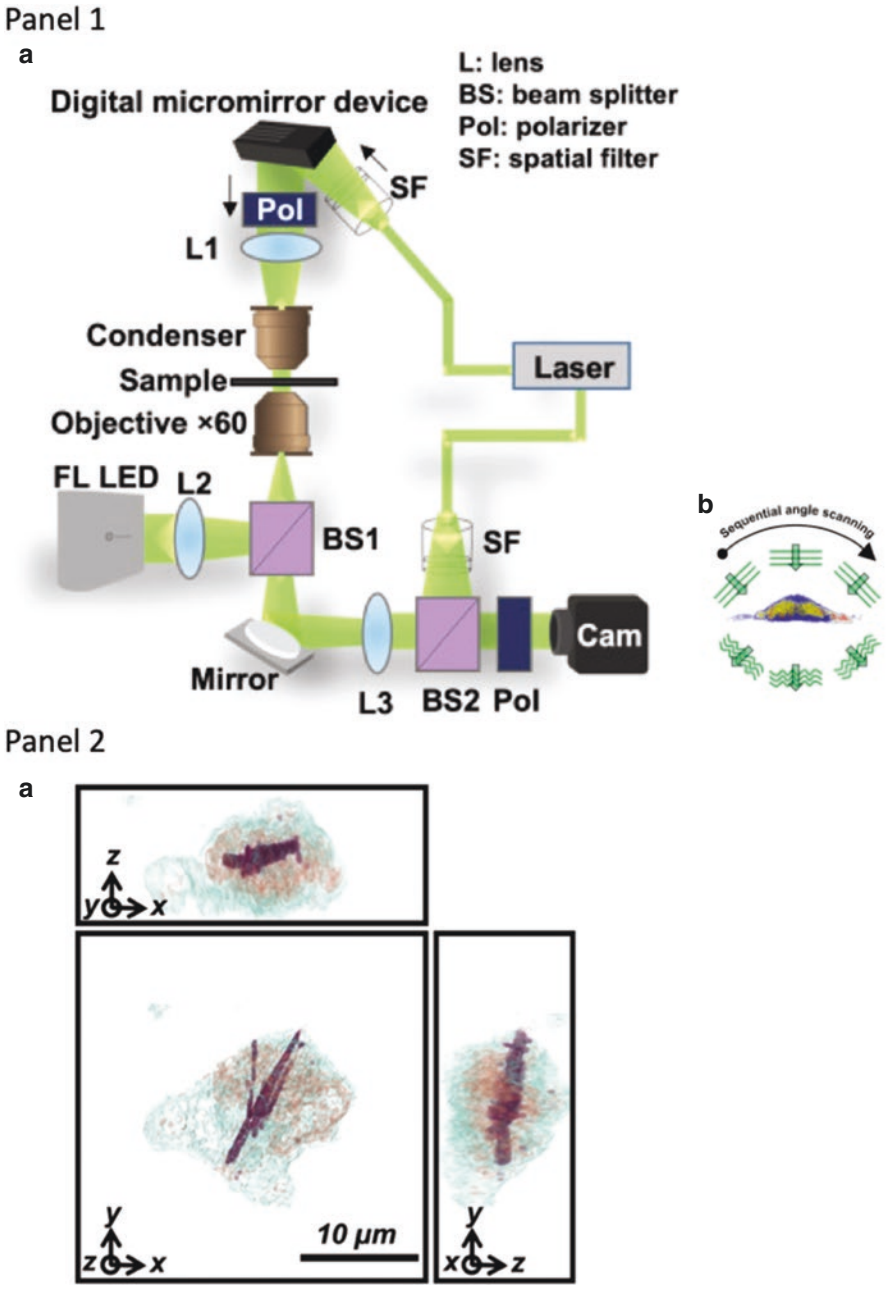

Fig. 14.2 Three-dimensional optical diffraction tomography (ODT) of MSU crystals. Panel 1: Schematic diagram of ODT setup. Panel 2: Intracellular cluster of MSU crystals viewed in 3 planes

Panel 2) [20]. In addition to 3D perspectives that show crystals in or adjacent to cells, the authors provide a time-lapse movie showing phagocytosis of an MSU crystal by a macrophage, based on data collected from 2-hour observation with images every 20-minutes. (Refer to https://www.nature.com/articles/s41598-021-89337-7#MOESM2.) They further report their findings of ten-fold increase in IL-1*B* production during macrophage ingestion of MSU crystals.

Benefits of ODT beyond enhanced imaging and digital data include (1) detailed 3-D structure of cells and crystals, (2) time-lapse observation of in vitro inflammatory cell response to crystals. The potential wealth of data likely comes with costs, extra time for data acquisition, and computational demands that may make this more useful for research instead of routine clinical applications.

Lens-Free Polarized Microscope Wide-Field Imaging

Lens-free polarized microscope wide-field imaging has been developed to detect MSU and CPP crystals [28, 29]. In this method, polarized light is passed through a synovial sample and directly detected by CMOS chip without the aid of lenses (see Fig. 14.3, Panel 1). Not dependent on lens magnification, the field of view becomes the area of the CMOS chip (~ 20 mm^2) compared with the standard 1, 0.16, and 0.01 mm^2 respectively for 10x, 40x, and 100x objectives (when paired with 10x ocular objective). Without lenses, optical image resolution is limited by CMOS (1.12 μm) pixel size, which is then enhanced using pixel-super resolution technique and deep neural network processing [16] (see Fig. 14.3, Panel B for sample images).

As currently described in publications, the lens-free method requires clinical validation and transition from bench to clinical instrumentation. Other lens-free applications from this lab have been adapted for use with current cell phone technology (using the mobile phone light source and CMOS chip) [13]. The potential development for use as point of care, bedside analysis (in clinic or emergency department setting), or in low resource regions is attractive. In addition to benefits of digitally acquired data (described above), the unique benefits of lens-free polarized microscopy include the wide field of view data acquisition, low-cost technology, and potential bedside or low resource setting.

Other Enhanced Synovial Fluid Analysis

Other authors have proposed using colorimetric methods that rely on the ability of urate and urate crystals to reduce silver nitrate. The authors argue that this could be developed into a quick (5-minute) bedside test to detect urate crystals [2, 21]. Though not addressed by the authors, the methodology would not be expected to detect other crystals (e.g., CPP or BCP).

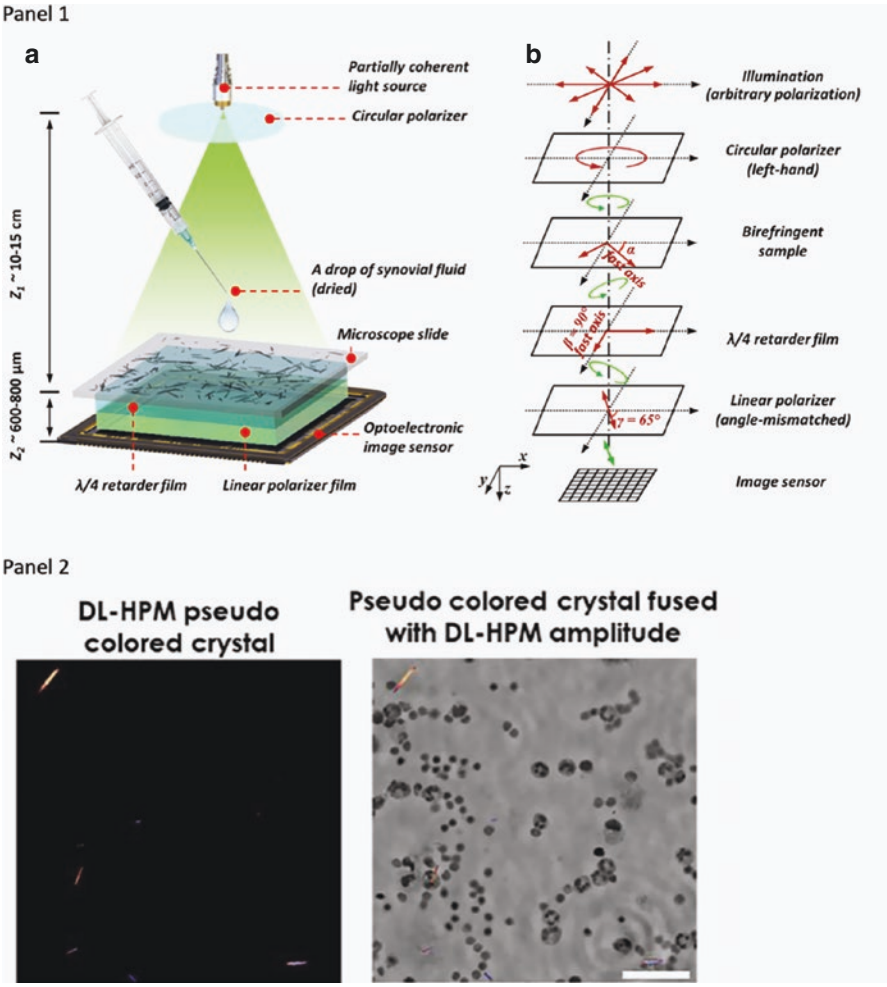

Fig. 14.3 Lens-free polarized microscope images of MSU crystals. Panel 1 (**a**) Schematic setup of lens-free differential holographic polarized microscopy. (**b**) Design of the polarization in this system. The light, which is propagating from top to bottom, passes through a left-hand circular polarizer, the birefringent sample, a λ/4 retarder film, a linear polarizer and reaches the image sensor. The orientations of the polarizing components are illustrated with red arrows, and the polarization states of the light between components are illustrated with green arrows. Panel 2 (**a**) Dark field image demonstrating birefriengent MSU crystals. (**b**) Same field of view fusing birefriengent crystal images with non-birefriengent celluar content and background

Raman Spectroscopy

Raman spectroscopy (RS) has the advantage of using the unique vibrational properties of chemical bonds to identify molecules and thus when crystals are detected, has 100% specificity for crystal identification [6]. Advances in development of RS have led to testing of a point of care RS machine (POCRS) [15]. At the time of reporting, a minimum of 0.5 ml of synovial fluid, treated with hyaluronidase is required for analysis. Concerns about sensitivity have been raised about Raman Spectroscopy [23]. Detection is dependent upon crystal concentration and volume of the sample rather than single crystal identification. POCRS can detect MSU crystals down to a threshold of 0.1 ug/mL and CPP to 2.5 ug/mL [15]. Despite prior concerns about RS sensitivity, POCRS demonstrated good agreement with CPLM findings; better for MSU crystals (k = 0.84) than CPP crystals (k = 0.61). POCRS detected MSU crystals in 38/174 (22%) slides compared to CPLM 44/174 (25%); and POCRS detected CPP crystals in 22/174 (13%) slides compared to CPLM 12/174 (7%) slides (see Table 14.1 for detail).

In vivo RS is an interesting concept that has been tested in patients with known gout [1, 7]. In vivo RS would share the advantage of ultrasound and other non-invasive imaging techniques (dual-energy CT). These preliminary in vivo RS studies were limited to a small number of patients (n = 10) with known gout. The diagnostic value of in vivo RS compared to other non-invasive or synovial fluid analyses is untested.

Other methods to enhance the sensitivity of RS include coating molecules or structures with metallic ions, a process referred to as surface-enhanced RS (SERS). Silver ions have been used to coat uric acid found in plasma [10], urine [12], or tears [19]. In a recent report, the findings from a Raman signal enhanced with coherent stimulate emission process, stimulated Raman scattering (SRS) can be paired with conventional microscope findings to detect and identify individual crystals or crystal clumps [28].

Table 14.1 Agreement between CPLM and POCRS methods

MSU		CPLM		
		Negative	Positive	Total
POCRS	Negative	128	8	136
	Positive	2	36	38
	Total	130	44	174

CPP		CPLM		
		Negative	Positive	Total
POCRS	Negative	151	1	152
	Positive	11	11	22
	Total	162	12	174

Other Imaging Techniques

Fourier transform infrared spectroscopy (FTIR) and X-ray diffraction are definitive methods for crystal characterization [22]. However, because of high cost, complex instrumentation, and limited availability outside the research setting they have limited clinical utility. FTIR evokes a crystal's inherent infrared wavelength absorption pattern. X-ray diffraction identifies a crystal's characteristic diffraction pattern of incident radiograph.

A summary and comparison of the various methodologies described above is provided in Table 14.2.

Table 14.2 Summary of potential benefits of new crystal detection methods

	Crystal detection[a]	Field of View	Point of Care	Non-invasive	Potential Cost	Comment
SCPLM	++	Standard			↑	Enhanced clinical images. Ultimate clinical utility dependent on development of detection and identification algorithms
ODT	+++	Standard			↑↑	Best imaging detail including 3D imaging Research > clinical potential utility given volume of data acquisition
Lens-free	+	20 mm^2	+		↓↓	Point of care, low-cost benefits. Large field of view may make up for lower optical resolution Clinical validity pending
Raman spectroscopy	+	N/A			?	Chemical detection of crystal molecular bonds
POCRS	+	N/A	+		?	Point of care machine. Similar agreement with CPLM for crystal identification
SRS paired microscopy	++	Standard			?	Enhanced Raman spectroscopy technique paired with standard microscope images. Clinical validity pending
In vivo RS	?	N/A	+	+	?	Point of care, non-invasive potential diagnostic instrument. Data available on only 10 patients to date. Clinical validity pending
Colorimetry	MSU only	N/A	+		↓	MSU limitation makes clinical use unclear

SCPLM Single Shot Computational Polarized Light Microscopy, *ODT* Optical Diffraction Tomography, *POCRS* Point of Care Raman Spectroscopy, *SRS* Stimulated Raman Scattering, *RS* Raman Spectroscopy, *N/A* Not applicable

[a]+ = similar to CPLM, ++/+++ = superior to CPLM

Conclusion

CPLM has been the gold standard for crystal identification from synovial fluid for over 50-years. While undeniably valuable, the limits of CPLM are well described. Newer crystal detection techniques, through enhanced imaging or analysis of molecular properties, show promise. All methods described above are in various stages of early development. The additional data provided through digital imaging may add better understanding about correlations of synovial fluid crystal content with clinical symptoms or phenotypes. Limits of crystal detection can be pushed through increased detection of smaller or more weakly birefringent crystals or increased number of FOV analyzed through automated techniques. Some of these applications may provide point of care results, which could expedite treatment resulting in improved outcomes for management of the acute inflammatory monoarthritic joint. Development of less expensive techniques may bring synovial fluid analysis to regions that don't have expensive clinical lab microscopes. The potential clinical benefits of enhanced detection and more detailed analysis of synovial fluid crystals are areas for future study.

Disclosures Dr. FitzGerald has had NIH funding within the last 24 months, for the development of Lens-Free synovial fluid analysis. Dr. FitzGerald is co-author on manuscripts cited in the Lens-Free and Single Shot Computational Microscope sections.

References

1. Abhishek A, Curran DJ, Bilwani F, Jones AC, Towler MR, Doherty M. In vivo detection of monosodium urate crystal deposits by Raman spectroscopy-a pilot study. Rheumatology (Oxford). 2016;55:379–80.
2. Anugu A, Monastero R, Pentyala S, Mustahsan VM, Cai Y, Rosenfeld J, Komatsu DE, Penna J, Hurst L, Pentyala SN. Methods Protoc. 2021;4(4):69. https://doi.org/10.3390/mps4040069. PMID: 34698258.
3. Bai B, Wang H, Liu T, Rivenson Y, Fitzgerald J, Ozcan A. Pathological crystal imaging with single-shot computational polarized light microscopy. J Biophotonics. 2020;13:e201960036.
4. Berendsen D, Neogi T, Taylor WJ, Dalbeth N, Jansen TL. Crystal identification of synovial fluid aspiration by polarized light microscopy. An online test suggesting that our traditional rheumatologic competence needs renewed attention and training. Clin Rheumatol. 2017;36:641–7.
5. Bjelle A, Crocker P, Willoughby D. Ultra-microcrystals in pyrophosphate arthropathy. Crystal identification and case report. Acta Med Scand. 1980;207:89–92.
6. Butler HJ, Ashton L, Bird B, Cinque G, Curtis K, Dorney J, Esmonde-White K, Fullwood NJ, Gardner B, Martin-Hirsch PL, Walsh MJ, Mcainsh MR, Stone N, Martin FL. Using Raman spectroscopy to characterize biological materials. Nat Protoc. 2016;11:664–87.
7. Curran DJ, Rubin L, Towler MR. Raman spectroscopy applied to the noninvasive detection of monosodium urate crystal deposits. Clin Med Insights Arthritis Musculoskelet Disord. 2015;8:55–8.
8. Dieppe P, Swan A. Identification of crystals in synovial fluid. Ann Rheum Dis. 1999;58:261–3.
9. Gordon C, Swan A, Dieppe P. Detection of crystals in synovial fluids by light microscopy: sensitivity and reliability. Ann Rheum Dis. 1989;48:737–42.

10. Gurian E, Giraudi P, Rosso N, Tiribelli C, Bonazza D, Zanconati F, Giuricin M, Palmisano S, De Manzini N, Sergo V, Bonifacio A. Differentiation between stages of non-alcoholic fatty liver diseases using surface-enhanced Raman spectroscopy. Anal Chim Acta. 2020;1110:190–8.
11. Hasselbacher P. Variation in synovial fluid analysis by hospital laboratories. Arthritis Rheum. 1987;30:637–42.
12. Hernandez S, Perales-Rondon JV, Heras A, Colina A. Determination of uric acid in synthetic urine by using electrochemical surface oxidation enhanced Raman scattering. Anal Chim Acta. 2019;1085:61–7.
13. I Bogoch, HCK, Tseng D, Ephraim R, Duah E, Tee J, Andrews J, Ozcan A. Evaluation of a mobile phone-based microscope for screening of Schistosoma haematobium infection in rural Ghana. Am J Tropical Med Hyg. 2017.
14. Ivorra J, Rosas J, Pascual E. Most calcium pyrophosphate crystals appear as non-birefringent. Ann Rheum Dis. 1999;58:582–4.
15. Li B, Singer NG, Yeni YN, Haggins DG, Barnboym E, Oravec D, Lewis S, Akkus O. A point-of-care Raman spectroscopy-based device for the diagnosis of gout and Pseudogout: comparison with the clinical standard microscopy. Arthritis Rheumatol. 2016;68:1751–7.
16. Liu T, De Haan K, Bai B, Rivenson Y, Luo Y, Wang H, Karalli D, Fu H, Zhang Y, Fitzgerald J, Ozcan A. Deep learning-based holographic polarization microscopy. ACS Photonics. 2020;7:3023–34.
17. Mccarty DJ, Hollander JL. Identification of urate crystals in gouty synovial fluid. Ann Intern Med. 1961;54:452–60.
18. Mcgill NW, York HF. Reproducibility of synovial fluid examination for crystals. Aust NZ J Med. 1991;21:710–3.
19. Narasimhan V, Siddique RH, Park H, Choo H. Bioinspired disordered flexible Metasurfaces for human tear analysis using broadband surface-enhanced Raman scattering. ACS Omega. 2020;5:12915–22.
20. Park S, Lee LE, Kim H, Kim JE, Lee SJ, Yoon S, Shin S, Kang H, Park Y, Song JJ, Lee S. Detection of intracellular monosodium urate crystals in gout synovial fluid using optical diffraction tomography. Sci Rep. 2021;11:10019.
21. Pentyala S, Monastero R, Palati S, Varghese E, Anugu A, Pentyala S, Mustahsan VM, Komatsu DE, Penna J, Hurst LC. Rapid gout detection method and kit. Diagnostics (Basel). 2019;9.
22. Rosenthal AK, Mandel N. Identification of crystals in synovial fluids and joint tissues. Curr Rheumatol Rep. 2001;3:11–6.
23. Rosenthal AK, Pascual E. Editorial: decreasing crystal-induced consternation: new methods of crystal identification. Arthritis Rheumatol. 2016;68:1574–7.
24. Schumacher Jr HR, Sieck MS, Rothfuss S, Clayburne GM, Baumgarten DF, Mochan BS, Kant JA. Reproducibility of synovial fluid analyses. A study among four laboratories. Arthritis Rheum. 1986;29:770–4.
25. Swan A, Amer H, Dieppe P. The value of synovial fluid assays in the diagnosis of joint disease: a literature survey. Ann Rheum Dis. 2002;61:493–8.
26. Von Essen R, Holtta AM, Pikkarainen R. Quality control of synovial fluid crystal identification. Ann Rheum Dis. 1998;57:107–9.
27. Zell M, Aung T, Kaldas M, Rosenthal AK, Bai B, Liu T, Ozcan A, Fitzgerald JD. Calcium pyrophosphate crystal size and characteristics. Osteoarthritis and Cartilage Open. 2021;3:100133.
28. Zhang B. Highly specific and label-free histological identification of microcrystals in fresh human gout tissues with stimulated Raman scattering. Theranostics. 2021;11:14.
29. Zhang YB, Lee SYC, Zhang Y, Furst D, Fitzgerald J, Ozcan A. Wide-field imaging of birefringent synovial fluid crystals using lens-free polarized microscopy for gout diagnosis. Sci Rep. 2016;6.

Chapter 15
Atlas of Images – Normal and Abnormal Synovial Fluid

Michael H. Pillinger

M. H. Pillinger (✉)
Division of Rheumatology, NYU Grossman School of Medicine/NYU Langone Medical Center, VA New York Harbor Health Care System, New York, NY, USA
e-mail: michael.pillinger@nyulangone.org

B. F. Mandell (ed.), *Synovial Fluid Analysis and The Evaluation of Patients With Arthritis*, https://doi.org/10.1007/978-3-030-99612-3_15

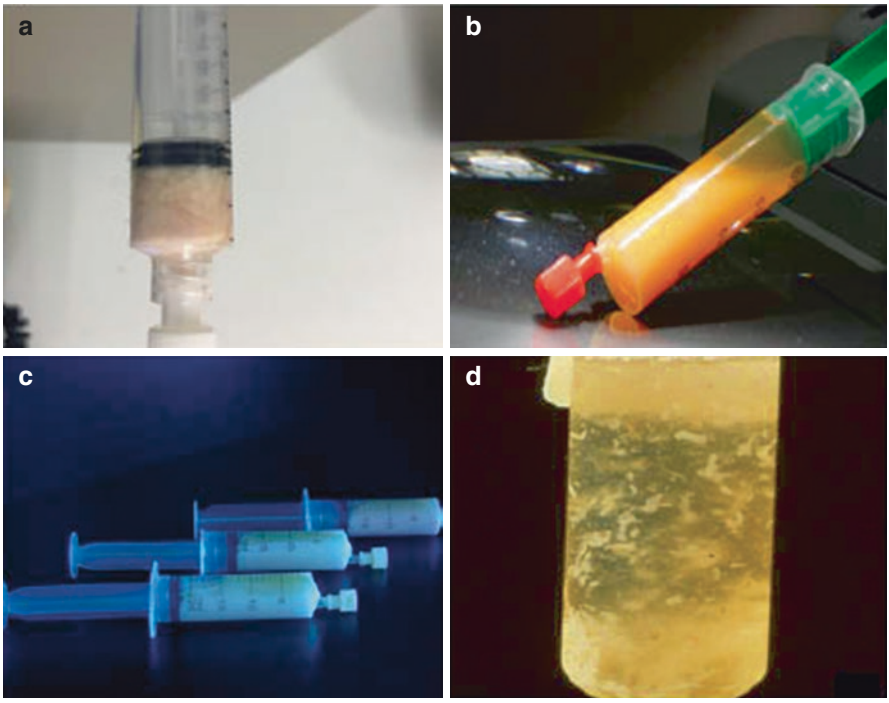

Fig. 15.1 Macroscopic appearance of synovial fluid aspirates from patients with several different conditions. (**a**), Aspirate from a chronically swollen, non-tender, and cool olecranon bursa. Patient had previously undiagnosed gout, with only one prior acute painful flare in a knee. The fluid contained rare neutrophils and large mononuclear cells, only a few with phagocytosed crystals, and sheets of negatively elongated, strongly birefringent, needle-shaped crystals. The milky color was due to large numbers of monosodium urate crystals. (**b**), Fluid aspirate from the bursa of a patient with rheumatoid arthritis that was found to be extensively populated with cholesterol crystals. The honey color seen in this picture may be more characteristic of cholesterol than other crystal types. (**c**), Inflammatory aspirate from the joint of a patient with gonococcal arthritis, showing a cloudy white fluid. The turbidity of the fluid is due mainly to a large number of neutrophils, whose myeloperoxidase in azurophilic granules may lend a very slight greenish tint. (**d**), "Rice bodies" – fibrin and synovial fragments – in the synovial fluid of a patient with longstanding RA. Such fragments are also seen in patients with chronic joint infections such as mycobacteria. Overall, it is very difficult to distinguish between the presence of various crystals and large numbers of leukocytes in synovial fluid on a macroscopic scale, and microscopic evaluation is always required for diagnosis. (Images courtesy of BF Mandell (**a**,), TL Jansen (**b**, **c**), and HR Schumacher and BF Mandell (**d**))

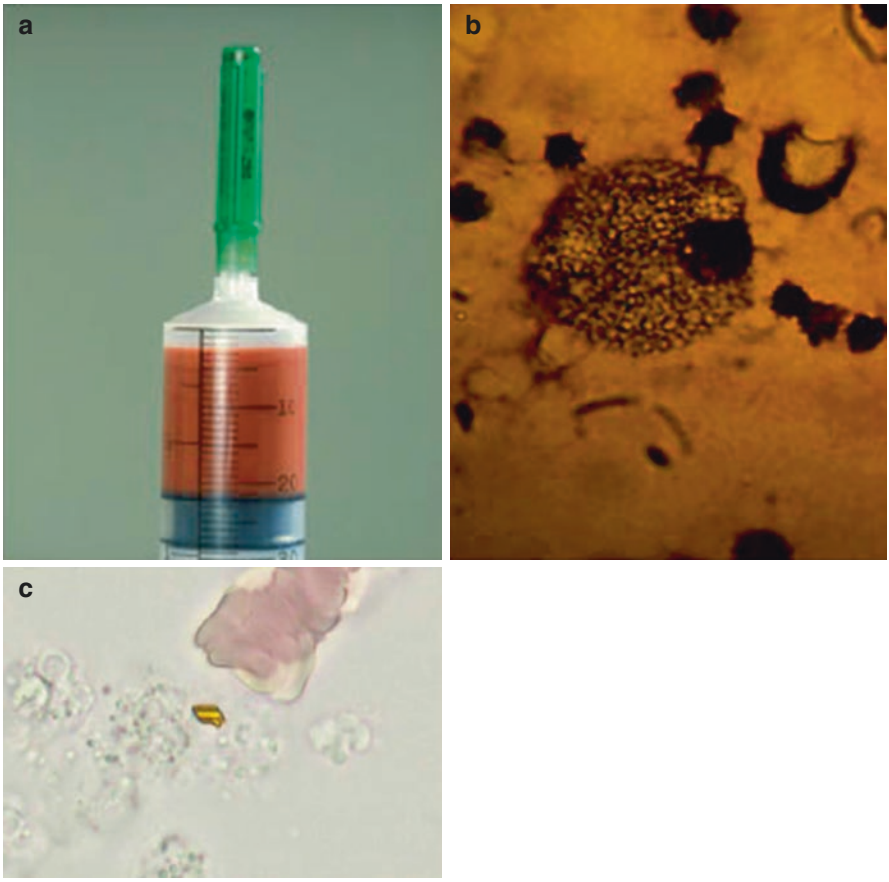

Fig. 15.2 Joint fluid in the setting of trauma. (**a**, **b**), Synovial fluid from the knee of a 29-year-old man following a traumatic patellar fracture. (**a**), Gross appearance of the aspirate. The "tomato soup" color is indicative of a traumatic hemarthrosis but is lighter than would be typical for a pure bloody aspirate, likely due to the presence of fat from marrow. (**b**), On microscopic examination the fluid contained, in addition to erythrocytes, many cells, leukocytes, and synoviocytes, containing a plethora of intracellular endocytosed fat globules (methylene blue stain, 400x standard light microscopy), consistent with marrow disruption and fat release from the bony fracture. (**c**), Hematoidin crystals are golden brown rhomboid-shaped crystals that represent a breakdown product of hemoglobin and may be seen in joints with prior intrasynovial hemorrhage. Hematoidin crystals may assist in diagnosis, but are not in themselves considered pathogenic. In this case, note also the several erythrocytes visible above the crystal. (Images courtesy of BF Mandell (**a**, **b**) and HR Schumacher and BF Mandell (**c**))

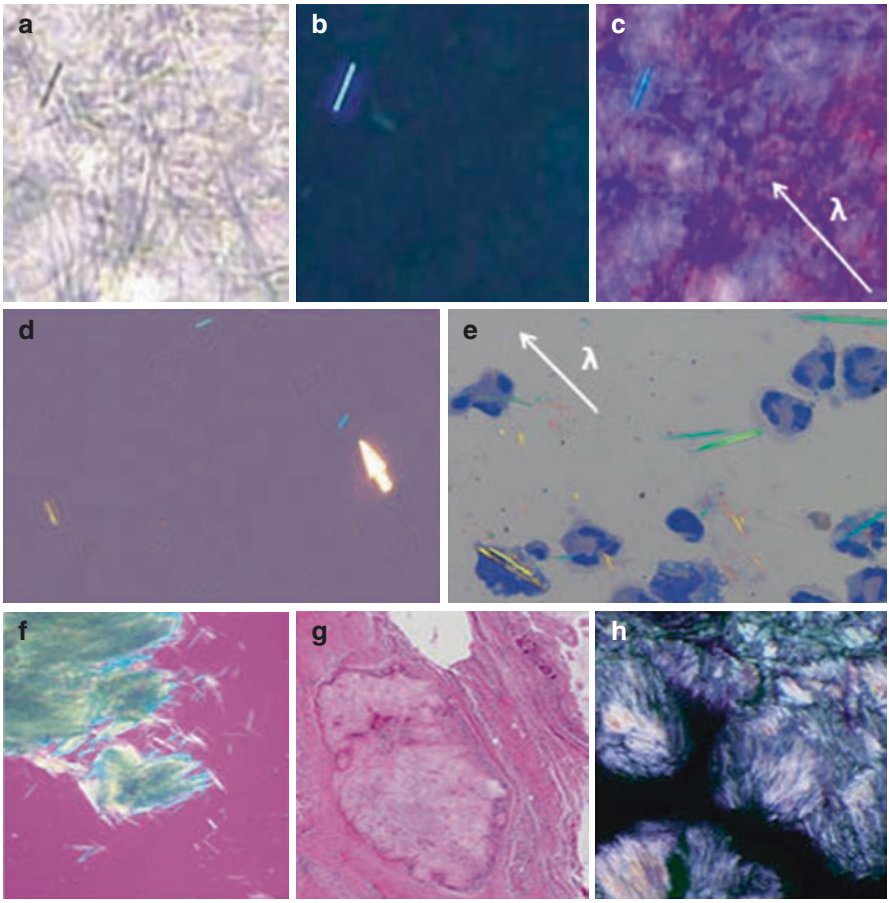

Fig. 15.3 Monosodium urate (MSU) crystals in synovial fluid. (**a**–**c**), A single MSU crystal from a synovial fluid joint aspiration as seen under standard brightfield light (**a**), uncompensated polarized (**b**), and compensated polarized microscopy (**c**). Note the needle shape of the crystal, with pointed ends. The arrow indicates the defined axis of the red compensator (and therefore the wave orientation of incoming polarized light), and the blue color of the crystal when perpendicular to the wave orientation indicates that it is negatively birefringent. (**d**), Several MSU crystals as viewed under compensated polarized microscopy. Careful examination reveals that these crystals are intracellular in neutrophils, by which they have likely been phagocytosed. Note the blue color of crystals perpendicular to, and the yellow color of crystals parallel to, the defined axis of the red compensator (white arrow). (**e**), MSU crystals in synovial fluid, with multiple neutrophils clearly visible under hematoxylin and eosin staining (compensated polarized microscopy). Some crystals are extracellular, but several are likely intracellular within neutrophils, including multiple crystals within a single neutrophil (bottom left). (**f**), A microtophus (MSU aggregate) aspirated from the synovial fluid of a patient with gout. (**g**). An actual tophus (intratissue MSU deposit) from a synovial biopsy of a patient with gout. Note that the tophus is surrounded by an inflammatory rind. (**h**), MSU crystals aspirated directly from a tophus, viewed under uncompensated polarized microscopy. (Images courtesy of F Olivero (**a**, **b**, **c**), GM McCarthy (**d**), N Haghi (**e**), NL Edwards (**f**), and R Bentley (**g**, **h**))

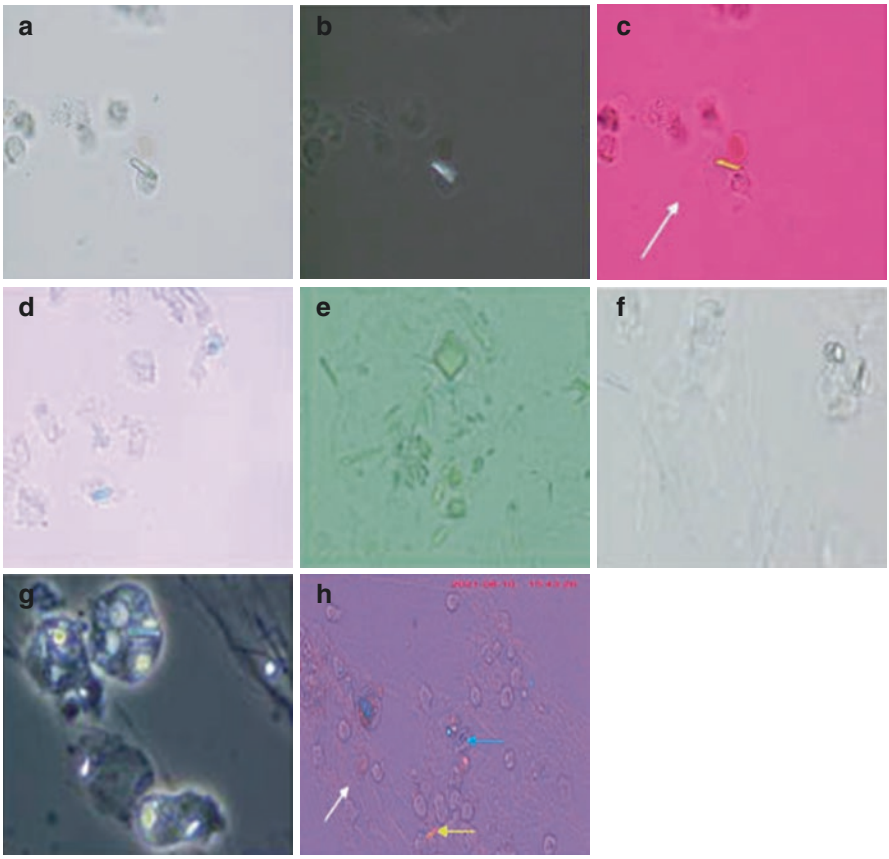

Fig. 15.4 Calcium pyrophosphate dihydrate (CPPD) crystals in synovial fluid. (**a**–**c**), A single, positively birefringent CPPD crystal is seen in the center of the field, demonstrating the short, squat rhomboid appearance typical of most (but not all) CPPD crystals. The panels show the crystal as seen under brightfield light (**a**), uncompensated polarized (**b**) and compensated polarized (**c**) microscopy. In contrast to monosodium urate crystals, a CPPD crystal if birefringent is yellow when perpendicular to the defined axis of the red compensator (white arrow) and would be blue when parallel to it. (**d**) Two rhomboid-shaped CPPD crystals viewed under polarized compensated microscopy. The pale quality of the crystals is common and reflects weak (or no) birefringence that may make recognition difficult. (**e**) Multiple CPPD crystals viewed under brightfield light microscopy, demonstrating the shape heterogeneity of CPPD crystals. While some crystals are rhomboid, others are square and still others are long and rod-like (although typically thicker than MSU crystals and without pointed ends). (**f**), Multiple CPPD crystals, of varying morphologies, that have been phagocytosed by neutrophils (brightfield light microscopy). (**g**), Phase microscopy showing multiple neutrophils containing multiple CPPD crystals of varying morphology. Crystals can be seen both within and outside of phagocytic vacuoles. (**h**), A mixed population of both CPPD and urate crystals in the same synovial fluid. The orientation of the red compensator is depicted by the white arrow; note the urate crystal that is yellow when parallel to the plane of polarization (yellow arrow), and the CPPD crystal that is blue parallel to the plane of polarization (blue arrow). (Images courtesy of E and M Andres (**a**–**c**, **e**–**g**), F Olivero (**d**), and (**g**) McCarthy (**h**))

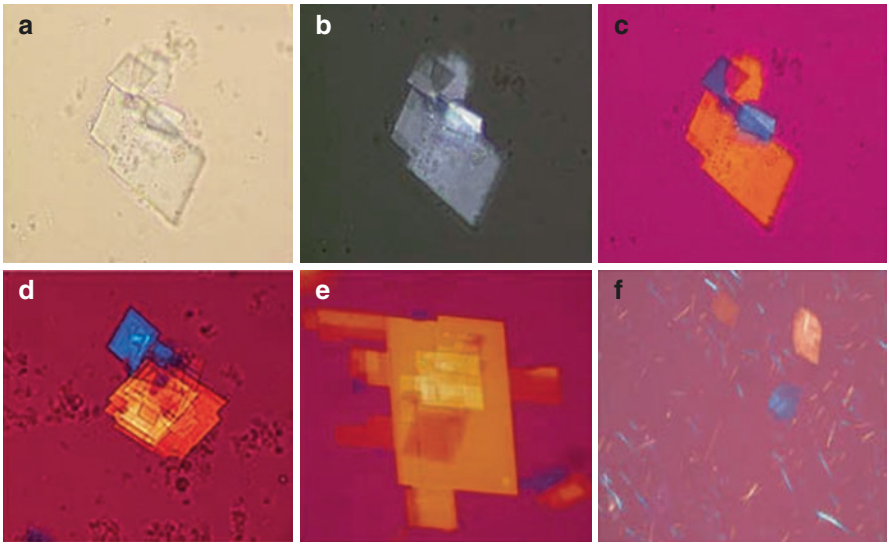

Fig. 15.5 Cholesterol crystals. (**a**–**c**), Cholesterol crystals from the joint of a patient with rheumatoid arthritis, as seen under bright field (**a**), uncompensated polarized (**b**), and compensated polarized light (**c**) microscopy. (**d**, **e**) Similar findings from other patients, under compensated polarized microscopy. In all cases, note the flat, stacked plates with characteristic notched corners sometimes referred to as a keystone appearance. (**f**) Cholesterol crystals, somewhat hazy, co-existing with negatively birefringent monosodium urate crystals (needle-shaped) in the synovial fluid of a patient with gout. Care must be taken in the interpretation of coexisting MSU and cholesterol crystals, as cholesterol plates when viewed on edge can mimic MSU crystals. (Images courtesy of E and M Andres (**a**–**c**), NL Edwards (**d**), and TL Jansen (**e**, **f**))

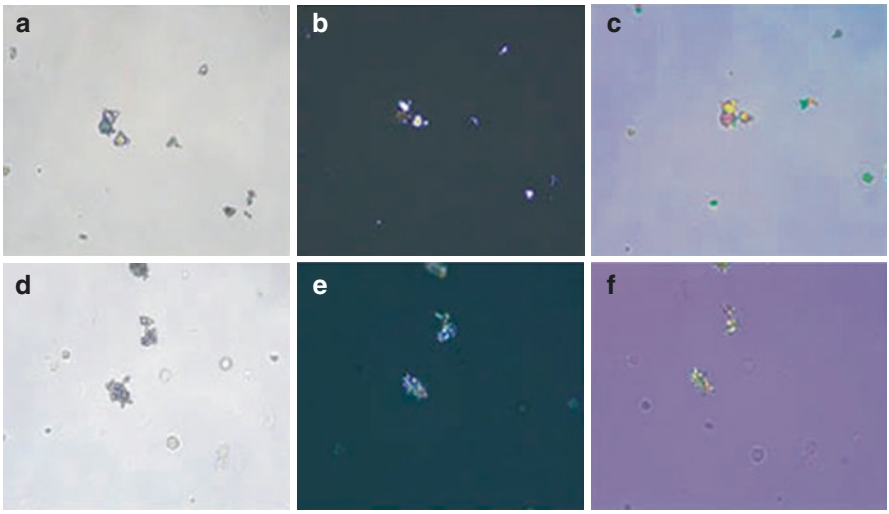

Fig. 15.6 Intraarticular deposit glucocorticoids are crystalline before dissolution and may be confused with an etiologic agent of disease (like CPPD). Shown are aspirates from two patients who had recently had glucocorticoid injections and underwent subsequent re-aspiration. Injection of crystalline glucocorticoids occasionally results in a transient inflammatory crystal response, before the glucocorticoids dissolve and exert their anti-inflammatory effect, which may trigger re-aspiration. (**a**–**c**), Triamcinolone acetonide (**d**–**f**), methylprednisolone acetate (**a**, **d**), brightfield light microscopy (**b**, **e**), uncompensated polarizing microscopy and (**c**, **f**) compensated polarizing microscopy. Other crystalline glucocorticoids that may be injected include prednisolone and betamethasone; the latter crystals are needle-shaped and may be mistaken for monosodium urate. Glucocorticoid crystals are typically extracellular. (Images courtesy of F Olivero)

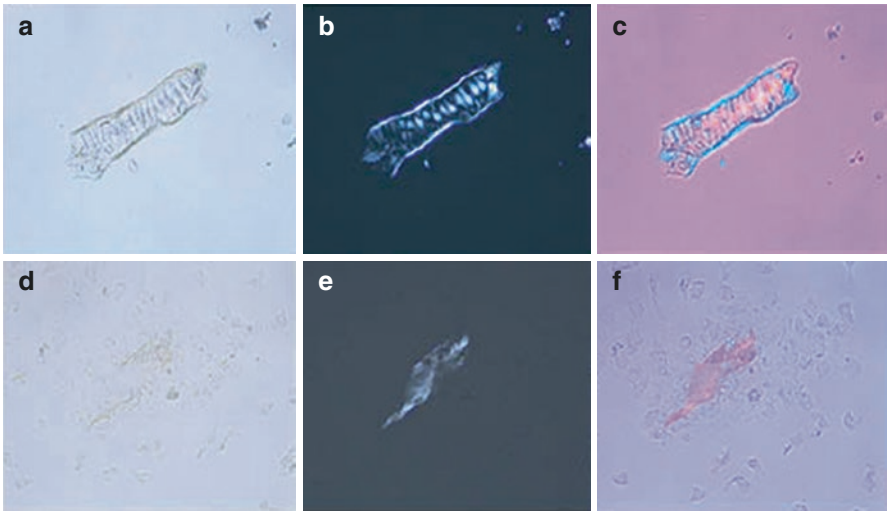

Fig. 15.7 Two examples of tissue fragments in synovial fluid. The folding and creasing of membrane structures can create the appearance of birefringent material. (**a**, **d**) Brightfield light microscopy. (**b**, **e**), Polarizing microscopy. (**c**, **f**) Compensated polarizing m5icroscopy. (Images courtesy of F Olivero)

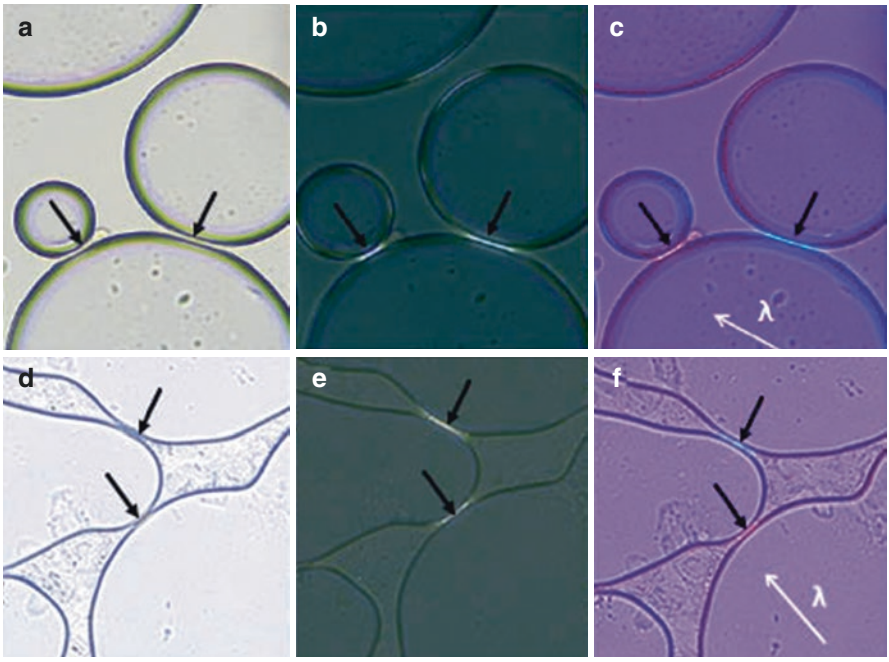

Fig. 15.8 Artifacts arising from pseudo-polarization at the interface of two surfaces (black arrows), in this case the surfaces of air bubbles. (**a**–**c**) note the birefringence at the interface of pairs of spherical air bubbles; (**d**–**f**), similar findings at the interface of air bubbles that are irregular in shape. (**a**, **d**) brightfield light microscopy; (**b**, **e**) uncompensated polarizing microscopy; (**c**, **f**) compensated polarizing microscopy. In (**c** and **f**) White arrows indicate the defined axis of the red compensator, and the interface effects are consistent with positive birefringence. These artifacts can also be observed at the interface of cells, especially of erythrocytes in serosanguinous or bloody synovial fluid. (Images courtesy of F Olivero)

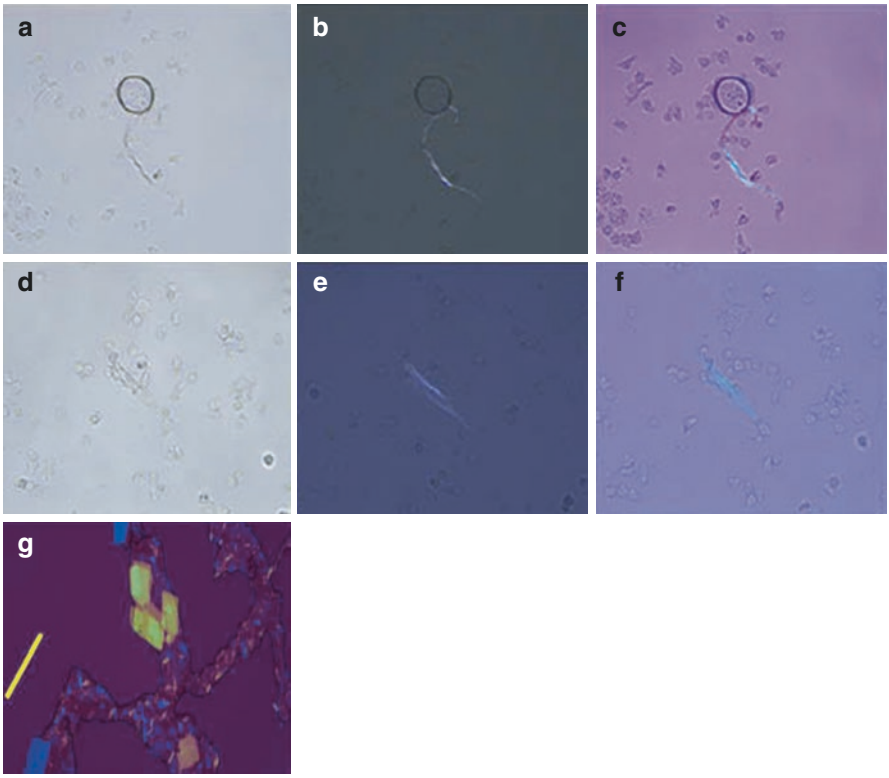

Fig. 15.9 Other birefringent artifacts. (**a**–**c**) show a contaminant fiber with birefringent properties. Fibers may be natural or iatrogenic (e.g., fibers from gauze, dust on microscope slide, etc.). (**d**–**f**) show an artefactual fragment of unknown provenance. (**g**), Artifacts of membrane drying. When large cells such as epithelial cells are subjected to drying during microscope slide preparation, aggregates may form that represent artifactual cholesterol crystals, and microfolds in the dried membranes may form needle-like structures that are birefringent and may be confused with MSU crystals. (Yellow bar indicates the defined axis of the red compensator.) (**a**, **d**) Brightfield light microscopy. (**b**, **e**) Uncompensated polarizing microscopy. (**c**, **f**, **g**) Compensated polarizing microscopy. (Images courtesy of F Oliviero (**a**–**f**) and TL Jansen (**g**))

Index

B. F. Mandell (ed.), *Synovial Fluid Analysis and The Evaluation of Patients With Arthritis*, https://doi.org/10.1007/978-3-030-99612-3